

THESIS 2003 4953429

LIBRARY
Michigan State >
University

This is to certify that the dissertation entitled

UNIVERSAL INTEGRAL CONTROLLERS WITH NONLINEAR GAINS

presented by

Hyon Sok Kay

has been accepted towards fulfillment of the requirements for the

Ph.D. degree in Electrical Engineering

Major Professor's Signature

May 16, 2003

Date

MSU is an Affirmative Action/Equal Opportunity Institution

PLACE IN RETURN BOX to remove this checkout from your record. TO AVOID FINES return on or before date due. MAY BE RECALLED with earlier due date if requested.

DATE DUE	DATE DUE	DATE DUE

6/01 c:/CIRC/DateDue.p65-p.15

UNIVERSAL INTEGRAL CONTROLLERS WITH NONLINEAR GAINS

By

Hyon Sok Kay

A DISSERTATION

Submitted to
Michigan State University
in partial fulfillment of the requirements
for the degree of

DOCTOR OF PHILOSOPHY

Department of Electrical and Computer Engineering

2003

ABSTRACT

UNIVERSAL INTEGRAL CONTROLLERS WITH NONLINEAR GAINS

By

Hyon Sok Kay

Various robust nonlinear control techniques have been developed for the regulation of nonlinear systems under uncertainties and disturbances. Among the controllers proposed for single-input single-output, input-output linearizable, minimum phase, nonlinear systems, the Universal Integral Controller has a simple structure that can be viewed as a natural extension of the classical PID controller and requires minimal information about the system. While robust nonlinear controllers ensure asymptotic regulation, they do not address the problem of transient performance. In this dissertation, we extend the structure of the Universal Integral Controller to provide more freedom that can be utilized to improve the transient performance. We allow the integral, proportional and derivative gains to be nonlinear functions of the tracking error and its derivatives. Two possible schemes for nonlinear integration are investigated: a nonlinearity placed before or after the integrator. Our analysis shows that the new Universal Integral Controller achieves regional and semiglobal regulation. More specific results are provided for the nonlinear PID controller, which is a special form of the Universal Integral Controller. By simulation, we demonstrate that the new freedom in designing the nonlinear gains can be used to improve the transient performance.

ACKNOWLEDGMENTS

I am deeply indebted to my advisor, Professor Hassan K. Khalil, for his encouragement and invaluable advice. I would like to extend my sincere thanks and appreciation to my parents, Lee Gil Kay and Yesil Kim, and my wife, Young Yi Yu, for their support and patience. I would also like to thank my children, Suyeon and Sumin, for their love and understanding.

Table of Contents

LI	ST C	OF TABLES	vii	
LI	ST (OF FIGURES	viii	
1	1 Introduction			
	1.1	Integral Control	2	
	1.2	Universal Integral Controller	3	
	1.3	High-gain Observers	5	
	1.4	Controllers with Variable Gains	6	
	1.5	Overview of the Thesis	7	
2	Universal Integral Controllers with Nonlinear Integral Gains			
	2.1	System Description	9	
	2.2	Sliding Mode Control	14	
	2.3	Design of Nonlinear Integral Gains	17	
	2.4	Closed-loop Analysis	26	
		2.4.1 Nonlinearity before the integrator	26	

		2.4.2 Nonlinearity after the integrator	36
	2.5	Simulation Results	40
	2.6	Conclusions	48
	Α	Stability of Nonlinear Integrators	49
	В	Derivation of (2.43)	51
3	Uni	versal Integral Controllers with Nonlinear Gains	56
	3.1	Introduction	56
	3.2	Design of Nonlinear Proportional and Derivative Gains	57
	3.3	Closed-loop Analysis	62
	3.4	Simulation Results	65
	3.5	Conclusion	69
	С	S-procedure for Lemma 1	72
4	Nor	alinear PID Controllers	75
	4.1	Introduction	75
	4.2	Closed-loop Analysis	79
	4.3	Simulation Results	90
	4.4	Conclusions	95
5	Con	aclusions	99

BIBLIOGRAPHY 102

List of Tables

3.1	Examples of	f sector conditions for stable systems determined by the	
	LMI	· • • • • • • • • • • • • • • • • • • •	61

List of Figures

1.1	Universal Integral Controller for relative-degree-one and two systems	4
2.1	Simulation results of the continuous sliding mode controller and Universal Integral Controller for the field-controlled DC motor	19
2.2	Nonlinearity $\psi(\hat{e}_a)$ for the Nonlinearity Before Integration scheme .	24
2.3	Two possible schemes for nonlinear integrators	25
2.4	Simulation results of Universal Integral Controllers with nonlinear integrators for the field-controlled DC motor	42
2.5	Nonlinearities $\psi_1(e_a)$ and $\psi_2(\sigma)$ for the simulation of the field-controlled DC motor	43
2.6	Simulation results of motion on a horizontal surface	44
2.7	Simulation results of the magnetic suspension system	46
2.8	Nonlinearity $\psi(e_a)$ for the simulation of the magnetic suspension system	47
2.9	Nonlinearity before integrator when $s=0$	50
3.1	Simulation results for the synchronous generator connected to an infinity bus	67
3.2	Nonlinear proportional gain $v_1(e_1) = k_1(e_1)e_1$ for the simulation of the synchronous generator connected to an infinite bus	68

3.3	Simulation results for the single link manipulator	70
3.4	Nonlinear proportional and derivative gains $k_1(e_1)$, $k_2(e_2)$, $k_3(e_3)$ for the simulation of the single link manipulator	71
4.1	Nonlinear PI controller for relative-degree-one systems and nonlinear PID controller for relative-degree-two systems	78
4.2	Simulation results of the nonlinear PID controllers for the field-controlled DC motor	91
4.3	Nonlinearities $\psi_1(e_a)$ and $\psi_2(e_1)$ for the simulation of the field-controlled DC motor	92
1.4	Simulation results of the nonlinear PID controllers for motion on a horizontal surface	93
4.5	Nonlinear proportional gain $k_1(e_1)$ for the simulation of the unstable second-order system $\ldots \ldots \ldots \ldots \ldots \ldots \ldots \ldots$	96
1.6	Simulation results for the second-order unstable system with nonlinear and linear proportional gains	97
1.7	Simulation results for the second-order unstable system with linear and nonlinear integrators	98

Chapter 1

Introduction

For input-output linearizable, minimum phase, nonlinear systems, the universal integral controller achieves robust asymptotic tracking. The controller which can be viewed as an extension of the classical PID controller, uses a feedback signal of the form

$$k_0 \int e_1 + k_1 e_1 + k_2 \frac{de_1}{dt} + \cdots + k_{
ho-1} \frac{d^{
ho-1}e_1}{dt^{
ho-1}} + \frac{d^{
ho}e_1}{dt^{
ho}}$$

where e_1 is the tracking error and the derivatives of the error are calculated using a high-gain observer. While it achieves robust steady-state performance, it does not address the problem of transient performance. In fact, most of the time, the improvement in the steady-state performance comes at the expense of degradation of the transient performance. The goals of this dissertation are

- 1. Extend the structure of the Universal Integral Controller by replacing the constant gains k_0 to $k_{\rho-1}$ by nonlinear functions of e_1 and its derivatives
- 2. Study the design of these nonlinear functions to improve the transient performance of the system
- 3. Prove the stability of the closed-loop system under Universal Integral Con-

trollers with variable gains

In the next sections, we briefly review the main background elements of this dissertation. In Section 1.1, we review integral control of nonlinear systems, which leads to the review of the Universal Integral Controller in Section 1.2. In Section 1.3, we review high-gain observers. The idea of using nonlinear gains as a tool for improving transient performance is not new in the control literature. In Section 2.4, we review the literature on this idea. Finally, we give an overview of the thesis in Section 2.5.

1.1 Integral Control

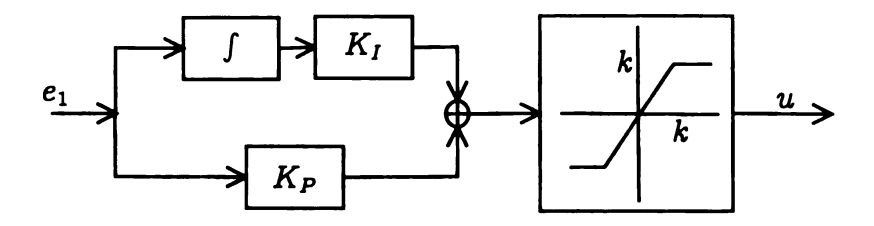
Integral control is extensively used in control system design. It achieves robust asymptotic tracking of a reference signal, which is constant or approaches a constant limit asymptotically, in the presence of external disturbances and unmodeled system dynamics. An integral controller is composed of two parts: the integrator and the stabilizing controller. Integration of the tracking error creates an equilibrium point, where the tracking error is zero, and the controller stabilizes the augmented system. While external disturbances or uncertainties of the system model move the equilibrium point, the integral action ensures that the tracking error is zero at equilibrium, as long as the stabilizing controller maintains the equilibrium point asymptotically stable. The control problem is to design a controller that stabilizes the equilibrium point of the augmented system in the domain of interest in the presence of unknown disturbances.

The theory of integral control for linear systems was developed in the seventies by Davison [8], Francis [12], and Desoer and Wang [9], among others. In the early nineties, the integral control theory was extended to nonlinear systems and local results were provided. Huang and Rugh [17],[18] used the extended linearization method and allowed slowly varying external signals. Isidori and Byrnes [21] derived necessary and sufficient conditions for local solutions. Regional and semiglobal results for input-output linearizable systems were reported later on. Freeman and Kokotovic [13] used backstepping to design a state feedback controller for systems with no zero dynamics. Mahmoud and Khalil [31], Khalil [25],[27] and Isidori [19] designed output feedback controllers, with high-gain observers, which achieve semiglobal regulation.

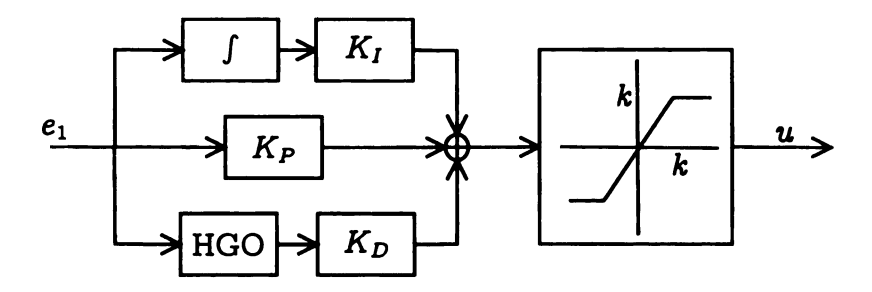
1.2 Universal Integral Controller

Mahmoud and Khalil [31] used integral control to design a robust min-max output feedback controller for a single-input single-output, input-output linearizable system with asymptotically stable zero dynamics. The integrator creates an equilibrium point at which the tracking error is zero. The robust controller brings the trajectory of the system to a positively invariant set. The size of that set can be made small by choice of some control parameters, and inside the set the controller acts as a high-gain controller stabilizing the equilibrium point. Khalil [27] carried the work of [31] further by designing Universal Integral Controllers, where continuous sliding mode control was used for robust nonlinear control. The control input has the form

$$u = -k \operatorname{sign}(\cdot) \operatorname{sat}\left(\frac{k_0 \sigma + k_1 e_1 + \dots + k_{\rho-1} e_{\rho-1} + e_{\rho}}{\mu}\right) \tag{1.1}$$



(a) A PI controller with $K_I = kk_1/\mu$, $K_P = k/\mu$ followed by saturation



(b) A PID controller with $K_I=kk_1/\mu,~K_P=kk_2/\mu,~K_D=k/\mu$ followed by saturation

Figure 1.1: Universal Integral Controller for relative-degree-one and two systems

where ρ is the relative degree of the system, σ is the integrator output, e_1 to e_ρ are the tracking error and its derivatives, and sat(·) is the saturation function. Only the information about the relative degree ρ of the plant and the sign of its high frequency gain sign(·) is necessary to design the controller, and the structure of the controller can be viewed as an extension of classical PID controller. In particular, for relative-degree-one systems, it is the classical PI controller followed by saturation, while for relative-degree-two systems, it is the classical PID controller followed by saturation. Figures 1.1 shows the structure of the controller for systems with relative degree one and two.

1.3 High-gain Observers

High-gain observers provide an important technique for the design of output feedback controllers for nonlinear systems. A high-gain observer estimates the derivatives of the output of a system. The observer gain depends on a small parameter ϵ , which can be adjusted to guarantee that the estimation error decays to the level $\mathcal{O}(\epsilon)$ in an arbitrarily small time interval. Esfandiari and Khalil [10] studied the use of high-gain observers in the design of output feedback control of nonlinear systems, which are minimum phase and input-output linearizable. A key contribution of their study is the use of saturation nonlinearities to overcome the peaking phenomenon associated with high-gain observers. The observer is designed to assign the observer eigenvalues at $\mathcal{O}(1/\epsilon)$ values in the open left-half complex plane. This results in exponential modes of the form $(1/\epsilon)^m \exp(-ta/\epsilon)$ for some positive constant a and positive integer m. While the decay of the exponential term $\exp(-ta/\epsilon)$ can be made faster by decreasing ϵ , the amplitude term $(1/\epsilon)^m$ grows larger with such decrease. This peaking phenomenon was known for linear systems, but Esfandiari and Khalil showed that its impact on nonlinear systems is more serious because it could destabilize the system. They proposed a technique to overcome the effect of peaking in the observer on the state of the system under control, i.e., the plant. The idea is to saturate the feedback control law outside a compact region of interest such that during peaking period the control saturates and protects the plant from the effects of peaking. Because the peaking transients decay rapidly, the saturation period is small. Since its introduction in 1992, the Esfandiari and Khalil technique has received a lot of attention in the control field and has been included in a few textbooks [33],[28],[20]. One of the important consequences of this technique is the ability to separate the design of output feedback control for nonlinear systems into a state feedback design followed by observer design, and to prove that the output feedback controller recovers the performance of the state feedback controller. Teel and Pray [41] developed a generic separation principle, which showed that a globally stabilizable system by state feedback with uniform observability can be stabilized semiglobally by output feedback. Atassi and Khalil [3] provided a more comprehensive separation principle and showed that the output feedback controller recovers the performance of the state feedback controller in the sense of recovering asymptotic stability of an equilibrium point, its region of attraction, and its trajectories. Extensive survey of the use of high-gain observers in nonlinear control can be found in [26].

1.4 Controllers with Variable Gains

Numerous researchers in various fields have proposed to use variable gains as a tool to improve the performance of controllers. The idea has been applied to aircraft control [39], traffic control [6], vibration control [1] and power systems [42], among other areas. In particular, as PID controllers are widely employed in control systems, controllers with nonlinear PID gains have been designed to improve the performance. Experimental and simulation results showing superior performance of nonlinear proportional and derivative gains are found in Fertik and Sharp [11], Clark [7], and Ni [32]. While integral control achieves asymptotic regulation, it has been observed that the integrator can degrade the transient performance. Krikelis [29] proposed 'intelligent' integrators where a deadzone nonlinearity was placed in a feedback loop around the integrator to prevent the buildup. This idea was

applied to digital systems by Ghreichi and Farison [15]. The idea of decreasing the integral gain when the error is large can be found in Luo, Jackson and Hill [30] and Fukuda, Fujiyoshi, Arai and Matsuura [14]. Shahruz and Schwartz [38] developed a computer aided design technique for tuning nonlinear PI controllers. Izuno [22] designed integral gain as a function of desired speed.

Only a few analytical results are available for nonlinear PI and PID controllers. Seraji [35],[36],[37] used Popov criterion to obtain the range of the nonlinear gains that stabilize the linear systems. Huang [16] showed Lyapunov stability of a nonlinear PD controller for second-order stable linear systems. Armstrong, Neevel and Kusik [2] showed the stability of a nonlinear PID controller for linear systems by switching off the nonlinearity which contributed to the positive terms of the derivative of Lyapunov function. Xu, Ma and Hollerbach [43] showed Lyapunov stability for second-order robotic systems.

1.5 Overview of the Thesis

In Chapter 2, we describe single-input single-output minimum phase systems with a well-defined normal form. A brief review of ideal sliding mode control, continuous sliding mode control and Universal Integral Controllers is provided. We find that the input-to-state stability of the dynamics of the system on the sliding surface is the essential property for the analysis. To prevent the buildup in the integrator, we propose to place a nonlinearity that satisfies a sector condition before or after the integrator. The nonlinear integrator is driven by an augmented error, which is a weighted sum of the tracking error and its derivatives. Our analysis shows that the controller with nonlinear integration achieves regional and semiglobal regulation.

We compare the performance of the controllers for linear integrator, nonlinearity before integration and nonlinearity after integration schemes.

In Chapter 3, we investigate the use of nonlinear proportional and derivative gains. We consider a nonlinear gain of the form $k_i = k_i(e_i)$ where $v(e_i) = k_i(e_i)e_i$ satisfies a sector condition. The dynamics of the system on the sliding surface can be represented as a Lure system. Linear Matrix Inequalities are used to find the sector condition for the nonlinear gains, so that a Lyapunov function on the sliding surface can be obtained. Our analysis shows that if the LMI problem is feasible, then the controller, with nonlinear proportional, integral and derivative gains, will achieve regional and semiglobal regulation. The effect of nonlinear gains on the performance is investigated by simulation.

In Chapter 4, we consider systems with relative degree two. A Universal Integral Controller with nonlinear gains reduces to a PID controller with nonlinear proportional and integral gains. In Chapters 2 and 3, the augmented error is used to drive the integrator for systems with higher relative degree. For relative degree two systems, we also consider nonlinear integrators driven by the tracking error, which is the classical form of the nonlinear integration found in the literature. In Chapter 3, LMIs were used to find sector conditions for proportional and derivative gains. For systems with relative degree two, a Lyapunov function is obtained analytically. Our analysis shows that a PID controller with nonlinear gains, with the nonlinear integrator driven by either the augmented error or the tracking error, achieves regional and semiglobal regulation. By simulation, we investigate the effect of nonlinear gains on the performance of the controller.

Our findings and some remarks are summarized in Chapter 5.

Chapter 2

Universal Integral Controllers with Nonlinear Integral Gains

2.1 System Description

Consider the single-input single-output nonlinear system

$$\dot{x} = f(x,\theta) + g(x,\theta)u, \quad y = h(x,\theta)$$
 (2.1)

where $x \in R^n$ is the state, $u \in R$ is the control input, $y \in R$ is the measured output, and $\theta \in R^l$ represents unknown constant disturbances and parameters. The functions f, g and h depend continuously on θ , which belongs to a compact set $\Theta \in R^l$. We assume that for all $\theta \in \Theta$, f, g and h are sufficiently smooth on U_{θ} , an open connected subset of R^n that could depend on θ .

In this work, we consider input-output linearizable, minimum phase nonlinear systems, which have well-defined normal forms.

Assumption 1 The system (2.1) has a uniform relative degree $\rho \leq n$ for all

 $x \in U_{\theta}$ and $\theta \in \Theta$, i.e.,

$$L_g h(x,\theta) = L_g L_f h(x,\theta) = \cdots = L_g L_f^{\rho-2} h(x,\theta) = 0$$

$$|L_g L_f^{\rho-1} h(x,\theta)| \ge c_0 > 0$$
 (2.2)

where c_0 is independent of θ . Moreover, there exists a diffeomorphism

$$\begin{bmatrix} \eta \\ \xi \end{bmatrix} = T(x,\theta) \tag{2.3}$$

of U_{θ} onto its image that transforms (2.1) into the normal form

$$\dot{\eta} = q(\eta, \xi, \theta)$$
 $\dot{\xi}_i = \xi_{i+1}, \quad for \ 1 \le i \le \rho - 1$
 $\dot{\xi}_{\rho} = b(\eta, \xi, \theta) + a(\eta, \xi, \theta)u$
 $y = \xi_1$

$$(2.4)$$

Under the conditions given in Byrnes and Isidori [5, Proposition 3.2b, Corollary 5.6], Assumption 1 holds locally or globally when $\theta = \theta_0$ is known. Global conditions when $\dot{\eta} = q(\eta, \xi)$ is also given in [5, Corollary 5.7]. In our assumption, the mapping in (2.3) is a diffeomorphism from U_{θ} onto its image. Necessary and sufficient conditions for a mapping from U to V to be a diffeomorphism of U onto V is provided in Sandberg [34]. A mapping $M: U \to M(U)$ is a diffeomorphism of U onto its image if and only if $\det J_p \neq 0$ for all $p \in U$ and M is a proper map of U into M(U), where J_p is the Jacobian matrix of M at $p \in U$. The results that guarantee the existence of a diffeomorphism for a given U_{θ} is not available in the literature. For most systems satisfying the local conditions, a region over which the

normal form exists is determined in the process of transforming the system into the normal form. While the requirement of the existence of normal form uniformly in θ is more restrictive, there are many examples of physical systems where the normal form exists uniformly over a compact set of system parameters.

We consider the tracking problem where y(t) is to asymptotically track a reference signal r(t). The reference signal has the following properties:

- r and its derivatives up to the ρ th derivative are bounded and $r^{(\rho)}$ is piecewise continuous, for all $t \geq 0$;
- $\lim_{t\to\infty} r(t) = w$ and $\lim_{t\to\infty} r^{(i)}(t) = 0$ for $1 \le i \le \rho$.

Define $\nu(t)$ by $\nu=[r-w,r^{(1)},\cdots,r^{(\rho-1)}]^T$. By construction, $\nu(t)$ is bounded for all $t\geq 0$ and $\lim_{t\to\infty}\nu(t)=0$. Let $W\subset R$, $\Lambda\subset R^\rho$, and $\Gamma\subset R$ be compact sets such that $w(t)\in W$, $\nu(t)\in \Lambda$, and $r^{(\rho)}(t)\in \Gamma$ for all $t\geq 0$. Set $d=(w,\theta)$ and $D=W\times\Theta$.

Assumption 2 For each $d \in D$, a unique equilibrium point $\bar{x} = \bar{x}(d) \in U_{\theta}$ and a unique control $\bar{u} = \bar{u}(d)$ exist such that

$$0 = f(\bar{x}, \theta) + g(\bar{x}, \theta)\bar{u}(d), \quad w = h(\bar{x}, \theta)$$

With the change of variables (2.3), the equilibrium point $\bar{x}(d)$ maps into $(\bar{\eta}(d), \bar{\xi}(d))$, where $\bar{\xi}(d) = [w, 0, \dots, 0]^T$.

For the tracking problem, let

$$egin{bmatrix} z \ e \end{bmatrix} = egin{bmatrix} \eta - ar{\eta} \ \xi - ar{\xi} -
u \end{bmatrix}$$

and rewrite the system (2.4) as

$$\dot{z} = q_0(z, e + \nu, d)$$
 $\dot{e}_i = e_{i+1}, \quad \text{for } 1 \le i \le \rho - 1$
 $\dot{e}_\rho = b_0(z, e + \nu, d, r^{(\rho)}) + a_0(z, e + \nu, d)u$
 $y_m = e_1$
(2.5)

where y_m is the measured tracking error.

Assumption 3 There exists positive constants r_1 and r_2 , independent of d, such that for all $d \in D$ and $\nu \in \Lambda$,

$$||e|| < r_1$$
 and $||z|| < r_2 \Rightarrow x \in U_{\theta}$

Define the balls $\mathcal{E}=\{e\in R^{\rho}: ||e||< r_1\}$ and $\mathcal{Z}=\{z\in R^{n-\rho}: ||z||< r_2\}.$ Since Λ is compact, there exists $r_3\geq 0$ such that

$$||\nu|| \le r_3$$
 for all $\nu \in \Lambda$ (2.6)

Therefore, $||e + \nu|| < r_1 + r_3$ for all $e \in \mathcal{E}$ and $\nu \in \Lambda$.

Assumption 4 There exist a C^1 proper function $V_0: \mathbb{Z} \to R_+$, possibly dependent on d, and class K functions $\alpha_1, \alpha_2, \alpha_3: [0, r_2) \to R_+$ and $\gamma: [0, r_1 + r_3) \to R_+$, independent of d, such that

$$\alpha_1(||z||) \leq V_0(t, z, d) \leq \alpha_2(||z||)$$
 (2.7)

$$\frac{\partial V_0}{\partial t} + \frac{\partial V_0}{\partial z} q_0(z, e + \nu, d) \le -\alpha_3(||z||) \quad \forall \ ||z|| \ge \gamma(||e + \nu||) \tag{2.8}$$

for all $e \in \mathcal{E}$, $z \in \mathcal{Z}$, $\nu \in \Lambda$ and $d \in D$. Furthermore,

$$\gamma(r_3) < \alpha_2^{-1}(\alpha_1(r_2))$$
 (2.9)

Moreover, the equilibrium point z=0 of $\dot{z}=q_0(z,0,d)$ is exponentially stable uniformly in d, i.e., there exist positive constants α_0 , β_0 and r_0 , independent of d, such that

$$||z(t)|| \le \beta_0 e^{-\alpha_0 t} ||z(0)||, \ \forall \ ||z(0)|| \le r_0, \ \forall \ t \ge 0$$
 (2.10)

The system $\dot{z}=q_0(z,e+\mu,d)$ is said to be input-to-state stable, viewing $(e+\nu)$ as the input, if there are a class \mathcal{KL} function $\beta(\cdot)$ and a class \mathcal{K} function $\alpha(\cdot)$ such that for any initial state z(0) and any bounded input $e(t)+\nu(t)$, the solution z(t) exists for all $t\geq 0$ and satisfies

$$||z(t)|| \leq \beta(||x(0)||,t) + \alpha \left(\sup_{0 \leq \tau \leq t} ||e(t) + \nu(t)|| \right)$$
 (2.11)

It is said to be locally input-to-stable if there exist positive constants c_1 and c_2 such that the inequality (2.11) is satisfied for $||z(t_0)|| \le c_1$ and $\sup_{t \ge 0} ||e(t) + \nu(t)|| < c_2$ [40].

The inequalities (2.7) and (2.8) in Assumption 4 imply that, viewing $(e + \nu)$ as the input, the system $\dot{z} = q_0(z, e + \nu, d)$ is locally input-to-state state in the domain of interest.

2.2 Sliding Mode Control

Robust asymptotic tracking can be achieved by sliding mode control. A sliding surface is chosen such that asymptotic tracking is achieved when motion is restricted to the surface. Then, a discontinuous control is designed to render the surface attractive and guarantee that all trajectories will reach the surface in finite time. Assumption 4 ensures that the system is minimum-phase and allows us to concentrate on stabilizing the motion of the e_i variables. Therefore, it is typical to choose the surface s=0 such that s is a weighted sum of the tracking error and its derivatives:

$$s = \sum_{i=1}^{\rho-1} k_i e_i + e_\rho$$

where the positive constants k_1 to $k_{\rho-1}$ are chosen such that the roots of

$$\lambda^{\rho-1} + k_{\rho-1}\lambda^{\rho-2} + \dots + k_2\lambda + k_1 = 0 \tag{2.12}$$

have negative real parts. The dynamics on the surface s = 0 are described by

$$\dot{\zeta} = egin{bmatrix} 0 & 1 & 0 & \cdots & 0 \ 0 & 0 & 1 & \cdots & 0 \ dots & & dots \ 0 & 0 & 0 & \cdots & 1 \ -k_1 & -k_2 & -k_3 & \cdots & -k_{
ho-1} \end{bmatrix} \zeta \stackrel{ ext{def}}{=} A \zeta$$

where $\zeta = [e_1, \cdots, e_{\rho-1}]^T$ and A is Hurwitz. The variable s satisfies a first-order differential equation of the form

$$\dot{s} = \Delta(\cdot) + (L_g L_f^{\rho-1} h) s$$

where $\Delta(\cdot)$ is a continuous function of z, e, d, ν and $r^{(\rho)}$. The sliding mode control

$$u = -k\operatorname{sign}(L_gL_f^{\rho-1}h)\operatorname{sgn}(s)$$

where

$$\operatorname{sgn}(s) = \begin{cases} 1, & \text{for } s > 0 \\ -1, & \text{for } s < 0 \end{cases}$$

ensures that

$$s\dot{s} \leq -p_0|s|$$
, for all $s \neq 0$

provided the control gain k is sufficiently large to satisfy

$$\left|\frac{\Delta(\cdot)}{L_g L_f^{\rho-1} h}\right| \leq k - p_0$$

over the domain of interest.

While ideal sliding mode control achieves zero steady-state error, it is well known [28, pages 198, 215] that, in practice, sliding mode controllers suffer from chattering due to nonideal effects such as switching delays and unmodeled dynamics. One approach to avoid chattering is to approximate the signum nonlinearity sgn(s)

by the saturation nonlinearity $sat(s/\mu)$, where

$$\operatorname{sat}(p) = egin{cases} 1, & ext{for } p > 1 \ p, & ext{for } |p| \leq 1 \ -1, & ext{for } p < -1 \end{cases}$$

and μ is a positive constant. In the presence of nonvanishing disturbance, the continuous sliding mode controller

$$u=-k\, ext{sign}(L_gL_f^{
ho-1}h)\, ext{sat}igg(rac{s}{\mu}igg)$$

can guarantee only ultimate boundness with respect to a compact set, which can be made arbitrarily small by decreasing μ . However, a too small value of μ will again induce chattering due to nonideal effects [28, page 215].

Zero steady-state error can be achieved by including integral action in the controller. This was done in Khalil [27] by augmenting the system with an integrator driven by the tracking error: $\dot{\sigma} = e_1$. The sliding surface is taken as

$$s = k_0 \sigma + \sum_{i=1}^{\rho-1} k_i e_i + e_\rho = 0$$
 (2.13)

where the positive constants k_0 to $k_{\rho-1}$ are chosen such that the roots of

$$\lambda^{\rho}+k_{\rho-1}\lambda^{\rho-1}+\cdots+k_1\lambda+k_0=0$$

have negative real parts. The augmentation of the integrator creates a closed-loop equilibrium point where the tracking error is zero. Since $s\dot{s}<-p_0|s|$ for $|s|>\mu$, s

reaches the boundary layer $\{s \leq |\mu|\}$ in finite time. The dynamics of σ and ζ are described by

$$\dot{\zeta}_{a} = \begin{bmatrix}
0 & 1 & 0 & \cdots & 0 \\
0 & 0 & 1 & \cdots & 0 \\
\vdots & & & \vdots \\
0 & 0 & 0 & \cdots & 1 \\
-k_{0} & -k_{1} & -k_{2} & \cdots & -k_{\rho-1}
\end{bmatrix}
\dot{\zeta}_{a} + \begin{bmatrix}
0 \\
0 \\
\vdots \\
0 \\
1
\end{bmatrix}
s$$

$$(2.14)$$

where $\zeta_a = [\sigma, e_1, \cdots, e_{\rho-1}]^T$ and A_a is Hurwitz. The fact that $\dot{\zeta}_a = A_a \zeta_a + B_a s$ is input-to-state stable, viewing s as input, together with Assumption 4, ensures that the trajectory of the system enters a positively invariant set. Inside the set, the controller acts as a high-gain controller that stabilizes the closed-loop equilibrium point. The controller of [27] is called "Universal Integral Controller" because it works for a class of nonlinear systems that have the same relative degree and sign of the high-frequency gain $L_g L_f^{\rho-1} h$. Only bounds on the uncertain terms are needed to tune the controller parameters.

2.3 Design of Nonlinear Integral Gains

While integral control ensures asymptotic tracking, it has been observed that the buildup in the integrator can cause poor transient performance. Simulation results of a continuous sliding mode controller and a Universal Integral Controller for a field-controlled DC motor are shown in Figure 2.1. A field-controlled DC

motor, described in a normalized form by [28, page 30]

$$egin{aligned} v_f &= i_f + rac{di_f}{dt} \ v_a &= c_1 i_f \omega + c_2 rac{di_a}{dt} + i_a \ rac{d\omega}{dt} &= c_3 i_f i_a - c_4 \omega \end{aligned}$$

has relative degree two, viewing the field voltage v_f as input and the angular velocity ω as output. For simulation, we use the numerical data $c_1=0.8484$, $c_2=0.1$, $c_3=4.242$, $c_4=1.2$. The control parameters are chosen as k=1, $\mu=0.5$, $k_0=1.5$ and $k_1=5$ and the reference signal is r=0.9. While Universal Integral Controller achieves zero steady-state regulation error, the buildup in the linear integrator causes large overshoot and settling time.

To prevent the integrator buildup and improve the transient performance, we propose to use a nonlinearity. We consider two possible design choices, where a nonlinearity is placed before the integrator:

$$\dot{\sigma} = \psi(e_1), \quad s = \sigma + \sum_{i=1}^{\rho-1} k_i e_i + e_{\rho}$$

or after the integrator:

$$\dot{\sigma}=e_1,\quad s=\psi(\sigma)+\sum_{i=1}^{\rho-1}k_ie_i+e_{
ho}$$

We would like to choose $\psi(\cdot)$ as a locally Lipschitz function that belongs to a sector (c_1, c_2) for some positive constants c_1 and $c_2 > c_1$, i.e.,

$$c_1 p^2 \le p \psi(p) \le c_2 p^2 \tag{2.15}$$

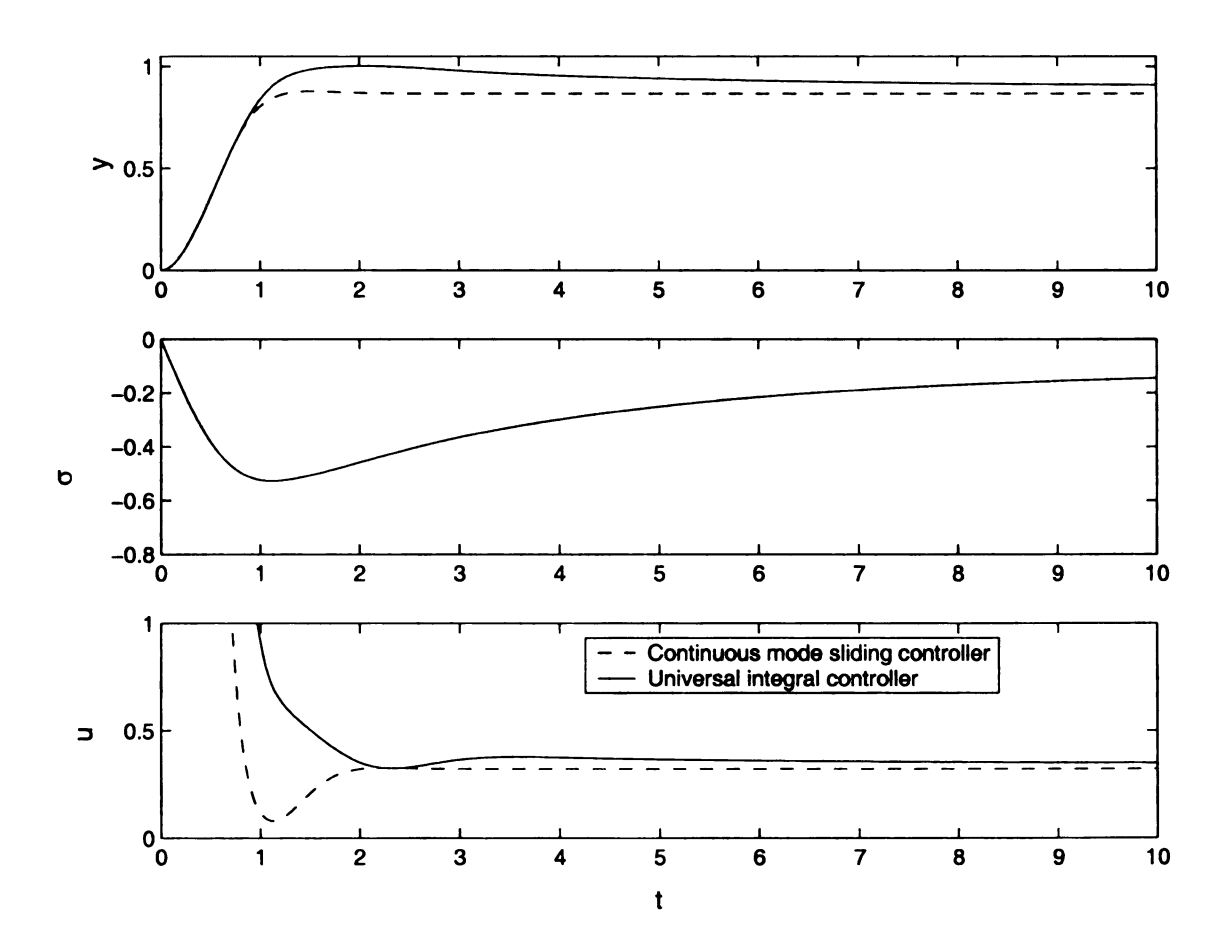


Figure 2.1: Simulation results of the continuous sliding mode controller and Universal Integral Controller for the field-controlled DC motor

The freedom in choosing the nonlinearity $\psi(\cdot)$ can be exploited to improve performance. For example, choosing $\psi(\cdot)$ to be small when $|e_1|$ is large reduces the effect of the integrator during the transient period. The presence of the nonlinearity $\psi(\cdot)$, however, complicates the dynamics of ζ_a . It is no longer true that the dynamics can be represented as a stable linear system driven by s, as in (2.14). The difficulties encountered in studying the stability of the system are discussed further in Appendix A where it is shown that such difficulties may be overcome if we use an augmented error, $e_a = \sum_{i=1}^{\rho-1} l_i e_i + e_{\rho}$. The two possible schemes are:

• a nonlinearity, driven by the augmented error, is placed before the integrator:

$$\dot{\sigma} = \psi(e_a), \quad s = \sigma + \sum_{i=1}^{\rho-1} k_i e_i + e_{\rho}$$
 (2.16)

• a nonlinearity is placed after the integrator, which is driven by the augmented error:

$$\dot{\sigma} = e_a, \quad s = \psi(\sigma) + \sum_{i=1}^{\rho-1} k_i e_i + e_{\rho}$$
 (2.17)

The foregoing integrators provide the desired integral action since, at steady state,

$$\dot{\sigma}=0 \Rightarrow (\psi(e_a)=0) \Rightarrow e_a=0 \Rightarrow e_1=0$$

due to the fact that e_2 to e_ρ are derivatives of e_1 . For the case of (2.16), the dynamics of the integrator have the form

$$\dot{\sigma} = \psi(s - \sigma + \sum_{i=1}^{\rho-1} l_i e_i - \sum_{i=1}^{\rho-1} k_i e_i)$$

and by choosing $l_i = k_i$ for $1 \le i \le \rho - 1$, we obtain

$$\dot{\sigma} = \psi(s - \sigma) \tag{2.18}$$

Similarly, for (2.17), with the same choice of l_i , the dynamics of σ are given by

$$\dot{\sigma} = s - \psi(\sigma) \tag{2.19}$$

For any $\psi(\cdot)$ in the sector (c_1, c_2) , the origin of $\dot{\sigma} = -\psi(\sigma)$ is asymptotically stable, and when $s \neq 0$ equations (2.18) and (2.19) are locally input-to-state stable viewing s as input. For the Nonlinearity Before Integration scheme, we choose the nonlinearity $\phi(\cdot)$ to satisfy the sector condition

$$c_1 p^2 \le p \psi(p) \le c_2 p^2$$
, for all $p \in \Omega$ (2.20)

where Ω is any compact set. When $|s| \leq c$, the solution σ of (2.18) is ultimately bounded with the ultimate bound $(1 + \delta)c$ where δ is a positive constant, i.e.,

$$|\sigma(t)| \leq (1+\delta)c$$
, for all $t \geq T$

for some $T \geq 0$. For the Nonlinearity After Integration scheme, the ultimate bound on $|\sigma|$ for (2.19), when $|s| \leq c$, is given by

$$|\sigma(t)| \leq rac{(1+\delta)c}{c_1}, \quad ext{for all } t \geq T$$

when we choose the nonlinearity $\psi(\cdot)$ to satisfy the sector condition

$$c_1 p^2 \le p \psi(p) \le c_2 p^2, \quad \text{for all } p \tag{2.21}$$

The dynamics of ζ are described by

$$\dot{\zeta} = A\zeta + B(s - \sigma)$$

and

$$\dot{\zeta} = A\zeta + B(s - \psi(\sigma))$$

respectively, and they are input-to-state stable since the roots of (2.12) have negative real parts; hence A is Hurwitz.

To design the output feedback controller, we estimate the state ζ using high-gain observer:

$$\dot{\hat{e}}_i = \hat{e}_{i+1} + (\beta_i/\epsilon^i)(e_1 - \hat{e}_1), \quad \text{for } 1 \le i \le \rho - 1
\dot{\hat{e}}_\rho = (\beta_\rho/\epsilon^\rho)(e_1 - \hat{e}_1)$$
(2.22)

where the positive constants β_1 to β_ρ are chosen such that the roots of

$$\lambda^{\rho} + \beta_1 \lambda^{\rho-1} + \dots + \beta_{\rho-1} \lambda + \beta_{\rho} = 0 \tag{2.23}$$

have negative real parts, while the positive constant ϵ is chosen to be small enough. To overcome the peaking phenomenon associated with high-gain observers, we want the right side of the $\dot{\sigma}$ equation to be a globally bounded function of of e_a [10]. This can be achieved by saturating e_a outside a compact set of interest. In particular, if L is greater than or equal to the maximum of $|e_a|$ over the domain of interest when

state feedback control is used, we can define the function $\mathcal L$ by

$$\mathcal{L}(p) = egin{cases} p, & ext{for } |p| \leq L \ L \operatorname{sgn}(p) & ext{for } |p| > L \end{cases}$$

and replace \hat{e}_a by $\mathcal{L}(\hat{e}_a)$. In the case when the nonlinearity is placed before the integrator, $\dot{\sigma}$ equation is given by

$$\dot{\sigma} = \psi(\mathcal{L}(\hat{e}_a))$$

We can combine $\psi(\cdot)$ and $\mathcal{L}(\cdot)$ in one nonlinearity defined by

$$c_1p^2 \leq p\psi(p) \leq c_2p^2, \quad ext{for } |p| \leq L$$

$$c_1L \leq |\psi(p)| \leq c_2L, \quad ext{for } |p| > L$$
 (2.25)

A nonlinearity satisfying (2.25) will lie in the shaded area of Figure 2.2. In summary, the Nonlinearity Before Integration scheme is described by

$$\hat{s} = \sigma + \hat{e}_a$$

$$\dot{\sigma} = \psi(\hat{e}_a) \qquad (2.26)$$

$$\hat{e}_a = k_1 e_1 + \sum_{i=2}^{\rho-1} k_i \hat{e}_i + \hat{e}_\rho$$

where $\psi(\cdot)$ satisfies (2.25). This scheme is shown in Figure 2.3(a). The Nonlinearity

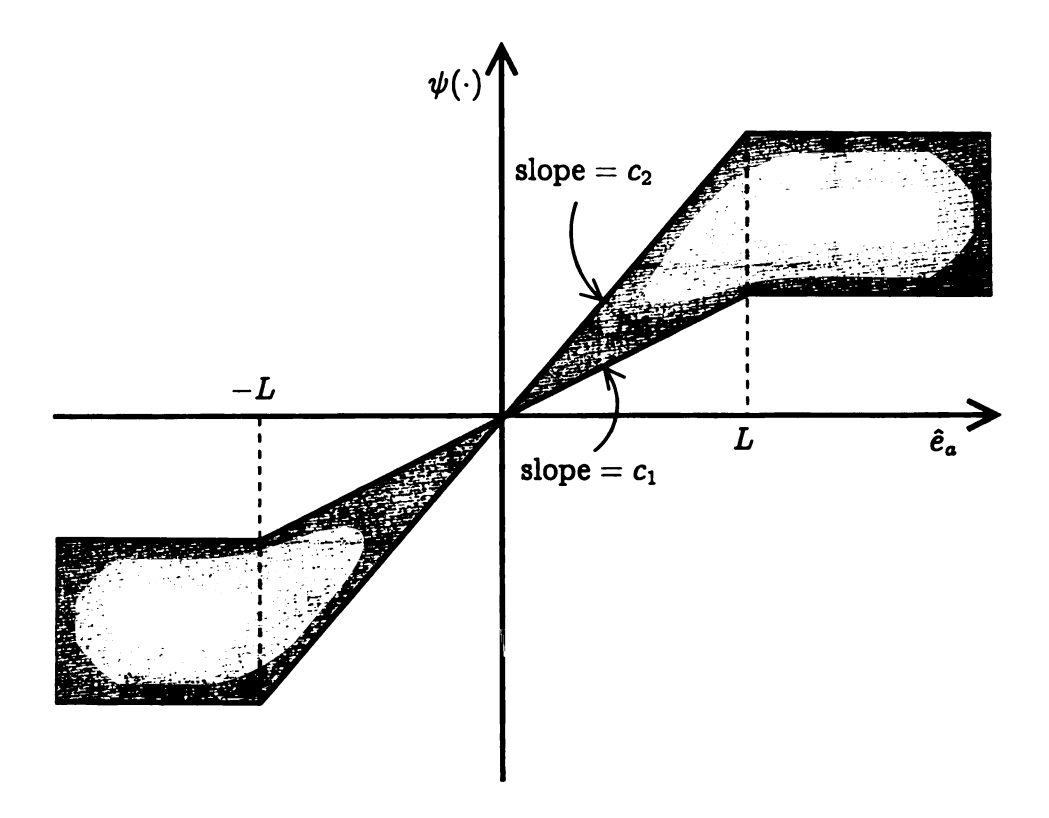


Figure 2.2: Nonlinearity $\psi(\hat{e}_a)$ for the Nonlinearity Before Integration scheme

After Integration scheme is described by

$$\hat{s} = \psi(\sigma) + \hat{e}_a$$

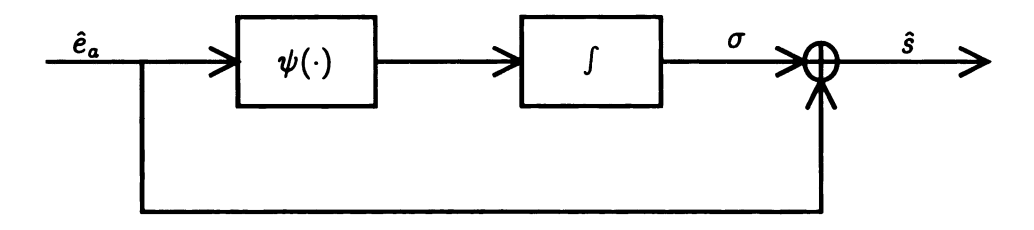
$$\dot{\sigma} = \mathcal{L}(\hat{e}_a)$$

$$\hat{e}_a = k_1 e_1 + \sum_{i=2}^{\rho-1} k_i \hat{e}_i + \hat{e}_\rho$$

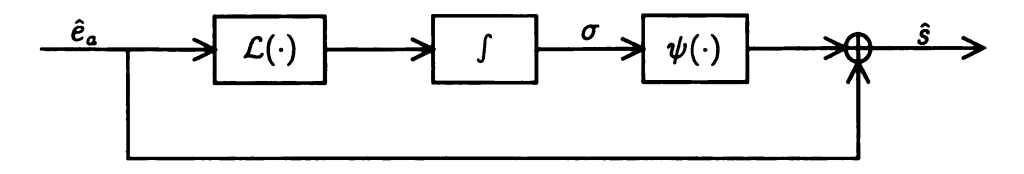
$$(2.27)$$

where $\psi(\cdot)$ satisfies the sector condition (2.21) and $\mathcal{L}(\cdot)$ is defined by (2.24). This scheme is shown in Figure 2.3(b).

To overcome chattering, we replace the signum nonlinearity $\operatorname{sgn}(s)$ by a continuous function $\phi(s/\mu)$. We do not limit ourselves to the choice of $\phi(p) = \operatorname{sat}(p)$ as in [27]. Instead, we allow any function $\phi(p)$ that is locally Lipschitz, odd, strictly



(a) Nonlinearity Before Integration



(b) Nonlinearity After Integration

Figure 2.3: Two possible schemes for nonlinear integrators

increasing for all |p|<1, increasing for all $|p|\geq 1$, $\phi(0)=0$, $\lim_{p\to\infty}\phi(p)=1$, and

$$(p_2-p_1)[\phi(p_2)-\phi(p_1)] \geq c_3(p_2-p_1)^2$$
, for $|p_1|,|p_2| \leq 1$ (2.28)

It follows that

$$|\phi(p)| \ge \phi(1) \ge c_3$$
, for $p \ge 1$ (2.29)

Typical examples are $\phi(p) = \operatorname{sat}(p)$, $\phi(p) = \operatorname{tanh}(p)$, $\phi(p) = (2/\pi) \arctan(\pi p/2)$, and $\phi(p) = p/(1+|p|)$. The continuous sliding mode control law is taken as

$$u = -k \operatorname{sign}(L_g L_f^{\rho-1} h) \phi\left(\frac{\hat{s}}{\mu}\right)$$
 (2.30)

with k_1 to $k_{\rho-1}$ and β_1 to β_{ρ} chosen such that (2.12) and (2.23) are Hurwitz, the remaining design parameters are the positive constants k, μ , and ϵ . The analysis of the next section will determine the conditions that should be satisfied by these constants.

2.4 Closed-loop Analysis

2.4.1 Nonlinearity before the integrator

For the integrator of the form (2.26), where a nonlinearity is placed before the integrator, the closed-loop system can be represented in the form

$$\dot{z} = q_0(z, e + \nu, d)$$
 $\dot{\zeta} = A\zeta + B(s - \sigma)$
 $\dot{\sigma} = \psi(s - N(\epsilon)\varphi - \sigma)$
 $\dot{s} = \Delta(\cdot) - k|a_0(\cdot)|\phi\left(\frac{s - N(\epsilon)\varphi}{\mu}\right)$
 $\epsilon\dot{\varphi} = A_f\varphi + \epsilon B_a\left[b_0(\cdot) - k|a_0(\cdot)|\phi\left(\frac{s - N(\epsilon)\varphi}{\mu}\right)\right]$

where

$$\Delta(z, e, \sigma, \nu, d, r^{(\rho)}) = \psi(s - N(\epsilon)\varphi - \sigma) + \sum_{i=1}^{\rho-1} k_i e_{i+1} + b_0(z, e + \nu, d, r^{(\rho)}) \quad (2.32)$$

$$egin{aligned} arphi = egin{bmatrix} arphi_1 \ dots \ \ dots \ \ dots \ dots \ \ dots \ dots \ dots \ \ d$$

and

$$N(\epsilon) = \begin{bmatrix} 0 & k_2 \epsilon^{\rho-2} & k_3 \epsilon^{\rho-3} & \cdots & k_{\rho-1} \epsilon & 1 \end{bmatrix}$$

With the parameter ϵ of the high-gain observer chosen sufficiently small, the closed-loop system has a singularly perturbed form where the scaled estimation error φ is the fast variable, and z, ζ , σ and s are slow variables. The matrices A and A_f are Hurwitz by design. Let $P=P^T>0$ be the solution of the Lyapunov equation

$$PA + A^TP = -I$$

and take $V(\zeta) = \zeta^T P \zeta$. Consider

$$\Omega_c \stackrel{\text{def}}{=} \{(z, e, \sigma) : |s| \le c, \ |\sigma| \le (1 + \delta)c, \ V(\zeta) \le c^2 \rho_1, \ V_0(t, z, d) \le \alpha_4(c\rho_2 + r_3)\}$$

where the positive constants c, δ , ρ_1 , ρ_2 and the class K function α_4 are to be specified. We require that our assumptions hold in the set Ω_c , i.e., $(z,e,\sigma)\in\Omega_c$ implies that $(z,e)\in\mathcal{Z}\times\mathcal{E}$. Since $e_{\rho}=s-\sigma-K\zeta$ where $K=[k_1,\cdots,k_{\rho-1}]$, the inequality

$$||e|| \le ||\zeta|| + |e_{\rho}| \le (1 + ||K||)||\zeta|| + |s| + |\sigma| \le c\rho_2 < r_1$$

should be satisfied, where

$$\rho_2 > (1 + ||K||) \sqrt{\frac{\rho_1}{\lambda_{\min}(P)}} + 2 + \delta$$
(2.33)

From inequality (2.7) we require that

$$||z|| \leq \alpha_1^{-1}(\alpha_4(c\rho_2+r_3)) < r_2$$

where the class K function α_4 is defined as $\alpha_4 \stackrel{\text{def}}{=} \alpha_2 \circ \gamma$, and from (2.9), α_4 satisfies the inequality $\alpha_4^{-1}(\alpha_1(r_2)) > r_3$. Thus, for any δ and ρ_1 , we can ensure that our assumptions are valid in the set Ω_c by choosing ρ_2 to satisfy (2.33) and then choosing c to satisfy

$$c\rho_2 \leq \min\{r_1, \alpha_4^{-1}(\alpha_1(r_2)) - r_3\}$$
 (2.34)

From (2.9), α_4 satisfies the inequality $\alpha_4^{-1}(\alpha_1(r_2)) > r_3$.

We start the analysis by showing that, for sufficiently small ϵ , the scaled estimation error φ will decay to a level of the order of $O(\epsilon)$ after some arbitrarily small time. Let $P_f = P_f^T > 0$ be the solution of the Lyapunov equation

$$P_f A_f + A_f^T P_f = -I$$

and take $V_f(\varphi) = \varphi^T P_f \varphi$. The derivative of V_f satisfies the inequality:

$$|\dot{V}_f \leq -rac{1}{\epsilon}||arphi||^2 + 2||arphi|||P_fB_a||\gamma_1(c)$$

where

$$\gamma_1(c) = \max\{|b_0(z, e + \nu, d)| + k|a_0(z, e + \nu, d)|\}$$

and the maximum is taken over all $(z,e,\sigma)\in\Omega_c$, $d\in D$, $\nu\in\Lambda$ and $r^{(\rho)}\in\Gamma$. In arriving at the preceding inequality, we have used the property $|\phi(p)|\leq 1$ for all p. For $V_f\geq\epsilon^2\rho_3$, where $\rho_3=16||P_fB_a||^2||P_f||\gamma_1^2(c)$, we have $\dot{V}_f<-\frac{1}{2\epsilon}||\varphi||^2$. Therefore, $\varphi(t)$ enters the set

$$\Sigma_{\epsilon} \stackrel{\mathrm{def}}{=} \left\{ arphi \in R^{
ho} : V_f(arphi) \leq \epsilon^2
ho_3
ight\}$$

within a finite time interval $[0,T_0(\epsilon)]$, and stays therein. We note that $\lim_{\epsilon\to 0}T_0(\epsilon)=0$.

Since the right side of the slow equation of (2.31) is bounded uniformly in ϵ , for all $(z(0), e(0), \sigma(0)) \in \Omega_b$ with b < c, there is a finite time T_1 , independent of ϵ , such that $(z(t), e(t), \sigma(t)) \in \Omega_c$ for $0 \le t \le T_1$. By choosing ϵ small enough, we can ensure that $T_0(\epsilon) < T_1$. Therefore, there exists $\epsilon_1^* > 0$ such that, for each $0 < \epsilon < \epsilon_1^*$, every trajectory, starting at a bounded $\hat{e}(0)$ with $(e(0), z(0), \sigma(0)) \in \Omega_b$, enters the set $\Omega_c \times \Sigma_{\epsilon}$ in finite time.

In the next step, we establish that the set $\Omega_c \times \Sigma_\epsilon$ is positively invariant. Let us choose μ small enough that $\mu(1+\delta) < c$ and ϵ small enough that $|N(\epsilon)\varphi| < \delta\mu$. For $\mu(1+\delta) \leq |s| \leq c$, we have

$$\operatorname{sign}\left(\phi\left(\frac{s-N(\epsilon)\varphi}{\mu}\right)\right)=\operatorname{sign}\left(\frac{s-N(\epsilon)\varphi}{\mu}\right)=\operatorname{sign}(s)$$

Using (2.29), we obtain

$$s\dot{s} \leq |\Delta(\cdot)||s| - c_3k|a_0||s| \tag{2.35}$$

We require the controller gain k to be large enough to overcome the disturbance. If k is designed to satisfy the condition

$$k \ge c_4 + \gamma_2(c) \tag{2.36}$$

where $c_4 > 0$ and

$$\gamma_2(c) = \max \left| rac{\Delta(z,e,\sigma,
u,d,r^{(
ho)})}{c_3 a_0(z,e+
u,d)}
ight|$$

with the maximum taken over all $(z,e,\sigma)\in\Omega_c,\ d\in D,\ \nu\in\Lambda$ and $r^{(\rho)}\in\Gamma,$ then $s\dot{s}<0$ on the boundary |s|=c. On the boundary $|\sigma|=(1+\delta)c$, since

 $|s - N(\epsilon)\varphi| < c + \delta\mu < |\sigma|$ and

$$\operatorname{sign}(\psi(s-N(\epsilon)\varphi-\sigma))=-\operatorname{sign}(\sigma)$$

we have

$$\sigma\dot{\sigma} = \sigma\psi(s - N(\epsilon)\varphi - \sigma) < 0$$

Due to the inequality

$$\dot{V} \le -||\zeta||^2 + 2||\zeta||||PB||(|s| + |\sigma|)
\le -||\zeta||^2 + 2||\zeta||||PB||c(2 + \delta)$$
(2.37)

we can show that $\dot{V} < 0$ on the boundary $V = c^2 \rho_1$, by choosing ρ_1 to satisfy

$$\rho_1 > 4||PB||^2||P||(2+\delta)^2 \tag{2.38}$$

From (2.7) and (2.8) and by defining the class \mathcal{K} function α_4 as $\alpha_4 \stackrel{\text{def}}{=} \alpha_2 \circ \gamma$, we can verify that $\dot{V_0} < 0$ on the boundary $V_0 = \alpha_4(c\rho_2 + r_3)$. Therefore, there exists $\mu_1^* > 0$ and $\epsilon_2^*(\mu) > 0$ such that for each $0 < \mu < \mu_1^*$ and $0 < \epsilon < \epsilon_2^*$, the set $\Omega_c \times \Sigma_\epsilon$ is positively invariant.

Next, we show that s(t) enters the boundary layer $\{|s| \leq \mu_1\}$ in finite time, where μ_1 is chosen as $\mu_1 = \mu(1-\delta)$ to ensure that $|(s-N(\epsilon)\varphi)/\mu| \leq 1$ inside the boundary layer. Let us consider s in the set $\{\mu_1 \leq |s| \leq c\}$ and choose δ to satisfy

$$\delta < \frac{c_4}{4k} < \frac{1}{4} \tag{2.39}$$

Notice that $\operatorname{sign}(\phi(\hat{s}/\mu)) = \operatorname{sign}(\hat{s}/\mu) = \operatorname{sign}(s)$, since $|N(\epsilon)\varphi| < \delta\mu < \mu(1-\delta) \le |s|$. If $|\hat{s}| \ge \mu$, inequality (2.35) holds and from (2.2) and (2.36) we can show that

$$s\dot{s} \leq -c_0c_3c_4|s|$$

On the other hand, if $|\hat{s}| < \mu$, using (2.28), (2.36), (2.39), and the fact that

$$egin{split} s\phiigg(rac{\hat{s}}{\mu}igg) &= s\, ext{sgn}(s)\left|\phiigg(rac{\hat{s}}{\mu}igg)
ight| \ &\geq rac{c_3}{\mu}|s||s-N(\epsilon)arphi| \geq rac{c_3}{\mu}|s|(\mu-2\delta\mu) \end{split}$$

we can show that

$$|s\dot{s}| \leq |\Delta(\cdot)||s| - k|a_0|soldsymbol{\phi}igg(rac{\hat{s}}{\mu}igg) \leq -rac{c_0c_3c_4}{2}|s|$$

The latter bound on $s\dot{s}$ holds for both cases and we conclude that s(t) reaches the boundary layer $\{|s| \leq \mu_1\}$ in finite time and stays therein. After s(t) reaches $\{|s| \leq \mu_1\}$, consider σ in the set $\{(1+\delta)\mu \leq |\sigma| \leq (1+\delta)c\}$. Since $|s-N(\epsilon)\varphi| < \mu < |\sigma|$, we have

$$ext{sign}(\psi(s-N(\epsilon)arphi-\sigma)) = ext{sign}(s-N(\epsilon)arphi-\sigma) = - ext{sign}(\sigma)$$
 $|s-N(\epsilon)arphi-\sigma| \geq |\sigma|-|s-N(\epsilon)arphi| > \delta\mu$

Moreover,

$$|s-N(\epsilon)arphi-\sigma| \leq \mu(1-\delta) + \mu\delta + (1+\delta)c = \mu + (1+\delta)c$$
 $|\psi(s-N(\epsilon)arphi-\sigma)| \geq ar{c}_1|s-N(\epsilon)arphi-\sigma|$

where

$$ar{c}_1 = c_1 \min\left\{1, rac{L}{\mu + (1+\delta)c}
ight\} > 0$$

Using these facts, we show that

$$\sigma\dot{\sigma} = \sigma\, ext{sign}(\psi(s-N(\epsilon)arphi-\sigma))|\psi(s-N(\epsilon)arphi-\sigma)| < -ar{c}_1\delta\mu|\sigma|$$

Thus, $\sigma(t)$ reaches the set $\{|\sigma| \leq (1+\delta)\mu\}$ in finite time and stays therein. Then, from inequality (2.37), we show that $\dot{V} \leq -\frac{1}{2}||\zeta||^2$ for $V(\zeta) \geq \mu^2 \rho_1$, by choosing ρ_1 to satisfy

$$\rho_1 \ge 64||PB||^2||P|| \tag{2.40}$$

Inequality (2.40) implies (2.38) and from now on, we fix ρ_1 as chosen above. Thus e(t) reaches the set $\{V(\zeta) \leq \mu^2 \rho_1\}$ in finite time and stays therein. From the inequality $||e|| \leq ||\zeta|| + |e_{\rho}|$, it follows that $||e|| < \mu \rho_2$. Since $\lim_{t \to \infty} \nu(t) = 0$, we have $||\nu(t)|| \leq \mu$ in finite time. Using $||e(t)|| + ||\nu(t)|| < \mu \rho_2 + \mu$ together with (2.7) and (2.8), we can show that for $V_0(z) \geq \alpha_4(\mu \rho_2 + \mu)$, $\dot{V_0} \leq -\alpha_3(||z||)$. Thus, z(t) reaches the set $\{V_0 \leq \alpha_4(\mu \rho_2 + \mu)\}$ in finite time and stays therein. Therefore, every trajectory in $\Omega_c \times \Sigma_\epsilon$ enters $\Psi_\mu \times \Sigma_\epsilon$ in finite time and stays therein, where the set Ψ_μ is defined as

$$\Psi_{\mu} \stackrel{\text{def}}{=} \{(z,e,\sigma) : |s| \leq \mu_1, \ |\sigma| \leq (1+\delta)\mu, \ V(\zeta) \leq \mu^2 \rho_1, \ V_0(t,z,d) \leq \alpha_4 (\mu \rho_2 + \mu)\}$$

Finally, we show that every trajectory in $\Psi_{\mu} \times \Sigma_{\epsilon}$ approaches an equilibrium point as time tends to infinity. When $\nu = 0$ and $r^{(\rho)} = 0$, the closed-loop system (2.31)

has a unique equilibrium point $(z = 0, e = 0, \sigma = \bar{\sigma}, \varphi = 0)$, where

$$ar{\sigma} = -\operatorname{sign}(L_g L_f^{
ho-1} h) \mu \phi^{-1}igg(rac{ar{u}(d)}{k}igg)$$

and $\phi^{-1}(p)$ is defined for all $|p| \leq 1$. Let $\bar{s} = \bar{\sigma}$ be the corresponding equilibrium value of s.

Inequality (2.10) of Assumption 4 implies that in some neighborhood of z=0 there is a Lyapunov function such that

$$||\lambda_1||z||^2 \le V_1 \le |\lambda_2||z||^2, \quad \frac{\partial V_1}{\partial z}q_0(z,0,d) \le -\lambda_3||z||^2, \quad \left\|\frac{\partial V_1}{\partial z}\right\| \le |\lambda_4||z|| \qquad (2.41)$$

for some positive constants λ_1 to λ_4 , independent of d. Consider

$$V_2 = V_1(z,d) + \lambda_5 \zeta^T P \zeta + \frac{1}{2} \lambda_6 \tilde{\sigma}^2 + \frac{1}{2} \tilde{s}^2 + \varphi^T P_f \varphi$$
 (2.42)

where λ_5 and λ_6 are positive constants to be chosen, $\tilde{\sigma} = \sigma - \bar{\sigma}$ and $\tilde{s} = s - \bar{s}$. The derivative of V_2 can be arranged in the form

$$\dot{V}_2 \leq -\chi^T P_2 \chi + (\lambda_7 ||\varphi|| + \lambda_8 |\tilde{s}| + \lambda_9 ||z||) ||\nu(t)|| + (\lambda_{10} ||\varphi|| + \lambda_{11} |\tilde{s}|) |r^{(\rho)}(t)| \quad (2.43)$$

where $\chi = [||z|| \ ||\zeta|| \ |\tilde{\sigma}| \ |\tilde{s}| \ ||\varphi||]^T$ and λ_7 to λ_{11} are positive constants. The sym-

metric matrix P_2 has the form

$$P_2 = egin{bmatrix} \lambda_3 & -\lambda_{12} & -\lambda_{13} & -\lambda_{14} & -\lambda_{15} \ \lambda_5 & -\lambda_{23} & -\lambda_{24} & -\lambda_{25} \ \lambda_6 c_1 & -\lambda_{34} & -\lambda_{35} \ & & rac{c_0 c_3 k}{\mu} - \lambda_{44} & -\lambda_{45} \ & & rac{1}{\epsilon} - \lambda_{55} \end{bmatrix}$$

where the nonnegative constants λ_{15} to λ_{55} are independent of ϵ , λ_{14} to λ_{34} are independent of μ , λ_{13} and λ_{23} are independent of λ_{6} , and λ_{12} is independent of λ_{5} . In arriving at (2.43), we have used (2.28). The detailed derivation of (2.43) and expressions for all the constants in P_{2} are given in Appendix B. By choosing λ_{5} large enough then λ_{6} large enough then μ small enough then ϵ small enough, we can make P_{2} positive definite. Since $\lim_{\epsilon \to \infty} \nu(t) = 0$ and $\lim_{\epsilon \to \infty} r^{(\rho)}(t) = 0$, there exists a ball \mathcal{B} around the equilibrium point, whose radius is independent of μ and ϵ , such that every trajectory in \mathcal{B} approaches the equilibrium point as time tends to infinity. We can choose μ and ϵ sufficiently small to ensure that $\Psi_{\mu} \times \Sigma_{\epsilon} \subset \mathcal{B}$. Hence, there exists $\mu_{2}^{*} > 0$ and $\epsilon_{3}^{*}(\mu) > 0$ such that for each $0 < \mu < \mu_{2}^{*}$ and $0 < \epsilon < \epsilon_{3}^{*}$, all trajectories in $\Psi_{\mu} \times \Sigma_{\epsilon}$ approaches the equilibrium point as time tends to infinity.

Our conclusions are summarized in the following theorem.

Theorem 1 Suppose that Assumptions 1 to 4 are satisfied and consider the closed-loop system (2.31) formed of the system (2.5), the observer (2.22), the nonlinear integrator (2.26) with nonlinearity satisfying the condition (2.25), and the output feedback controller (2.30). Suppose $\hat{e}(0)$ is bounded and

 $(z(0), e(0), \sigma(0)) \in \Omega_b$, where b < c and c satisfies (2.34) and (2.36). Then, there exists $\mu^* > 0$ and for each $0 < \mu < \mu^*$, there exists $\epsilon^* = \epsilon^*(\mu) > 0$ such that for each $0 < \mu < \mu^*$ and $0 < \epsilon < \epsilon^*(\mu)$, all the state variables of the closed-loop system are bounded and $\lim_{t\to\infty} e(t) = 0$.

The estimate of the region of attraction Ω_b is limited by two factors: the region of the validity of our assumptions shown (2.34), and the requirement (2.36) on the controller gain k. If all the assumptions hold globally and k can be chosen arbitrarily large, the controller can achieve semiglobal regulation.

Corollary 1 Suppose that Assumptions 1 to 4 are satisfied globally, i.e., $U_{\theta} = R^n$, α_1 , α_2 , α_3 and γ are class \mathcal{K}_{∞} functions. For any given compact sets $\mathcal{N} \in R^{n+1}$ and $\mathcal{M} \in R^{\rho}$, choose c > b > 0 and $r_3 \geq 0$ such that $\mathcal{N} \in \Omega_b$, and choose k large enough to satisfy (2.36). Then, there exists $\mu^* > 0$ and for each $0 < \mu < \mu^*$, there exists $\epsilon^* = \epsilon^*(\mu) > 0$ such that for each $0 < \mu < \mu^*$ and $0 < \epsilon < \epsilon^*(\mu)$, and for all initial states $(z(0), e(0), \sigma(0)) \in \mathcal{N}$ and $\hat{e}(0) \in \mathcal{M}$, the state variables of the closed-loop system (2.31) are bounded and $\lim_{t \to \infty} e(t) = 0$.

The control parameter k can be chosen as the maximum magnitude of the actuator. The choice of small μ is limited by the system and controller delays, since too small μ can cause chattering problem. Since high-gain observer is an approximate differentiator, in practice, the choice of small ϵ is limited by measurement noise and unmodeled high-frequency dynamics of the senor.

2.4.2 Nonlinearity after the integrator

For the integrator of the form (2.27), where a nonlinearity is placed after the integrator, the closed-loop system can be represented in a form similar to (2.31):

$$\dot{z} = q_0(z, e + \nu, d)$$
 $\dot{\zeta} = A\zeta + B(s - \psi(\sigma))$
 $\dot{\sigma} = \mathcal{L}(s - N(\epsilon)\varphi - \psi(\sigma))$
 $\dot{s} = \Delta(\cdot) - k|a_0(\cdot)|\phi\left(\frac{s - N(\epsilon)\varphi}{\mu}\right)$
 $\epsilon\dot{\varphi} = A_f\varphi + \epsilon B_a\left[b_0(\cdot) - k|a_0(\cdot)|\phi\left(\frac{s - N(\epsilon)\varphi}{\mu}\right)\right]$

where

$$\Delta(z,e,\sigma,
u,d,r^{(
ho)})=\psi'(\sigma)(s-N(\epsilon)arphi-\psi(\sigma))+\sum_{i=1}^{
ho-1}k_ie_{i+1}+b_0(z,e+
u,d,r^{(
ho)})$$

Only the dynamics of ζ and σ and the disturbance term $\Delta(\cdot)$ are different from (2.31) and the analysis follows the same steps. We will mention only the parts that are different from the previous section. Consider

$$\Omega_c \stackrel{\mathrm{def}}{=} \{(z,e,\sigma): |s| \leq c, \; |\sigma| \leq rac{(1+\delta)}{c_1}c, \; V(\zeta) \leq c^2
ho_1, \; V_0(t,z,d) \leq lpha_4(c
ho_2+r_3)\}$$

We can show that our assumptions are valid in the set Ω_c by choosing ρ_2 to satisfy (2.45) and then choosing c to satisfy (2.34), since from $e_{\rho} = s - \psi(\sigma) - K\zeta$, the inequality

$$||e|| \le ||\zeta|| + |e_{\rho}| \le (1 + ||K||)||\zeta|| + |s| + |\psi(\sigma)| \le c\rho_2 < r_1$$

should be satisfied, where

$$ho_2 > (1 + ||K||) \sqrt{\frac{
ho_1}{\lambda_{\min}(P)}} + 1 + \frac{c_2}{c_1} (1 + \delta)$$
 (2.45)

As in the previous section, we show that every trajectory, starting at a bounded $\hat{e}(0)$ with $(e(0), z(0), \sigma(0)) \in \Omega_b$, with b < c, enters the set $\Omega_c \times \Sigma_\epsilon$ in finite time. After showing that $s\dot{s} < 0$ on the boundary |s| = c, consider σ on the boundary $|\sigma| = (1 + \delta)c/c_1$. We have

$$\sigma\dot{\sigma} = \sigma\mathcal{L}(s - N(\epsilon)\varphi - \psi(\sigma)) < 0$$

since

$$|s-N(\epsilon)arphi| < c + \delta\mu < c_1 |\sigma| < |\psi(\sigma)|$$
 $ext{sign}(\mathcal{L}(s-N(\epsilon)arphi - \psi(\sigma))) = ext{sign}(s-N(\epsilon)arphi - \psi(\sigma)) = - ext{sign}(\sigma)$

Due to the inequality

$$\dot{V} \leq -||\zeta||^2 + 2||\zeta||||PB||(|s| + |\psi(\sigma)|)
\leq -||\zeta||^2 + 2||\zeta||||PB||c\left(1 + \frac{c_2}{c_1}(1+\delta)\right)$$
(2.46)

we can show that $\dot{V} < 0$ on the boundary $V = c^2 \rho_1$, by choosing ρ_1 to satisfy

$$\rho_1 > 4||PB||^2||P|| \left(1 + \frac{c_2}{c_1}(1+\delta)\right)^2$$
(2.47)

Then we verify that $\dot{V}_0 < 0$ on the boundary $V_0 = \alpha_4(c\rho_2 + r_3)$. Therefore, the set $\Omega_c \times \Sigma_{\epsilon}$ is positively invariant.

After showing that s(t) reaches $\{|s| \leq \mu_1\}$ in finite time, consider σ in the set $\{(1+\delta)\mu/c_1 \leq |\sigma| \leq (1+\delta)c/c_1\}$. Since $|s-N(\epsilon)\varphi| < \mu < c_1|\sigma| < |\psi(\sigma)|$, we have

$$\operatorname{sign}(\mathcal{L}(s-N(\epsilon)arphi-\psi(\sigma))) = \operatorname{sign}(s-N(\epsilon)arphi-\psi(\sigma)) = -\operatorname{sign}(\sigma) \ |s-N(\epsilon)arphi-\psi(\sigma)| \geq c_1|\sigma|-|s-N(\epsilon)arphi| > \delta\mu$$

Moreover,

$$|s-N(\epsilon)arphi-\psi(\sigma)| \leq \mu(1-\delta) + \mu\delta + rac{c_2}{c_1}(1+\delta)c = \mu + rac{c_2}{c_1}(1+\delta)c$$
 $|\mathcal{L}(s-N(\epsilon)arphi-\sigma)| \geq ar{c}_1|s-N(\epsilon)arphi-\sigma|$

where

$$ar{c}_1=\min\left\{1,rac{L}{\mu+rac{c_2}{c_1}(1+\delta)c}
ight\}>0$$

Thus,

$$\sigma\dot{\sigma} = \sigma\, ext{sign}(\mathcal{L}(s-N(\epsilon)arphi-\psi(\sigma)))|\mathcal{L}(s-N(\epsilon)arphi-\psi(\sigma))| < -ar{c}_1\delta\mu|\sigma|$$

Therefore, $\sigma(t)$ reaches the set $\{|\sigma| \leq (1+\delta)\mu/c_1\}$ in finite time and stays therein. Then, from inequality (2.46), $\dot{V} \leq -\frac{1}{2}||\zeta||^2$ for $V(\zeta) \geq \mu^2 \rho_1$ if

$$\rho_1 > 16||PB||^2||P|| \left(1 + \frac{c_2}{c_1}(1+\delta)\right)^2$$
(2.48)

By choosing ρ_1 to satisfy Inequality (2.48), which implies (2.47), e(t) reaches the set $\{V(\zeta) \leq \mu^2 \rho_1\}$ in finite time and stays therein. Thus, z(t) reaches the set

 $\{V_0 \leq \alpha_4(\mu\rho_2 + \mu)\}$ in finite time and stays therein. Therefore, every trajectory in $\Omega_c \times \Sigma_\epsilon$ enters $\Psi_\mu \times \Sigma_\epsilon$ in finite time and stays therein, where the set Ψ_μ is defined as

$$\Psi_{\mu} \stackrel{\mathrm{def}}{=} \{(z,e,\sigma) : |s| \leq \mu_1, \ |\sigma| \leq \frac{(1+\delta)}{c_1} \mu, \ V(\zeta) \leq \mu^2 \rho_1, \ V_0(t,z,d) \leq \alpha_4 (\mu \rho_2 + \mu) \}$$

When $\nu=0$ and $r^{(\rho)}=0$, the closed-loop system (2.44) has a unique equilibrium point $(z=0,e=0,\sigma=\bar{\sigma},\varphi=0)$, where

$$ar{\sigma} = \psi^{-1}(ar{s}) = -\operatorname{sign}(L_g L_f^{
ho-1} h) \psi^{-1} \left(\mu \phi^{-1} \left(rac{ar{u}(d)}{k}
ight)
ight)$$

provided $\psi^{-1}(\cdot)$ exists in the neighborhood of \bar{s} . Considering the composite Lyapunov function of the form (2.42), we can show that all trajectories in $\Psi_{\mu} \times \Sigma_{\epsilon}$ approaches this equilibrium point as time tends to infinity.

Our analysis shows that the sector condition (2.15) is not sufficient to guarantee asymptotic tracking of Universal Integral Controller with nonlinear integral gain (2.27). The nonlinearity $\psi(\cdot)$ should be invertible in the neighborhood of \bar{s} . In practice, due to unknown system dynamics and disturbances, we cannot predict \bar{s} , thus the nonlinearity should be designed such that

$$\psi^{-1}(p)$$
 exists for $0 \le p \le \mu$ (2.49)

Notice that the sets Ω_c and Ψ_{μ} are dependent on the sector condition (c_1, c_2) . The conditions for ρ_1 and ρ_2 , in (2.48) and (2.45), include the term c_2/c_1 , and the bound of σ is proportional to $1/c_1$.

The following theorem summarizes the conclusion of our analysis.

Theorem 2 Suppose that Assumptions 1 to 4 are satisfied and consider the closed-loop system formed of the system (2.5), the observer (2.22), the nonlinear integrator (2.27), with nonlinearity satisfying the conditions (2.21) and (2.49), and the output feedback controller (2.30). Suppose $\hat{e}(0)$ is bounded and $(z(0), e(0), \sigma(0)) \in \Omega_b$, where b < c, the size of Ω_b depends on the sector condition (2.21) and c satisfies (2.34) and (2.36). Then, there exists $\mu^* > 0$ and for each $0 < \mu < \mu^*$, there exists $\epsilon^* = \epsilon^*(\mu) > 0$ such that for each $0 < \mu < \mu^*$ and $0 < \epsilon < \epsilon^*(\mu)$, all the state variables of the closed-loop system (2.44) are bounded and $\lim_{t\to\infty} e(t) = 0$.

When the controller gain k can be chosen arbitrarily large, the controller achieves semiglobal regulation.

Corollary 2 Suppose that Assumptions 1 to 4 are satisfied globally, i.e., $U_{\theta} = R^n$, α_1 , α_2 , α_3 and γ are class \mathcal{K}_{∞} functions, and k can be chosen arbitrarily large. For any given compact sets $\mathcal{N} \in R^{n+1}$ and $\mathcal{M} \in R^{\rho}$, choose c > b > 0 and $r_3 \geq 0$ such that $\mathcal{N} \in \Omega_b$, and choose k large enough to satisfy (2.36). Then, there exists $\mu^* > 0$ and for each $0 < \mu < \mu^*$, there exists $\epsilon^* = \epsilon^*(\mu) > 0$ such that for each $0 < \mu < \mu^*$ and $0 < \epsilon < \epsilon^*(\mu)$, and for all initial states $(z(0), e(0), \sigma(0)) \in \mathcal{N}$ and $\hat{e}(0) \in \mathcal{M}$, the state variables of the closed-loop system (2.44) are bounded and $\lim_{t \to \infty} e(t) = 0$.

2.5 Simulation Results

Example 1: In Figure 2.4, the simulation results for the field-controlled DC motor is shown. We use the same parameters as the simulation of Figure 2.1, and take $\mathcal{L}(\cdot)$ with L=5. The tracking error, integrator output and control effort are shown

for controllers with linear integral gain and the following nonlinear integral gains:

$$\dot{\sigma} = \psi_1(\hat{e}_a), \quad \hat{s} = \sigma + \hat{e}_a \tag{2.50}$$

$$\dot{\sigma} = \mathcal{L}(\hat{e}_a), \quad \hat{s} = \psi_2(\sigma) + \hat{e}_a \tag{2.51}$$

We use the nonlinearities shown in Figure 2.5. The buildup in the linear integrator causes overshoot and large settling time. The transient performance of the nonlinear integrator (2.50), where the nonlinearity is placed before the integrator, shows no overshoot and smallest settling time. The nonlinearity $\psi_1(\cdot)$ is designed so that the gain is small when the augmented error is large to prevent the buildup in the integrator during the reaching phase. It behaves similar to a PD controller until it reaches the boundary layer; then during the sliding phase the integrator drives the tracking error to zero. The transient performance of the controller with the nonlinear integrator (2.51), where the nonlinearity is placed after the integrator, shows better settling time compared to the linear integrator, but it does not improve the overshoot. To satisfy the conditions (2.21) and (2.49), we choose $\psi_2(\cdot)$ as a monotonically increasing function, which restricts the freedom of choosing a nonlinearity that reduces the effect of integration on the control input during the transient period.

Example 2: The advantage of the Nonlinearity Before Integration Scheme is demonstrated for the motion on a horizontal surface with friction and disturbance.

$$\ddot{y}+0.1\dot{y}^2=u-1$$

The control gains are chosen as $\mu=0.5, k=2.5, k_0=0.98, k_1=1.4$ and L=5.

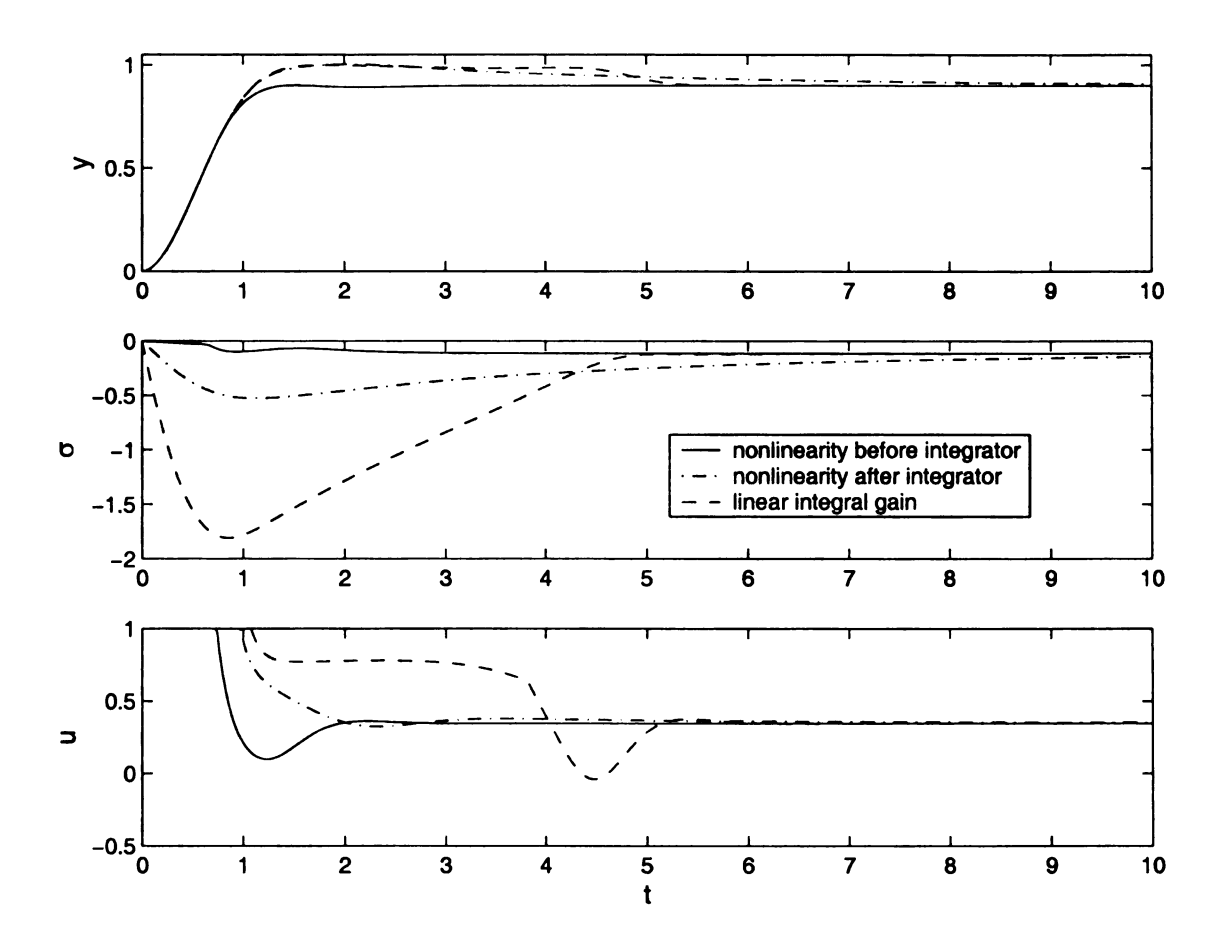


Figure 2.4: Simulation results of Universal Integral Controllers with nonlinear integrators for the field-controlled DC motor

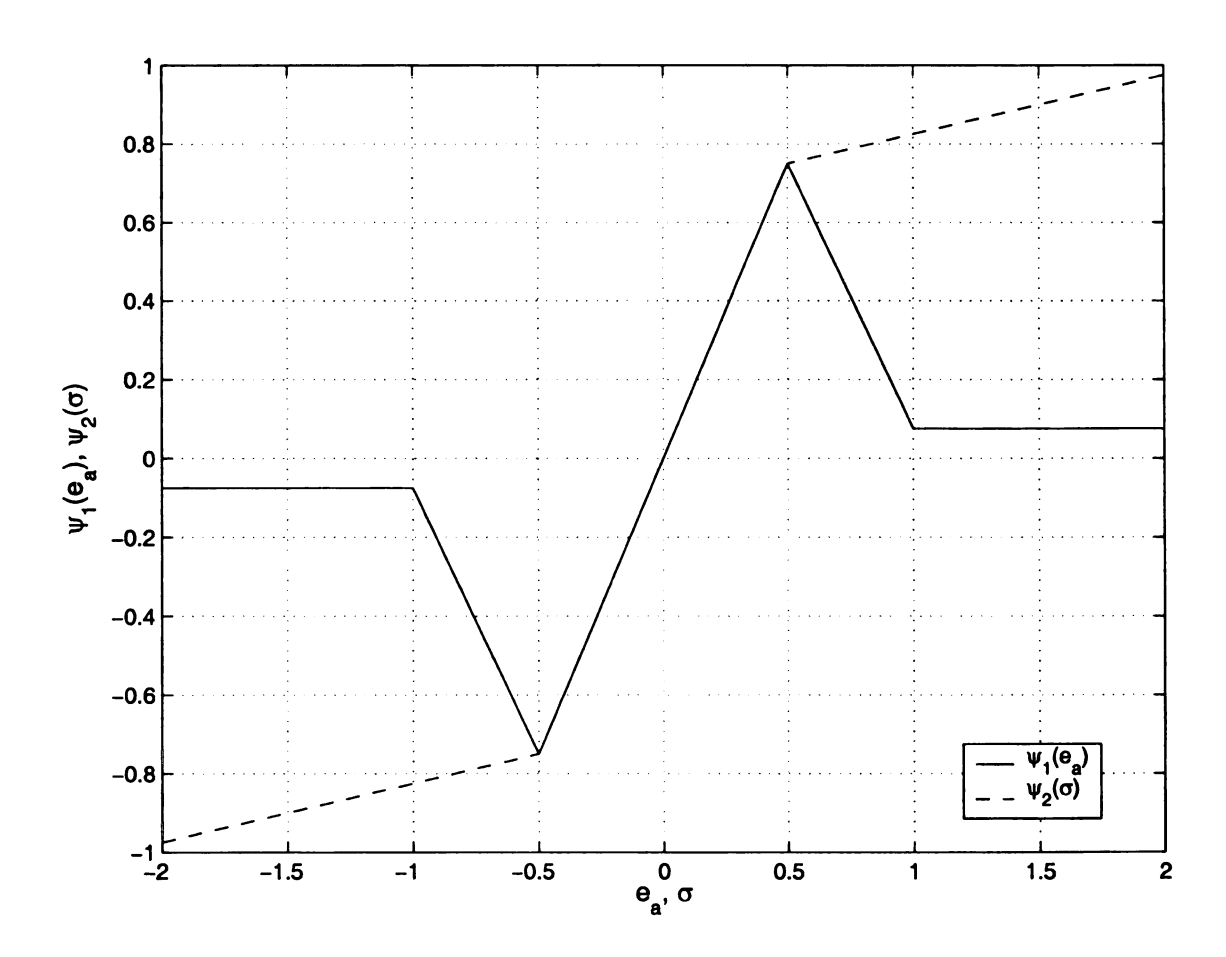


Figure 2.5: Nonlinearities $\psi_1(e_a)$ and $\psi_2(\sigma)$ for the simulation of the field-controlled DC motor

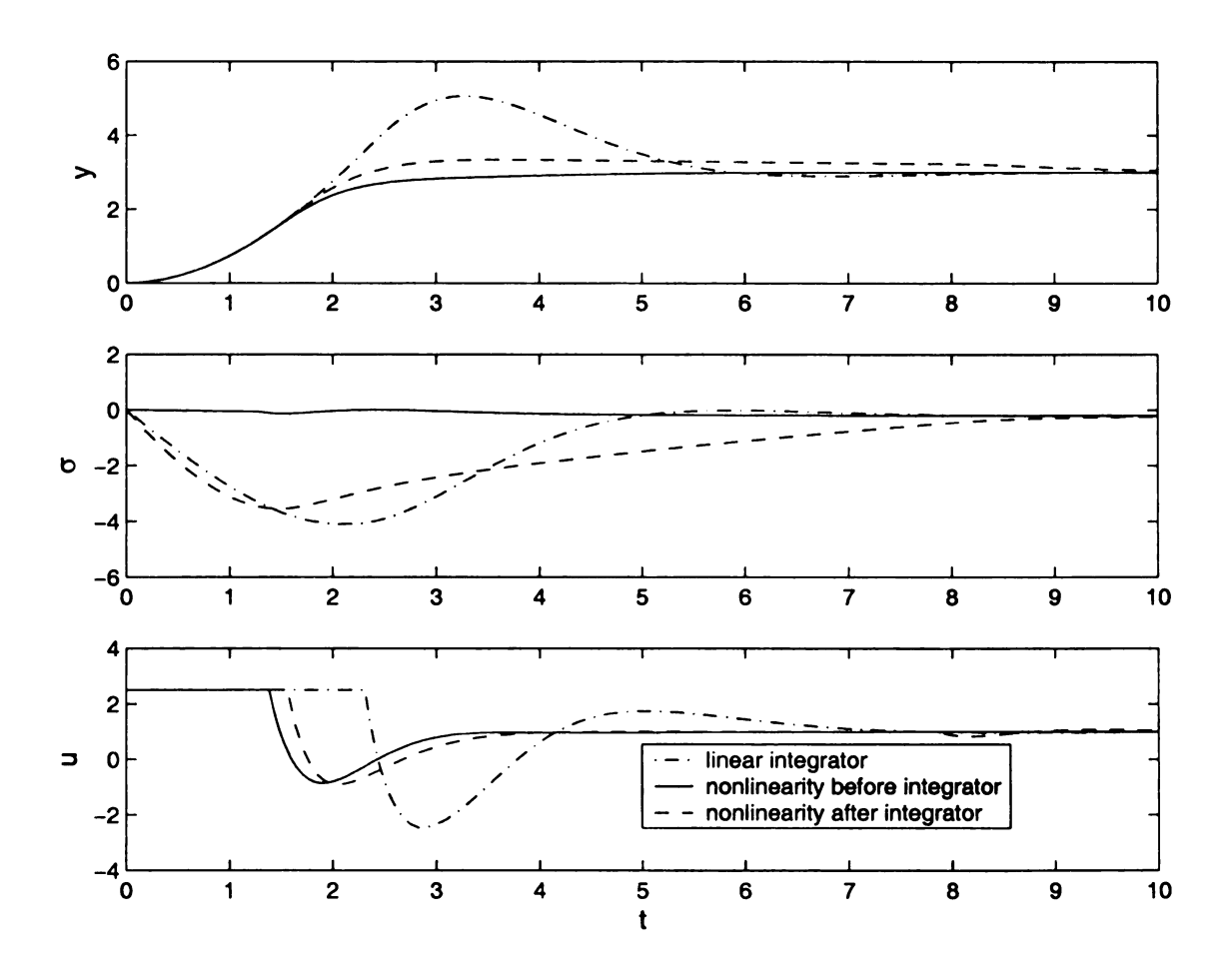


Figure 2.6: Simulation results of motion on a horizontal surface

We use the nonlinearities shown in Figure 2.5. The simulation results are shown in Figure 2.6. The Nonlinearity Before Integration scheme maintain the integrator output small and shows better performance than the Nonlinearity After Integration scheme. The settling time for the Nonlinear After Integration Scheme is increased by 100%. The buildup in the linear integrator causes 68% overshoot.

Example 3: A magnetic suspension system, where a ball of magnetic material is suspended by an electromagnet whose current is controlled by the ball position, is described by [28, page 31]

$$egin{align} m\ddot{y}&=-k\dot{y}+mg+F(y,i) & F(y,i)&=-rac{L_0i^2}{2a(1+y/a)^2} \ v&=\dot{\phi}+Ri, \quad \phi=L(y)i & L(y)&=L_1+rac{L_0}{1+y/a} \ \end{array}$$

With the vertical position of the ball y as output and voltage v of a voltage source which controls the electromagnet as input, the system has relative degree three. For simulations, we use m=0.01 kg, k=0.001 N/m/sec, g=9.81m/sec², a=0.05 m, $L_0=0.01$ H, $L_1=0.02$ H and $R=10\Omega$. The controller gain is chosen as $\mu=0.05$, k=40, $k_0=1$, $k_1=2$, $k_2=2$ and L=0.5 for nonlinear integration. Simulation results for controllers with linear integration $\dot{\sigma}=e_1$ and nonlinear integration $\dot{\sigma}=\psi(e_a)$, with $\psi(\cdot)$ designed as in Figure 2.8, are shown in Figure 2.7.

While controllers with nonlinear integration improves transient performance, the augmented error e_a is small and the nonlinear integration is operating in the linear region: $\dot{\sigma}=e_a$. This suggests that we may gain the benefits of the nonlinear integrator if we simply drive the linear integrator by the augmented error. This is indeed the case since the input-to-state stable dynamics of the integrator, $\dot{\sigma}=s-\sigma$ keeps the integrator output small when s reaches the boundary layer fast. Linear

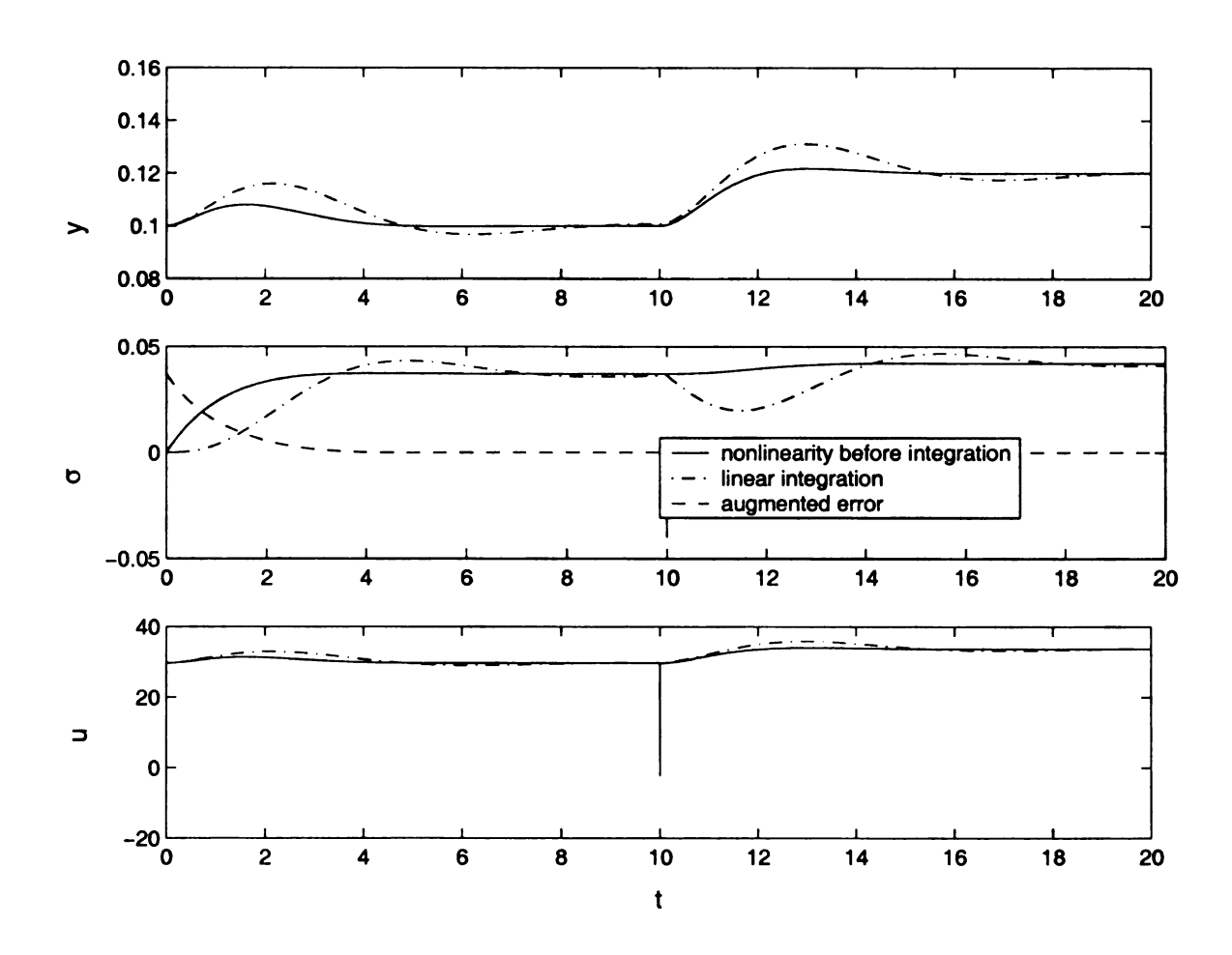


Figure 2.7: Simulation results of the magnetic suspension system

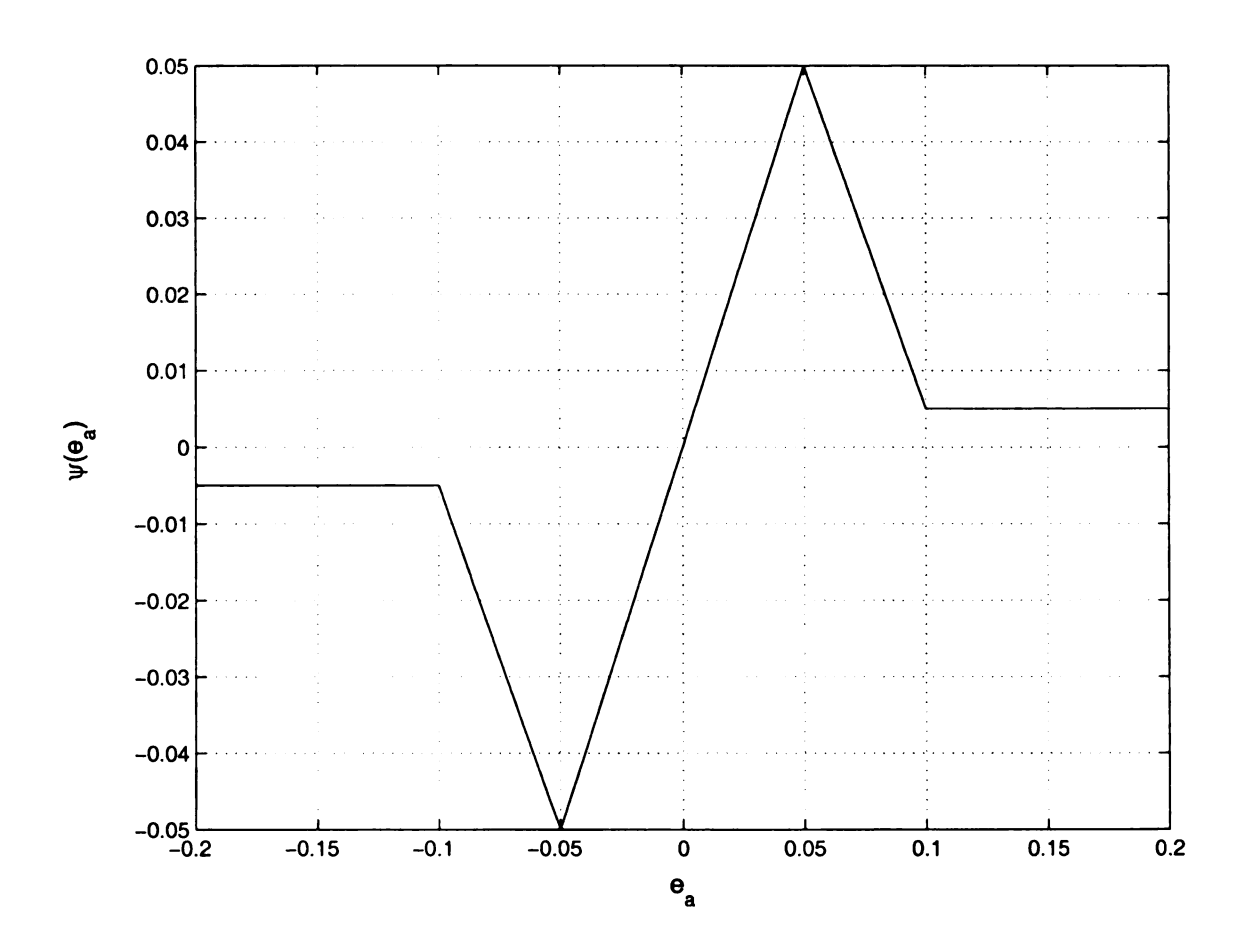


Figure 2.8: Nonlinearity $\psi(e_a)$ for the simulation of the magnetic suspension system

integrators driven by the augmented error, $\dot{\sigma} = e_a$, can be used to prevent integrator buildup if the maximum control level k is large enough to force s to reach the boundary layer fast.

2.6 Conclusions

We designed Universal Integral Controllers with nonlinear integrators driven by the augmented error. We considered two possible schemes: Nonlinearity Before Integration and Nonlinearity After Integration. Our analysis shows that the controller achieves regional and semiglobal regulation. Simulation results show that the Nonlinearity Before Integration scheme prevents the integrator buildup and achieves better transient performance than the Nonlinearity After Integration scheme and the linear integrator, when the maximum permissible control level k is not large enough to ensure fast reaching phase. In the case of fast reaching phase, the benefit of using a nonlinearity may not be significant, but driving the linear integrator by the augmented error rather than the tracking error may still improve the transient performance.

Appendix A Stability of Nonlinear Integrators

Consider the case

$$\dot{\sigma} = \psi(e_1), \quad s = \sigma + \sum_{i=1}^{\rho-1} k_i e_i + e_{
ho}$$

On the surface s=0,

$$e_{\rho} = -\sigma - \sum_{i=1}^{\rho-1} k_i e_i$$

and the system can be represented by the feedback connection of Figure 2.9 with

$$G(s) = \frac{1}{s(s^{\rho-1} + k_{\rho-1}s^{\rho-2} + \cdots + k_1)}$$

The transfer function G(s) has all poles in the left half plane, except a simple pole at the origin. Application of the Popov criterion [28, Exercise 7.8] shows that the feedback connection will be absolutely stable for ψ in the sector (0, k] if we can choose a positive constant η such that

$$\frac{1}{k} + \text{Re}[(1+j\omega\eta)G(j\omega)] > 0, \quad \forall \ \omega$$

For this inequality to hold with arbitrarily large k, we need the Nyquist plot of

$$(1+\eta s)G(s)=rac{(1+\eta s)}{s(s^{
ho-1}+k_{
ho-1}s^{
ho-2}+\cdots+k_1)}$$

to lie in the right-half plane, which is possible only if $(1+\eta s)G(s)$ has relative degree zero or one. This will be the case if $\rho=1$ or $\rho=2$. For $\rho\geq 3$, $(1+\eta s)G(s)$ will have relative degree higher than one and its Nyquist plot must cross in the left-half plane. To overcome this difficulty we can use $\dot{\sigma}=\psi(e_a)$ instead of $\dot{\sigma}=\psi(e_1)$, where

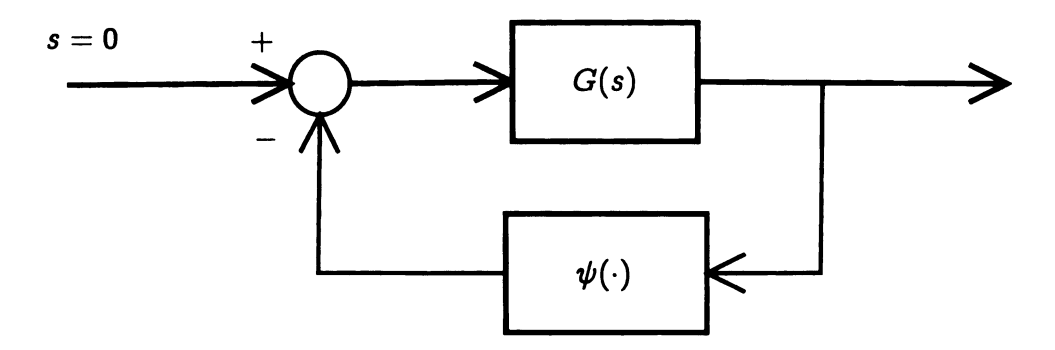


Figure 2.9: Nonlinearity before integrator when s = 0

 $e_a = \sum_{i=1}^{\rho-1} l_i e_i + e_{\rho}$. In this case the system, on the sliding surface s = 0, will be represented by the feedback connection of Figure 2.9 with

$$G(s) = rac{1}{s} \left[rac{(l_{
ho-1} - k_{
ho-1}) s^{
ho-2} + \cdots + (l_1 - k_1)}{s^{
ho-1} + k_{
ho-1} s^{
ho-2} + \cdots + k_1} + 1
ight]$$

so that the transfer function $(1 + \eta s)G(s)$ will have relative degree zero. In fact, the choice

$$l_i = k_i$$
, for $1 \le i \le \rho - 1$

yields G(s) = 1/s and for any $\eta > 0$, the Nyquist plot of $(1 + \eta s)/s$ will be in the right half plane.

Appendix B Derivation of (2.43)

The derivative of V_2 of (2.42) is given by

$$\dot{V}_{2} = \frac{\partial V_{1}}{\partial z} q_{0}(z, e + \nu, d)
- \lambda_{5} ||\zeta||^{2} + 2\lambda_{5} \zeta^{T} P B(s - \sigma)
+ \lambda_{6} \tilde{\sigma} \psi(s - N(\epsilon)\varphi - \sigma)
+ \tilde{s} \left[\psi(s - N(\epsilon)\varphi - \sigma) + \sum_{i=1}^{\rho-1} k_{i} e_{i+1} + b_{0}(\cdot) - k|a_{0}|(\cdot)\phi \left(\frac{s - N(\epsilon)\varphi}{\mu} \right) \right]
- \frac{1}{\epsilon} ||\varphi||^{2} + 2\varphi^{T} P_{f} B_{a} \left[b_{0}(\cdot) - k|a_{0}|(\cdot)\phi \left(\frac{s - N(\epsilon)\varphi}{\mu} \right) \right]$$
(2.52)

We arrange (2.52) in a quadratic form of $\chi = [||z|| \ ||\zeta|| \ |\tilde{\sigma}| \ |\tilde{s}| \ ||\varphi||]^T$. From (2.42), we have

$$egin{aligned} rac{\partial V_1}{\partial z}q_0(z,e+
u,d) &= rac{\partial V_1}{\partial z}q_0(z,0,d) + rac{\partial V_1}{\partial z}[q_0(z,e+
u,d) - q_0(z,0,d)] \ &\leq -\lambda_3||z||^2 + \lambda_4 L_q||z||(||e|| + ||
u||)) \end{aligned}$$

where L_q is a Lipschitz constant of $q_0(\cdot)$. Since

$$||e|| = ||s - \sigma - K\zeta|| = ||\tilde{s} - \tilde{\sigma} - K\zeta|| \le ||K|| ||\zeta|| + |\tilde{s}| + |\tilde{\sigma}|$$

where $K=[k_1,\cdots,k_{\rho-1}]$, the first term of (2.52) satisfies

$$\frac{\partial V_1}{\partial z} q_0(z, e + \nu, d) \le -\lambda_3 ||z||^2 + \lambda_4 L_q ||z|| (||K|| ||\zeta|| + |\tilde{\sigma}| + |\tilde{s}| + ||\nu||)$$
 (2.53)

The following inequality is satisfied for the second term of (2.52).

$$-\lambda_5||\zeta||^2+2\lambda_5\zeta^TPB(s-\sigma)<-\lambda_5||\zeta||^2+2\lambda_5||PB||||\zeta||(|\tilde{s}|+|\tilde{\sigma}|)$$
 (2.54)

We choose μ small enough that

$$L \geq (2+\delta)\mu > |s-N(\epsilon)\varphi-\sigma|$$

then $c_1p^2 \leq p\psi(p) \leq c_2p^2$ and the third term of (2.52) is arranged in the form

$$\lambda_{6}\tilde{\sigma}\psi(s-N(\epsilon)\varphi-\sigma)$$

$$=\lambda_{6}\tilde{\sigma}\psi(\tilde{s}-N(\epsilon)\varphi-\tilde{\sigma})$$

$$=-\lambda_{6}(\tilde{s}-N(\epsilon)\varphi-\tilde{\sigma})\psi(\tilde{s}-N(\epsilon)\varphi-\tilde{\sigma})+\lambda_{6}(\tilde{s}-N(\epsilon)\varphi)\psi(\tilde{s}-N(\epsilon)\varphi-\tilde{\sigma})$$

$$\leq -\lambda_{6}c_{1}(\tilde{s}-N(\epsilon)\varphi-\tilde{\sigma})^{2}+\lambda_{6}c_{2}|\tilde{s}-N(\epsilon)\varphi||\tilde{s}-N(\epsilon)\varphi-\tilde{\sigma}|$$

$$\leq -\lambda_{6}c_{1}\tilde{\sigma}^{2}+\lambda_{6}(c_{2}-c_{1})\tilde{s}^{2}+\lambda_{6}(c_{2}-c_{1})||N(\epsilon)||^{2}\varphi^{2}+\lambda_{6}(2c_{1}+c_{2})|\tilde{s}||\tilde{\sigma}|$$

$$+\lambda_{6}(2c_{1}+c_{2})||N(\epsilon)||||\varphi|||\tilde{\sigma}|+2\lambda_{6}(c_{1}+c_{2})||N(\epsilon)||||\varphi|||\tilde{s}| \qquad (2.55)$$

Consider the fourth term of (2.52) and divide it into three parts. The first part satisfies the inequality

$$\tilde{s}\psi(s-N(\epsilon)\varphi-\sigma) = \tilde{s}\psi(\tilde{s}-N(\epsilon)\varphi-\tilde{\sigma})$$

$$\leq c_2|\tilde{s}|(|\tilde{s}|+||N(\epsilon)||||\varphi||+|\tilde{\sigma}|) \tag{2.56}$$

The second part can be rewritten as

$$\tilde{s} \sum_{i=1}^{\rho-1} k_i e_{i+1} = \tilde{s} \left[\sum_{i=1}^{\rho-2} k_i e_{i+1} + k_{\rho-1} e_{\rho} \right] \\
= \tilde{s} \left[\sum_{i=1}^{\rho-2} k_i e_{i+1} + k_{\rho-1} (s - \sigma - K\zeta) \right] \\
\leq \tilde{s} (||K_1|| ||\zeta|| + k_{\rho-1} |\tilde{s}| + k_{\rho-1} |\tilde{\sigma}|)$$
(2.57)

where $K_1 = [-k_{\rho-1}k_1, k_1 - k_{\rho-1}k_2, \cdots, k_{\rho-2} - k_{\rho-1}^2]$. Since

$$ar{u}(d) = -k \operatorname{sign}(L_g L_f^{
ho-1} h) \phi\left(rac{ar{s}}{\mu}
ight)$$

we can arrange the remaining part of the fourth term of (2.52) as

$$b_{0}(z, e + \nu, d, r^{\rho}) - k|a_{0}(z, e + \nu, d)|\phi\left(\frac{s - N(\epsilon)\varphi}{\mu}\right)$$

$$= b_{0}(z, e + \nu, d, r^{\rho}) - b_{0}(0, 0, d, 0) + b_{0}(0, 0, d, 0) + a_{0}(0, 0, d)\bar{u}(d)$$

$$+ k|a_{0}(0, 0, d)|\phi\left(\frac{\bar{s}}{\mu}\right) - k|a_{0}(0, 0, d)|\phi\left(\frac{\bar{s} + \bar{s} - N(\epsilon)\varphi}{\mu}\right)$$

$$+ k|a_{0}(0, 0, d)|\phi\left(\frac{s - N(\epsilon)\varphi}{\mu}\right) - k|a_{0}(z, e + \nu, d)|\phi\left(\frac{s - N(\epsilon)\varphi}{\mu}\right)$$
(2.58)

Recalling that at equilibrium,

$$b_0(0,0,d,0) + a_0(0,0,d)\bar{u}(d) = 0$$

and inside the boundary layer Ψ_{μ} ,

$$\phi\left(\frac{s-N(\epsilon)\varphi}{\mu}\right)\leq 1$$

we have

$$\tilde{s} \left[b_{0}(z, e + \nu, d, r^{\rho}) - k |a_{0}(z, e + \nu, d)| \phi \left(\frac{s - N(\epsilon) \varphi}{\mu} \right) \right] \\
\leq |\tilde{s}| \left[L_{b}(||z|| + ||e|| + ||\nu|| + |r^{\rho}|) + k L_{a}(||z|| + ||e|| + ||\nu||) \right] \\
+ \tilde{s} \left[k |a_{0}(0, 0, d)| \phi \left(\frac{\bar{s}}{\mu} \right) - k |a_{0}(0, 0, d)| \phi \left(\frac{\bar{s} + \bar{s} - N(\epsilon) \varphi}{\mu} \right) \right]$$
(2.59)

where L_a and L_b are Lipschitz constants of $a_0(\cdot)$ and $b_0(\cdot)$, respectively. Moreover, using property (2.29) of $\phi(\cdot)$, namely

$$(p_1-p_2)(\phi(p_1)-\phi(p_2)) \geq c_3(p_1-p_2)^2$$

and the minimum c_0 of $a_0(\cdot)$, as in (2.2),

$$\tilde{s}\left[k|a_{0}(0,0,d)|\phi\left(\frac{\bar{s}}{\mu}\right)-k|a_{0}(0,0,d)|\phi\left(\frac{\tilde{s}+\bar{s}-N(\epsilon)\varphi}{\mu}\right)\right] \\
=-k|a_{0}(0,0,d)|(\tilde{s}-N(\epsilon)\varphi+N(\epsilon)\varphi)\left[\phi\left(\frac{\tilde{s}+\bar{s}-N(\epsilon)\varphi}{\mu}\right)-\phi\left(\frac{\bar{s}}{\mu}\right)\right] \\
\leq -\frac{c_{3}k}{\mu}|a_{0}(0,0,d)|(\tilde{s}-N(\epsilon)\varphi)^{2}+\frac{kL_{\phi}}{\mu}|a_{0}(0,0,d)||N(\epsilon)\varphi||\tilde{s}-N(\epsilon)\varphi| \\
\leq -\frac{c_{0}c_{3}k}{\mu}(\tilde{s}-N(\epsilon)\varphi)^{2}+\frac{kL_{\phi}}{\mu}|a_{0}(0,0,d)||N(\epsilon)|||\varphi||(|\tilde{s}|+||N(\epsilon)||||\varphi||) \tag{2.60}$$

where L_{ϕ} is the Lipschitz constant of $\phi(\cdot)$. From (2.58), the last term of (2.52) satisfies

$$-\frac{1}{\epsilon}||\varphi||^{2} + 2\varphi^{T}P_{f}B_{a}\left[b_{0}(\cdot) - k|a_{0}|(\cdot)\phi\left(\frac{s - N(\epsilon)\varphi}{\mu}\right)\right]$$

$$\leq -\frac{1}{\epsilon}||\varphi||^{2} + 2||\varphi||||P_{f}B_{a}||\left[L_{b}(||z|| + ||e|| + ||\nu|| + |r^{\rho}|) + kL_{a}(||z|| + ||e|| + ||\nu||)\right]$$

$$+ 2||\varphi||||P_{f}B_{a}||\left[\frac{kL_{\phi}}{\mu}|a_{0}(0, 0, d)|(|\tilde{s}| + ||N(\epsilon)||||\varphi||)\right]$$
(2.61)

We choose ϵ small enough that $||N(\epsilon)|| \leq N_1$ for some positive constant $N_1 > 1$. From (2.53) to (2.57) and (2.59) to (2.61), we set

$$\begin{split} \lambda_{12} &= \frac{1}{2} (\lambda_4 L_q || K ||) \\ \lambda_{13} &= \frac{1}{2} (\lambda_4 L_q) \\ \lambda_{23} &= \lambda_5 || PB || \\ \lambda_{14} &= \frac{1}{2} (\lambda_4 L_q + L_b + k L_a) \\ \lambda_{24} &= \frac{1}{2} [2 \lambda_5 || PB || + || K_1 || + || K || (L_b + k L_a)] \\ \lambda_{34} &= \frac{1}{2} [\lambda_6 (2 c_1 + c_2) + c_2 + k_{\rho-1} + L_b + k L_a] \\ \lambda_{44} &= \lambda_6 (c_2 - c_1) + c_2 + k_{\rho-1} + L_b + k L_a \\ \lambda_{15} &= || P_f B_a || (L_b + k L_a) \\ \lambda_{25} &= || P_f B_a || || K || (L_b + k L_a) \\ \lambda_{35} &= \frac{1}{2} [\lambda_6 (2 c_1 + c_2) N_1 + 2 || P_f B_a || (L_b + k L_a)] \\ \lambda_{45} &= \frac{1}{2} \left[c_2 N_1 + 2 \lambda_6 (c_1 + c_2) N_1 + \frac{2 c_0 c_3 k N_1}{\mu} + \frac{k L_{\phi} |a_0(0, 0, d)| N_1}{\mu} + 2 || P_f B_a || \left(L_b + k L_a + \frac{k L_{\phi} |a_0(0, 0, d)|}{\mu} \right) \right] \\ \lambda_{55} &= \lambda_6 (c_2 - c_1) N_1^2 + \frac{k L_{\phi} |a_0(0, 0, d)| N_1^2}{\mu} + \frac{2 k || P_f B_a || L_{\phi} |a_0(0, 0, d)| N_1}{\mu} \\ \lambda_7 &= 2 || P_f B_a || (L_b + k L_a) \\ \lambda_8 &= L_b + k L_a \\ \lambda_9 &= \lambda_4 L_q \\ \lambda_{10} &= 2 || P_f B_a || L_b \\ \lambda_{11} &= L_b \end{split}$$

Chapter 3

Universal Integral Controllers with Nonlinear Gains

3.1 Introduction

In Chapter 2, we designed Universal Integral Controllers with nonlinear integral gains. In this chapter, we investigate the use of nonlinear proportional and derivative gains in addition to nonlinear integral gains. We consider only the Nonlinearity Before Integration scheme, which showed the best transient performance in simulations. Nonlinear proportional and derivative gains provide us more freedom in designing a controller and can be utilized to further improve transient performance.

For a Universal Integral Controller with a nonlinearity placed before the integrator, from the closed-loop equation (2.31), the error dynamics have the form of a stable linear system driven by $(s - \sigma)$:

$$\dot{\zeta} = A\zeta + B(s - \sigma)$$

If the nonlinearity is designed to hold the integrator output σ small, the response of the system depends on the eigenvalues of A, which are determined by the gains k_1 to $k_{\rho-1}$. But, the design of the proportional and derivative gains k_i is limited by the control level k. Large k_i 's increase the disturbance term $\Delta(\cdot)$ in (2.32), and a higher controller gain k is required to overcome the disturbance (2.36), which may violate the actuator limit.

We propose to replace the constant proportional and derivative gains k_i with nonlinear gains $k_i(\cdot)$, which can be functions of the tracking error and its derivatives ζ . Our goal is to design a Universal Integral Controller with nonlinear proportional, integral and derivative gains that improve the transient performance, while preserving the stability properties of the systems, both regional and semiglobal.

3.2 Design of Nonlinear Proportional and Derivative Gains

Taking nonlinear proportional and derivative gains is equivalent to designing a nonlinear sliding surface:

$$egin{aligned} s &= k_0 \sigma + \sum_{i=1}^{
ho-1} k_i(\cdot) e_i + e_
ho \ &\stackrel{ ext{def}}{=} k_0 \sigma + \sum_{i=1}^{
ho-1} v_i(\cdot) + e_
ho \end{aligned}$$

where $k_i(\cdot)$ is a nonlinear function of e_1 to $e_{\rho-1}$ and $v_i(\cdot)=k_i(\cdot)e_i$. The dynamics of $\zeta=[e_1,\cdots,e_{\rho-1}]^T$ have the form

$$\dot{\zeta} = \begin{bmatrix}
0 & 1 & 0 & \cdots & 0 \\
0 & 0 & 1 & \cdots & 0 \\
\vdots & & & \vdots \\
0 & 0 & 0 & \cdots & 1 \\
0 & 0 & 0 & \cdots & 0
\end{bmatrix}
\begin{pmatrix}
v_1(\cdot) \\
v_2(\cdot) \\
\vdots \\
v_{\rho-2}(\cdot) \\
v_{\rho-1}(\cdot)
\end{pmatrix} + \begin{bmatrix}
0 \\
0 \\
\vdots \\
0 \\
0 \\
1
\end{bmatrix} (s - \sigma)$$

$$\stackrel{\text{def}}{=} A_m \zeta + B_m v(\cdot) + B(s - \sigma) \tag{3.1}$$

where $v(\cdot) = [v_1(\cdot), \cdots, v_{\rho-1}(\cdot)]^T$. Finding a class of nonlinear functions $v_i(\cdot)$, which ensure that the dynamics of ζ are asymptotically stable when $(s - \sigma) = 0$, is a challenging problem. In this work, we consider nonlinear gains of the form

$$v_i = v_i(e_i) = k_i(e_i)e_i$$

where $v_i(e_i)$ satisfies the sector conditions

$$l_i e_i^2 \le e_i v_i(e_i) \le m_i e_i^2$$
, for $1 \le i \le \rho - 1$ (3.2)

i.e., the nonlinear gains $k_i(e_i)$ that are bounded by

$$l_i < k_i(e_i) < m_i$$
, for $i = 1, \dots, \rho - 1$

Then, the study of stability of the system (3.1) with the given sector conditions (3.2) reduces to a Lure problem. For Lure systems, Lyapunov functions have been found analytically only for systems of order two. When $s - \sigma = 0$, the derivative of

the Lyapunov function

$$V = \zeta^T P \zeta + 2 \lambda_1 \int_0^{\zeta_1} v_1(au) d au, \quad P = P^T = egin{bmatrix} p_{11} & p_{12} \ p_{12} & p_{22} \end{bmatrix} > 0$$

with the choice of $\lambda_1 = p_{22}$, satisfies the inequality

$$\dot{V} \leq -\zeta^T egin{bmatrix} 2p_{12} & -p_{11} + p_{12}m_2 \ -p_{11} + p_{12}m_2 & 2(p_{22}l_2 - p_{12}) \end{bmatrix} \zeta = -\zeta^T Q \zeta$$

and $Q=Q^T$ can be made positive definite by choosing $p_{12}>0$ and p_{22} large. For higher order systems, Linear Matrix Inequalities can be applied to determine the stability for the given sector conditions $v_i(e_i) \in (l_i, m_i)$ [4, Chapter 8].

Lemma 1 Consider

$$\dot{\zeta} = A_m \zeta + B_m v(\zeta)$$

with $v(\zeta)$ satisfying the sector conditions (3.2). There is a Lyapunov function of the form

$$V = \zeta^T P \zeta + 2 \sum_{i=1}^{\rho-1} \lambda_i \int_0^{\zeta_i} v_i(\tau) d\tau$$
 (3.3)

where $P = P^T > 0$ and λ_i are positive constants, and its derivative satisfies the inequality

$$\dot{V} = 2(\zeta^T P + v^T(\zeta)\Lambda)(A_m \zeta + B_m v(\zeta)) \le -\zeta^T \zeta \tag{3.4}$$

where

$$\Lambda = \operatorname{diag}(\lambda_1, \cdots, \lambda_{\rho-1})$$

if the LMI problem

$$\begin{bmatrix} A_m^T P + P A_m + I - 2T K_p & P B_m + A_m^T \Lambda + T K_s \\ B_m^T P + \Lambda A_m + K_s T & \Lambda B_m + B_m^T \Lambda - 2T \end{bmatrix} \le 0$$
 (3.5)

is feasible, where

$$egin{align} K_p &= \operatorname{diag}(l_1 m_1, \cdots, l_{
ho-1} m_{
ho-1}) \ & K_s &= \operatorname{diag}(l_1 + m_1, \cdots, l_{
ho-1} + m_{
ho-1}) \ & T &= \operatorname{diag}(au_1, \cdots, au_{
ho-1}) \ \end{aligned}$$

and τ_1 to $\tau_{\rho-1}$ are nonnegative constants.

Lemma 1 results from the S-procedure [4, page 23] and detailed steps are shown in Appendix C.

For relative-degree- ρ systems, we determine the desired range of the nonlinear gains and solve the LMI problem. If the LMI problem is feasible, our analysis in the next section shows that the controller achieves regional and semiglobal regulation. Examples of sector conditions which ensure the stability for second, third and fourth-order systems are computed by the MATLAB LMI toolbox and are shown in Table 3.1. For example, in the second column of the table, we started solving the LMI problem for relative-degree-three systems with $(l_1, m_1) = (3.9, 4.1)$, $(l_2, m_2) = (5.9, 6.1)$, and $(l_3, m_3) = (3.9, 4.1)$ and increased the range of the nonlinear gains until the LMI problem was infeasible.

Table 3.1: Examples of sector conditions for stable systems determined by the LMI

	2nd	3rd	3rd	4th	4th
l_1	0.1	2.5	16	13	180
m_1	1000	5.5	48	21	332
l_2	0.1	3.5	12	18	134
m_2	1000	7.5	36	30	250
l_3		2.5	6	14	58
m_3		5.5	10	22	86
14				4	9
m_4				7.5	15

In summary, a Universal Integral Controller with nonlinear proportional, integral and derivative gains is taken as

$$u = -k \operatorname{sign}(L_g L_f^{\rho-1} h) \phi\left(\frac{\hat{s}}{\mu}\right)$$
 (3.6)

where

$$\hat{s} = \sigma + \hat{e}_a$$

$$\dot{\sigma} = \psi(\hat{e}_a) \tag{3.7}$$

and the augmented error \hat{e}_a is given by

$$\hat{e}_a = v_1(e_1) + \sum_{i=2}^{
ho-1} v_i(\hat{e}_i) + \hat{e}_{
ho}$$

The nonlinear integral gain $\psi(\sigma)$ satisfies the condition (2.25), and the nonlinear proportional and derivative gains $v_i = v_i(e_i)$ are continuous, piecewise differentiable and satisfy the sector conditions (3.2).

3.3 Closed-loop Analysis

The closed-loop system can be represented in the singularly perturbed form

$$\dot{z} = q_0(z, e + \nu, d)$$

$$\dot{\zeta} = A_m \zeta + B_m v(\zeta) + B(s - \sigma)$$

$$\dot{\sigma} = \psi(s - N_m(\zeta, s, \varphi, \epsilon) - \sigma)$$

$$\dot{s} = \Delta(\cdot) - k|a_0(\cdot)|\phi\left(\frac{s - N_m(\zeta, s, \varphi, \epsilon)}{\mu}\right)$$

$$\epsilon \dot{\varphi} = A_f \varphi + \epsilon B_a \left[b_0(\cdot) - k|a_0(\cdot)|\phi\left(\frac{s - N_m(\zeta, s, \varphi, \epsilon)}{\mu}\right)\right]$$
(3.8)

where

$$egin{aligned} \Delta(z,e,\sigma,
u,d,r^{(
ho)}) &= \psi(s-N_m(\zeta,s,arphi,\epsilon)-\sigma) + \sum_{i=1}^{
ho-1} v_i'(e_i)e_{i+1} + b_0(z,e+
u,d,r^{(
ho)}) \ N_m(\zeta,s,arphi,\epsilon) &= \sum_{i=2}^{
ho-1} (v_i(e_i)-v_i(\hat{e}_i)) + \hat{e}_
ho - e_
ho \end{aligned}$$

Only the dynamics of ζ , the estimation error $N_m(\zeta, s, \varphi, \epsilon) = s - \hat{s}$ and the disturbance term $\Delta(\cdot)$ are different from (2.31). We present in detail only the part of the analysis that is different from Section 2.4.1.

Suppose that $v(\zeta)$ is chosen such that the LMI problem (3.5) is feasible. Take the Lyapunov function V of the form (3.3) whose derivative satisfies the inequality (3.4). Consider

$$\Omega_c \stackrel{\mathrm{def}}{=} \{(z,e,\sigma): |s| \leq c, \ |\sigma| \leq (1+\delta)c, \ V(\zeta) \leq c^2 \rho_1, \ V_0(t,z,d) \leq \alpha_4 (c\rho_2 + r_3)\}$$

We show that our assumptions hold in the set Ω_c , by choosing ρ_2 to satisfy (3.9)

and then choosing c to satisfy (2.34). Since $e_{\rho} = s - \sigma - \sum_{i=1}^{i=\rho-1} v_i(\zeta_i)$, the inequality

$$||e|| \le ||\zeta|| + |e_{\rho}| \le (1 + ||K_m||)||\zeta|| + |s| + |\sigma| \le c\rho_2 < r_1$$

should be satisfied, where $K_m = [m_1, \cdots, m_{
ho-1}]$ and

$$\rho_2 > (1 + ||K_m||) \sqrt{\frac{\rho_1}{\lambda_{\min}(P)}} + 2 + \delta$$
(3.9)

In the first step, we show that every trajectory, starting at a bounded $\hat{e}(0)$ with $(e(0), z(0), \sigma(0)) \in \Omega_b$, and b < c, enters the set $\Omega_c \times \Sigma_{\epsilon}$ in finite time.

From the continuity of $v_i(\cdot)$, we can choose ϵ small enough so that $|N_m(\zeta, s, \varphi, \epsilon)| < \delta \mu$. Then we show that $s\dot{s} < 0$ on the boundary |s| = c and $\sigma \dot{\sigma} < 0$ on the boundary $|\sigma| = (1 + \delta)c$. Consider ζ on the boundary $V = c^2 \rho_1$, where ρ_1 is to be specified. From (3.2) and (3.4),

$$\dot{V} \le -\|\zeta\|^2 + 2\|\zeta\|(\|PB\| + \lambda_{\rho-1}m_{\rho-1})(|s| + |\sigma|)$$

$$\le -\|\zeta\|^2 + 2\|\zeta\|(\|PB\| + \lambda_{\rho-1}m_{\rho-1})c(2 + \delta)$$
(3.10)

and we can show that $\dot{V} < 0$ on the boundary $V = c^2 \rho_1$, by choosing ρ_1 to satisfy

$$\rho_1 > 4(||PB|| + \lambda_{\rho-1}m_{\rho-1})^2(||P|| + \max_{1 \le i \le \rho-1} \{\lambda_i m_i\})(2+\delta)^2$$
 (3.11)

Then we verify that $\dot{V}_0<0$ on the boundary $V_0=lpha_4(c
ho_2+r_3)$. Therefore, the set $\Omega_c imes\Sigma_\epsilon$ is positively invariant.

In the next step, we show that s(t) reaches the boundary layer $\{|s| \leq \mu_1\}$ and $\sigma(t)$ reaches the set $\{|\sigma| \leq (1+\delta)\mu\}$ in finite time. Then, from (3.10), we show

that $\dot{V} \leq -\frac{1}{2}||\zeta||^2$ for $V(\zeta) \geq \mu^2 \rho_1$ if

$$\rho_1 > 64(||PB|| + \lambda_{\rho-1}m_{\rho-1})^2(||P|| + \max_{1 \le i \le \rho-1} \{\lambda_i m_i\})$$
 (3.12)

Since (3.12) implies (3.11), by fixing ρ_1 to satisfy (3.12), we show that $\zeta(t)$ reaches the set $\{V(\zeta) \leq \mu^2 \rho_1\}$ in finite time and stays therein. Then, z(t) reaches the set $\{V_0 \leq \alpha_4(\mu \rho_2 + \mu)\}$ in finite time and stays therein. Therefore, every trajectory in $\Omega_c \times \Sigma_{\epsilon}$ enters $\Psi_{\mu} \times \Sigma_{\epsilon}$ in finite time and stays therein, where the set Ψ_{μ} is defined as

$$\Psi_{\mu} \stackrel{\text{def}}{=} \{(z, e, \sigma) : |s| \leq \mu_1, \ |\sigma| \leq (1 + \delta)\mu, \ V(\zeta) \leq \mu^2 \rho_1, \ V_0(t, z, d) \leq \alpha_4(\mu \rho_2 + \mu)\}$$

When $\nu=0$ and $r^{(\rho)}=0$, the closed-loop system (3.8) has a unique equilibrium point $(z=0,e=0,\sigma=\bar{\sigma},\varphi=0)$, where

$$ar{\sigma} = -\operatorname{sign}(L_g L_f^{
ho-1} h) \mu \phi^{-1} igg(rac{ar{u}(d)}{k}igg)$$

Following steps similar to Appendix B, we conclude that all trajectories in $\Psi_{\mu} \times \Sigma_{\epsilon}$ approaches the equilibrium point as time tends to infinity.

Our conclusions are summarized in the following theorem and corollary.

Theorem 3 Suppose Assumptions 1 to 4 are satisfied and consider the closed-loop system formed of the system (2.5), the observer (2.22), the nonlinear integral gain (3.7) satisfying condition (2.25), nonlinear proportional and derivative gain satisfying (3.2), and the output feedback controller (3.6). Suppose the LMI problem (3.5) is feasible, $\hat{e}(0)$ is bounded, and $(z(0), e(0), \sigma(0)) \in \Omega_b$, where b < c and c satisfies (2.34) and (2.36). Then, there exists $\mu^* > 0$ and

for each $0 < \mu < \mu^*$, there exists $\epsilon^* = \epsilon^*(\mu) > 0$ such that for each $0 < \mu < \mu^*$ and $0 < \epsilon < \epsilon^*(\mu)$, all the state variables of the closed-loop system are bounded and $\lim_{t\to\infty} e(t) = 0$.

If all the assumptions hold globally and k can be chosen arbitrarily large, the controller can achieve semiglobal regulation.

Corollary 3 Suppose Assumptions 1 to 4 are satisfied globally, i.e., $U_{\theta} = R^n$, α_1 , α_2 , α_3 and γ are class \mathcal{K}_{∞} functions, the LMI problem (3.5) is feasible, and k can be chosen arbitrarily large. For any given compact sets $\mathcal{N} \in R^{n+1}$ and $\mathcal{M} \in R^p$, choose c > b > 0 and $r_3 \geq 0$ such that $\mathcal{N} \in \Omega_b$, and choose k large enough to satisfy (2.36). Then, there exists $\mu^* > 0$ and for each $0 < \mu < \mu^*$, there exists $\epsilon^* = \epsilon^*(\mu) > 0$ such that for each $0 < \mu < \mu^*$ and $0 < \epsilon < \epsilon^*(\mu)$, and for all initial states $(z(0), e(0), \sigma(0)) \in \mathcal{N}$ and $\hat{e}(0) \in \mathcal{M}$, the state variables of the closed-loop system (3.8) are bounded and $\lim_{t \to \infty} e(t) = 0$.

3.4 Simulation Results

Example 1: A synchronous generator connected to an infinite bus can be described [28, page 25-26] by

$$M\ddot{\delta}=P-D\delta-\eta_1 E_q \sin \delta \
onumber \
onumb$$

The system has relative degree three viewing the field voltage E_{FD} as input and the angle δ as output, for $0 < \delta < \pi$. For simulations, we use P = 0.815, $\eta_1 = 2.0$, $\eta_2 = 2.7$, $\eta_3 = 1.7$, $\tau = 6.6$, M = 0.0147 and D/M = 4. The simulation results

shown in Figure 3.1 are for the controllers with linear and nonlinear proportional gains. Since s enters the boundary layer fast, we drive the integrator with the augmented error $4e_a$ without using nonlinearity. Controller parameters $\mu=0.5$, k=2.5 and limit L=10 for the integrators are chosen for the simulation. The error dynamics inside the boundary layer is given by

$$\dot{\zeta} = A\zeta + B(s-\sigma) = egin{bmatrix} 0 & 1 \ -k_1 & -k_2 \end{bmatrix} egin{bmatrix} e_1 \ e_2 \end{bmatrix} + egin{bmatrix} 0 \ 1 \end{bmatrix} (s-\sigma)$$

When the linear gains are chosen as $k_1 = 8$ and $k_2 = 4$, the system $\dot{\zeta} = A\zeta$ is underdamped and shows fast response with overshoot, while the linear gains $k_1 = 6$ and $k_2 = 5$ remove the overshoot but increase the settling time. The nonlinear proportional gain increases to $k_1(e_1) = 12.5$ when the tracking error is large for fast rise time, and decreases to $k_1(e_1) = 6$ as the error becomes small to prevent overshoot. The nonlinear proportional is shown in Figure 3.2. The derivative gain was fixed as $k_2 = 5$. The simulation results show that the nonlinear proportional gain achieves comparable settling time with the linear gains $k_1 = 8$ and $k_2 = 4$, without showing overshoot.

Example 2: The nonlinear model of a single-link manipulator with flexible joints [28, page 25], damping ignored, is described by

$$I\ddot{q}_1 + MgL\sin q_1 + k(q_1 - q_2) = 0$$
 $J\ddot{q}_2 - K(q_1 - q_2) = u$

Viewing the angular position q_1 as output and the torque u as input, the system has relative degree four. For simulations, the numerical values $I = 0.5 \text{ kg/m}^2$,

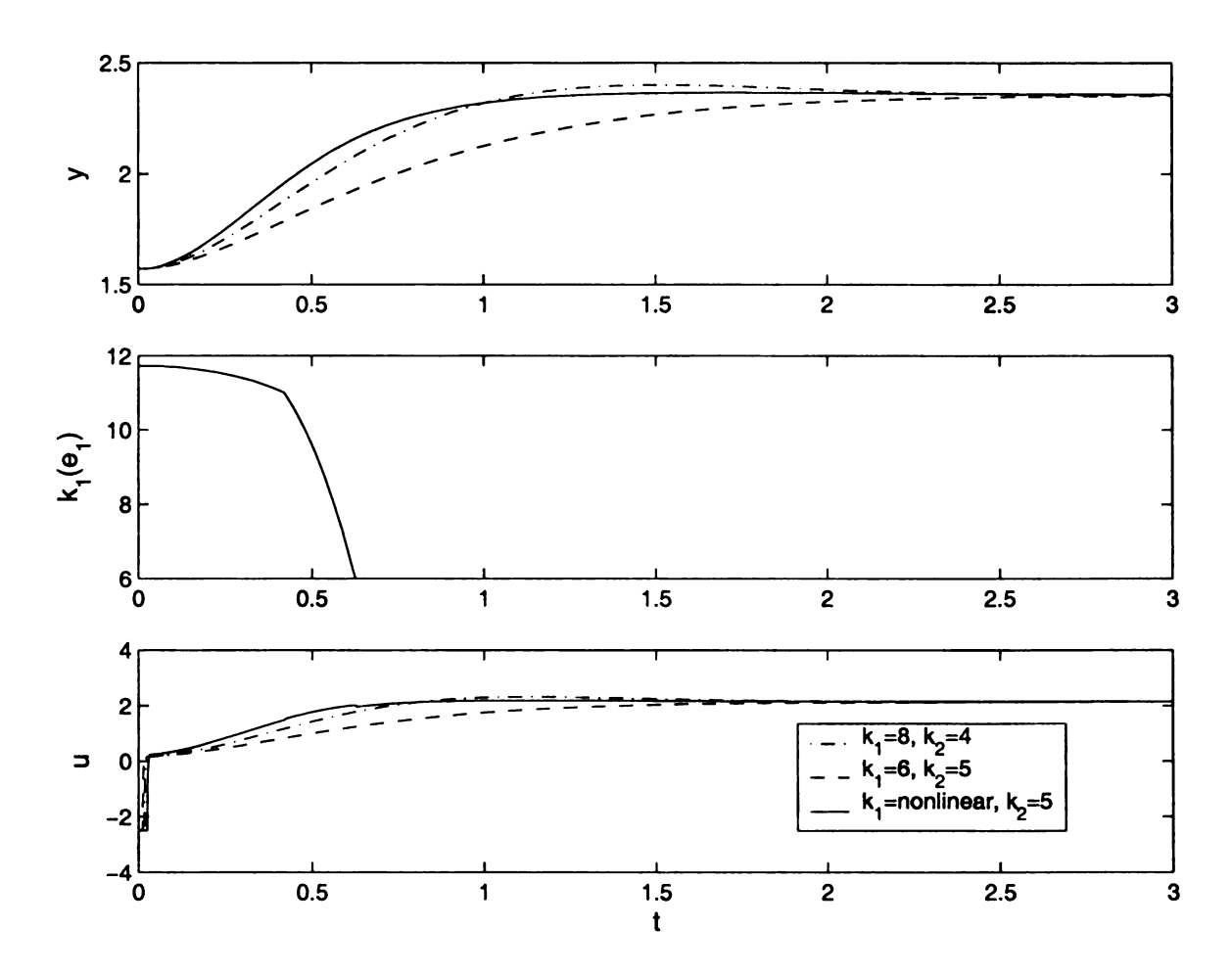


Figure 3.1: Simulation results for the synchronous generator connected to an infinity bus

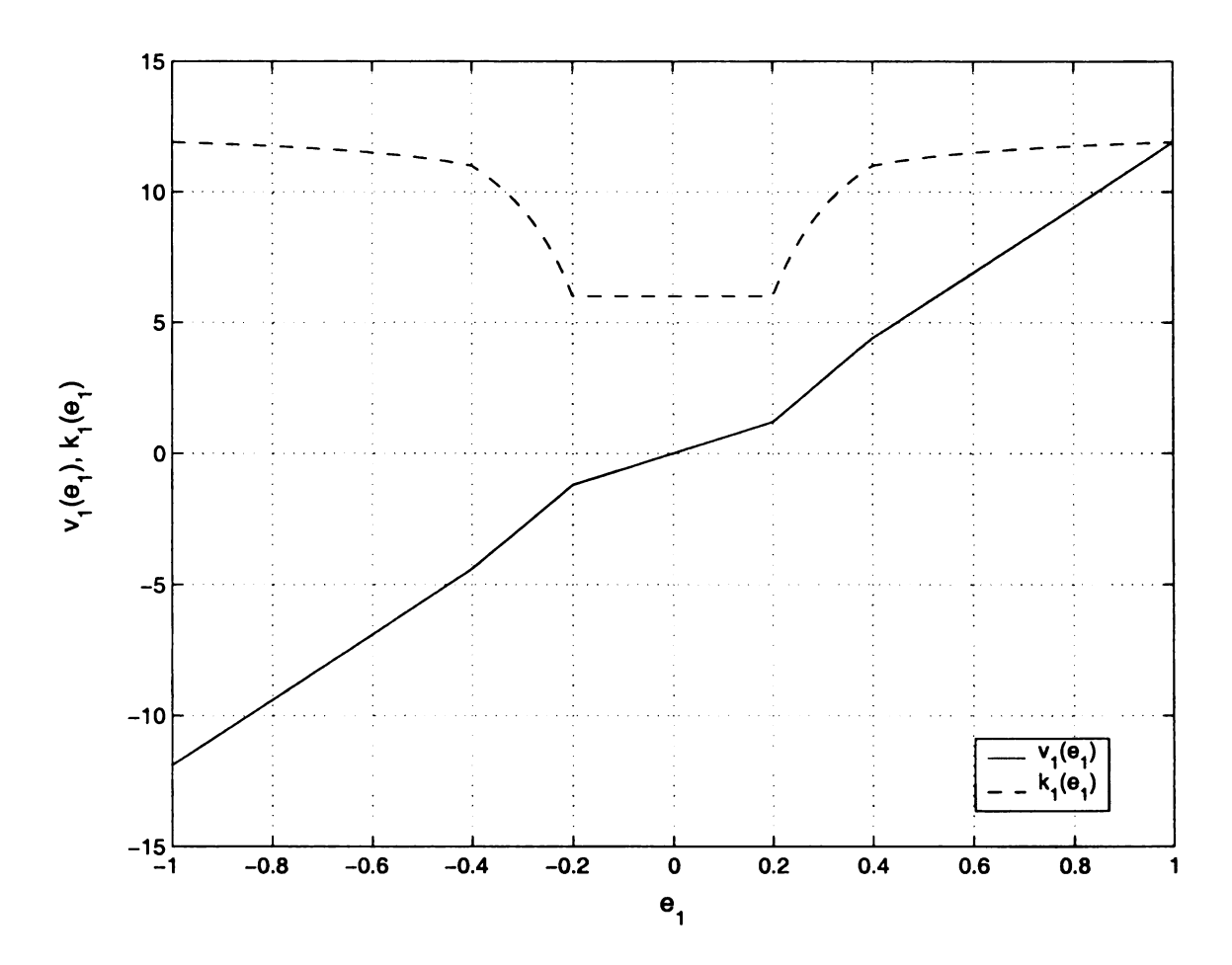


Figure 3.2: Nonlinear proportional gain $v_1(e_1) = k_1(e_1)e_1$ for the simulation of the synchronous generator connected to an infinite bus

 $J=0.5~{
m kg/m^2},~M=1~{
m kg},~g=9.8~{
m m/sec^2},~L=1~{
m m}$ and $k=20~{
m N/m}$ are used. In Figure 3.3, we compare the performance of the controllers with the linear and nonlinear proportional and derivative gains. The maximum control level is set as k=12, and the linear gains are chosen as $k_1=31.25,~k_2=25$ and $k_3=7.5$. The nonlinear gains are designed to satisfy the conditions $31.25 \le k_1(e_1) \le 45$, $25 \le k_2(e_2) \le 28$ and $6 \le k_3(e_3) \le 7.5$. For the range of the nonlinear gains chosen, the LMI problem is feasible, as shown in Table 1. The nonlinear gains are plotted in Figure 3.4. The integrator is driven with $2e_a$ with the limit L=90. For the reference r=2 with the initial condition y(0)=0, the nonlinear gains achieve better settling time but show small damping. When the reference r=1 is applied at t=4, the nonlinear gains reduce the settling time without overshoot. Since the nonlinear gains $k_i(e_i)$ are functions of different variables, it is difficult to design the gains to change the poles of $\dot{\zeta}=A\zeta$ as the tracking error becomes small.

3.5 Conclusion

In this chapter, we designed Universal Integral Controller with nonlinear integral, proportional and derivative gains. We showed that, if the LMI problem in Lemma 1 is feasible for the nonlinear gains, the controller stabilizes the system regionally and semiglobally. The nonlinear gains provide us freedom to alter the error dynamics inside the boundary layer as the state of the system changes. The simulation results showed that the nonlinear gains can be chosen to improve the transient performance for relative-degree-three systems. It is more challenging to design the gains for higher relative degree.

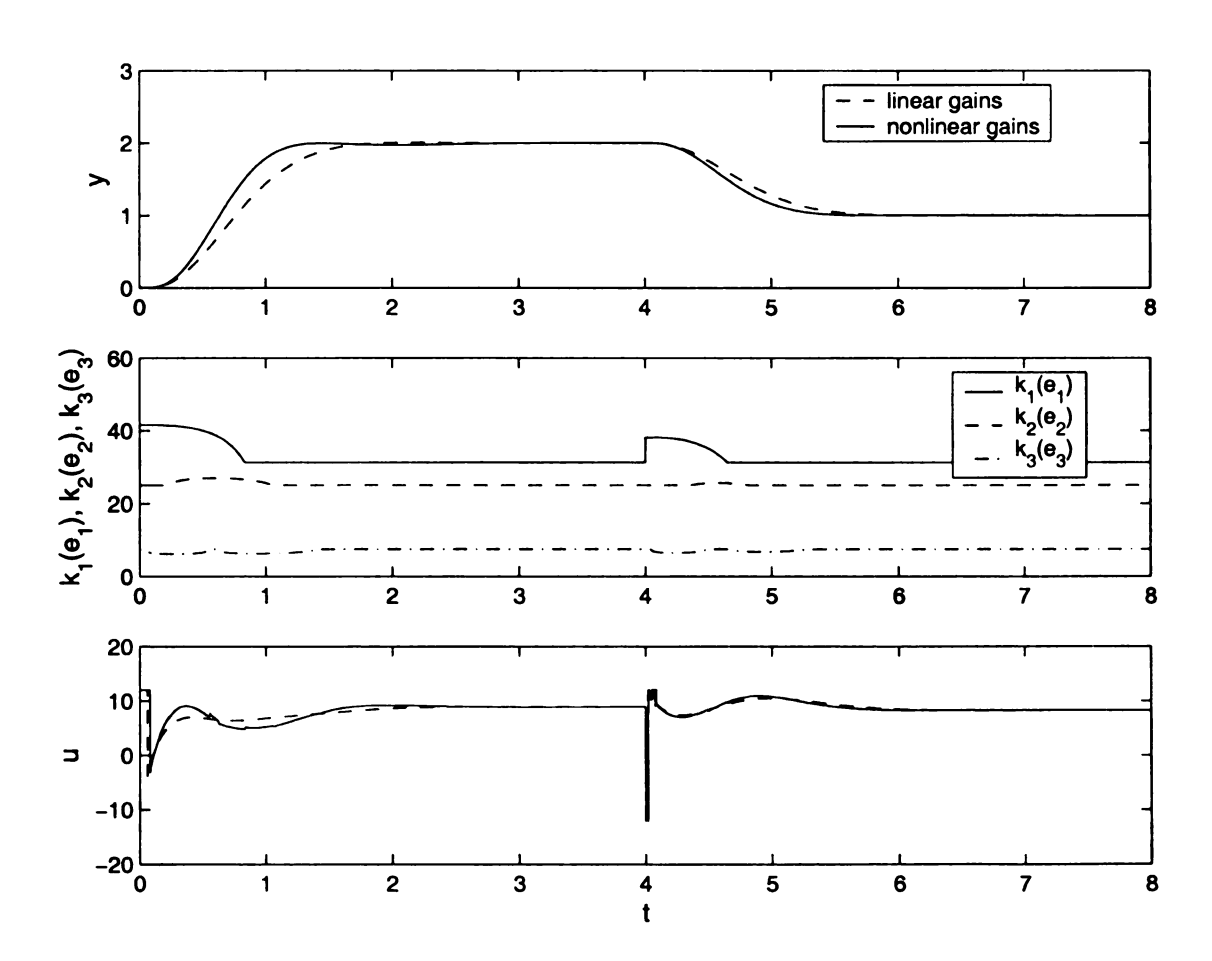


Figure 3.3: Simulation results for the single link manipulator

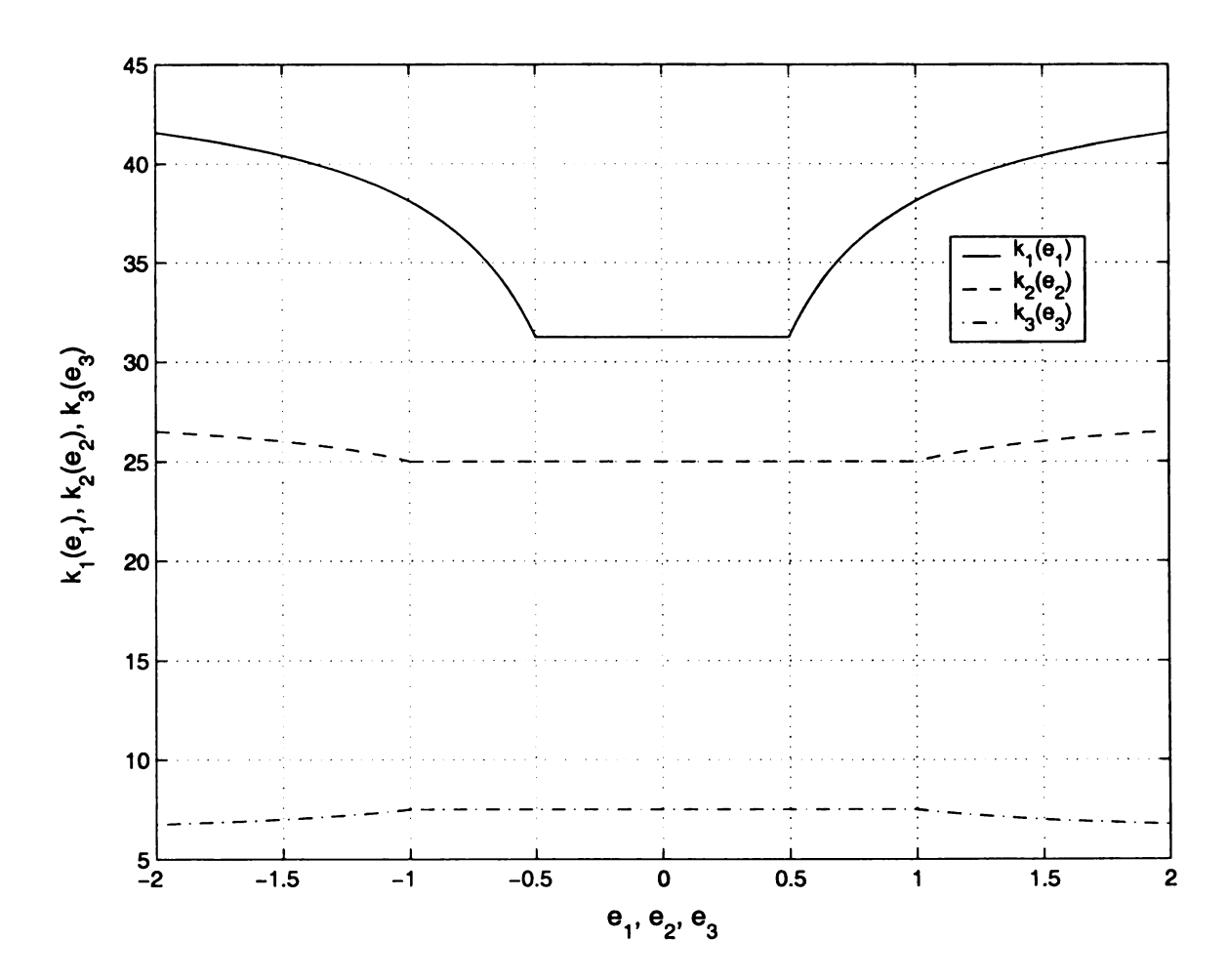


Figure 3.4: Nonlinear proportional and derivative gains $k_1(e_1)$, $k_2(e_2)$, $k_3(e_3)$ for the simulation of the single link manipulator

Appendix C S-procedure for Lemma 1 [4]

A linear matrix inequality (LMI) has the form

$$F(x) = F_0 + \sum_{i=1}^m x_i F_i > 0$$

where $x \in R^m$ is the variable and $F_i = F_i^T \in R^{n \times n}$ are given. The LMI is equivalent to a set of n polynomial inequalities in x. The convex constraint on x, i.e. $\{x : F(x) > 0\}$ can represent a wide variety of convex constraint on x. The LMI problem is to find x such that F(x) > 0 or determine that the LMI is infeasible. Efficient algorithms have been developed for LMI problems, which often represent constraints in control design.

For the constraint that some quadratic functions be nonnegative whenever some other quadratic functions are nonnegative, the S-procedure can be applied to form an LMI that is a conservative approximation of the constraints. Let G_0, \dots, G_p be quadratic functions of the variable $\xi \in \mathbb{R}^n$:

$$G_i(\xi) = \xi^T T_i \xi + 2\omega_i^T \xi + \eta_i$$
, for $i = 0, \dots, p$

where $T_i = T_i^T$. Consider the following condition on G_0, \dots, G_p :

$$G_0 \geq 0$$
 for all ξ such that $G_i(\xi) \geq 0$, for $i = 1, \dots, p$

The above constraint holds if

there exist
$$\tau_1 \geq 0, \cdots, \tau_p \geq 0$$
 such that for all ξ , $G_0(\xi) - \sum_{i=1}^p \tau_i G_i(\xi) \geq 0$

The sufficient condition can also be represented as

$$egin{bmatrix} T_0 & \omega_0 \ \omega_0^T & \eta_0 \end{bmatrix} - \sum_{i=1}^p au_i egin{bmatrix} T_i & \omega_i \ \omega_i^T & \eta_i \end{bmatrix} \geq 0$$

Note that in Lemma 1, we require inequality (3.4) be true if every nonlinear gain $v_i(\cdot)$ satisfies the section condition (3.2); both inequalities can be arranged in quadratic forms. We apply the S-procedure to find the sufficient condition. From (3.4), we have

$$\begin{split} &2(\zeta^T P + v^T(\zeta)\Lambda)(A_m \zeta + B_m v(\zeta)) + \zeta^T \zeta \\ &= \zeta^T (2PA_m + I)\zeta + 2\zeta^T (PB_m + A_m^T \Lambda)v(\zeta) + 2v^T(\zeta)\Lambda B_m v(\zeta) \\ &= \begin{bmatrix} \zeta \\ v(\zeta) \end{bmatrix}^T \begin{bmatrix} A_m^T P + PA_m + I & PB_m + A_m^T \Lambda \\ B_m^T P + \Lambda A_m & \Lambda B_m + B_m^T \Lambda \end{bmatrix} \begin{bmatrix} \zeta \\ v(\zeta) \end{bmatrix} \\ &\stackrel{\text{def}}{=} \zeta_m^T T_0 \zeta_m \leq 0 \end{split}$$

The sector conditions (3.2) can be arranged as

$$2(v_i(\zeta_i) - l_i\zeta_i)(v_i(\zeta_i) - m_i\zeta_i)$$

$$= \begin{bmatrix} \zeta \\ \zeta \\ \vdots \\ 0 \end{bmatrix}^T \begin{bmatrix} 0 & \cdots & 0 & 0 & \cdots & 0 \\ \vdots & 2l_im_i & \vdots & \vdots & -(l_i + m_i) & \vdots \\ 0 & \cdots & 0 & 0 & \cdots & 0 \\ \vdots & \cdots & 0 & 0 & \cdots & 0 \\ \vdots & -(l_i + m_i) & \vdots & \vdots & 2 & \vdots \\ 0 & \cdots & 0 & 0 & \cdots & 0 \end{bmatrix} \begin{bmatrix} \zeta \\ \zeta \\ v(\zeta) \end{bmatrix}$$

$$\stackrel{\text{def}}{=} \zeta_m^T T_i \zeta_m \leq 0$$

for $i = 1, \dots, \rho-1$, where the elements of T_i are zero except the *i*th diagonal element of each submatrix. Thus, the inequality (3.4) is true, for $v_i(\zeta_i)$ that satisfies the sector condition (3.2), if

$$T_0 - \sum_{i=1}^{\rho-1} \tau_i T_i = T_0 - \begin{bmatrix} -2TK_P & TK_s \\ K_s T & -2T \end{bmatrix} \leq 0$$

which is the LMI problem of (3.5).

Chapter 4

Nonlinear PID Controllers

4.1 Introduction

For relative-degree one or two nonlinear systems, the controllers designed in the previous two chapters specialize to nonlinear versions of the classical PI and PID controllers. In this chapter we study the special case of relative degree one or two systems for various reasons. First, there has been a lot of interest in the control literature to develop nonlinear PID controllers, or more precisely PID controllers with nonlinear gains, in order to improve the performance of the system. In Chapter 1, we described the various ideas that have been proposed in the literature and the analytical results that are available for some of those ideas. It is important to emphasize that all the results available in the literature are for the case when the plant is linear or for nonlinear robotic systems. Second, by specializing to the case of relative degree one or two systems, we can obtain results sharper than those we obtained in Chapter 3 for the general relative degree case. In Chapter 3, we could not obtain an analytically verifiable stability condition. What we obtained was a condition in the form of feasibility of an LMI problem, which could be checked only

numerically. In this chapter we derive analytical stability conditions. Third, in the case of relative degree one or two systems we can consider new structures for the nonlinear integrator that we cannot consider in the general relative degree case. We saw in Appendix A of Chapter 1 that for relative degree higher than two, we need to drive the integrator by an augmented error. For relative-degree-two systems, we can also consider nonlinear integrators that are driven by the tracking error. For relative-degree-one systems, we have the controller

$$u = -k \operatorname{sign}(L_g h) \phi\left(\frac{\sigma + e_1}{\mu}\right)$$

$$\dot{\sigma} = \psi(e_1)$$
 (4.1)

which is a special case of the controller (2.26) when $\rho = 1$. For relative-degree-two systems, we consider two different controllers:

$$u = -k \operatorname{sign}(L_g L_f h) \phi \left(\frac{\sigma + k(e_1)e_1 + \hat{e}_2}{\mu} \right)$$

$$\dot{\sigma} = \psi(k_1(e_1)e_1 + \hat{e}_2)$$
(4.2)

and

$$u = -k \operatorname{sign}(L_g L_f h) \phi \left(\frac{\sigma + k(e_1)e_1 + \hat{e}_2}{\mu} \right)$$
 (4.3) $\dot{\sigma} = \psi(e_1)$

The controller (4.2) is a special case of the controller (3.6) when $\rho = 2$. The controller (4.3) is a new structure in which the integrator is driven by a nonlinear function of the tracking error e_1 instead of the augmented error

$$\hat{e}_a = k_1(e_1) + \hat{e}_2$$

In both (4.2) and (4.3) the estimate \hat{e}_2 is obtained by the high-gain observer

$$\dot{\hat{e}}_1 = \hat{e}_2 + \frac{\beta_1}{\epsilon} (e_1 - \hat{e}_1)$$

$$\dot{\hat{e}}_2 = \frac{\beta_2}{\epsilon^2} (e_1 - \hat{e}_1)$$
(4.4)

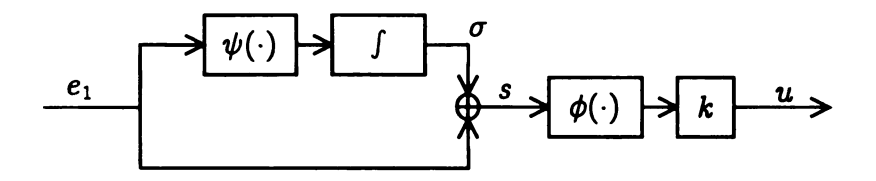
where β_1 , β_2 and ϵ are positive constants with ϵ chosen sufficiently small. To overcome the peaking phenomenon that can be induced by high-gain observers, we require the nonlinearity $\psi(\hat{e}_a)$ for the controller (4.2) be a globally bounded function of \hat{e}_a :

$$c_1p^2 \le p\psi(p) \le c_2p^2$$
, for $|p| \le L$
$$c_1L < |\psi(p)| < c_2L$$
, for $|p| > L$ (4.5)

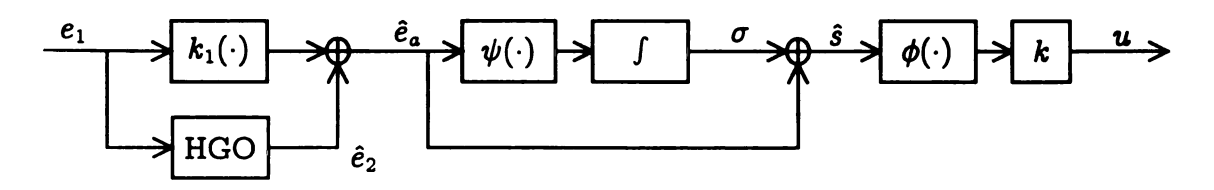
while the nonlinearity $\psi(e_1)$ for the controllers (4.1) and (4.3) satisfies the sector condition

$$c_1 p^2 \le p \psi(p) \le c_2 p^2 \tag{4.6}$$

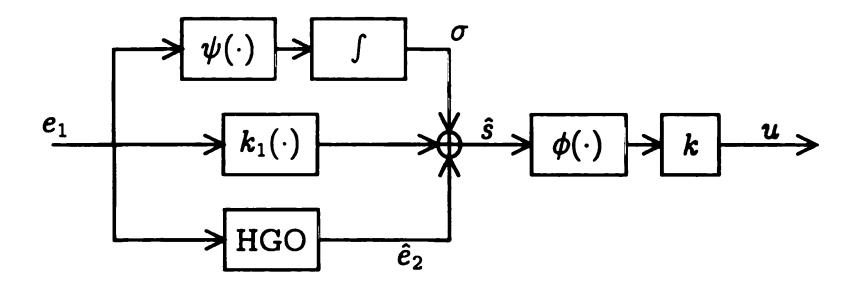
Schematic diagrams of the controllers (4.1), (4.2) and (4.3) are shown in Figure 4.1. All the schemes are versions of classical PI or PID controllers with nonlinear gains and with saturation nonlinearity $\phi(\cdot)$. It is worthwhile to note that the PI and PID controllers considered in [27] as special cases of the Universal Integral Controller when $\rho = 1$, and $\rho = 2$, respectively, are special cases of (4.1) and (4.3), with $\psi(e_1) = k_0 e_1$, $k_1 = \text{constant}$, and $\phi(\cdot) = \text{sat}(\cdot)$.



(a) Nonlinear PI controller



(b) Nonlinear PID controller with nonlinear integrator driven by the augmented error



(c) Nonlinear PID controller with nonlinear integrator driven by the tracking error

Figure 4.1: Nonlinear PI controller for relative-degree-one systems and nonlinear PID controller for relative-degree-two systems

4.2 Closed-loop Analysis

We present the proof of regional and semiglobal regulation of the nonlinear PID controllers (4.2) and (4.3) for relative-degree-two systems. The closed-loop system for the controller (4.2) can be represented in the singularly perturbed form

$$\dot{z} = q_0(z, e + \nu, d)$$
 $\dot{\sigma} = \psi(s - N\varphi - \sigma)$
 $\dot{e}_1 = -\sigma - k_1(e_1)e_1 + s$
 $\dot{s} = \Delta(\cdot) - k|a_0(\cdot)|\phi\left(\frac{s - N\varphi}{\mu}\right)$
 $\epsilon \dot{\varphi} = A_f \varphi + \epsilon B_a \left[b_0(\cdot) - k|a_0(\cdot)|\phi\left(\frac{s - N\varphi}{\mu}\right)\right]$

where

$$s=\sigma+k_1(e_1)e_1+e_2 \ \Delta(z,e,\sigma,
u,d,\ddot{r})=\psi(s-Narphi-\sigma)+k_1(e_1)e_2+k_1'(e_1)e_1e_2+b_0(z,e+
u,d,\ddot{r}) \ arphi=egin{bmatrix} rac{1}{\epsilon}(e_1-\hat{e}_1)\ e_2-\hat{e}_2 \end{pmatrix},\quad A_f=egin{bmatrix} -eta_1\ -eta_2\ 0 \end{pmatrix},\quad B_a=egin{bmatrix} 0\ 1 \end{pmatrix},\quad N=egin{bmatrix} 0\ 1 \end{pmatrix},$$

For the controller (4.3), the closed-loop system is given by

$$\dot{z} = q_0(z, e + \nu, d)$$
 $\dot{\sigma} = \psi(e_1)$
 $\dot{e}_1 = -\sigma - k_1(e_1)e_1 + s$
 $\dot{s} = \Delta(\cdot) - k|a_0(\cdot)|\phi\left(\frac{s - N\varphi}{\mu}\right)$
 $\epsilon \dot{\varphi} = A_f \varphi + \epsilon B_a \left[b_0(\cdot) - k|a_0(\cdot)|\phi\left(\frac{s - N\varphi}{\mu}\right)\right]$

where

$$\Delta(z, e, \sigma, \nu, d, \ddot{r}) = \psi(e_1) + k_1(e_1)e_2 + k'_1(e_1)e_1e_2 + b_0(z, e + \nu, d, \ddot{r})$$

The dynamics of σ and the disturbance $\Delta(\cdot)$ are different between (4.7) and (4.8). We present the analysis for (4.7), and remark on the part that is different for (4.8). For (4.7), consider

$$\Omega_c \stackrel{\mathrm{def}}{=} \{(z,e,\sigma): |s| \leq c, \ |\sigma| \leq (1+\delta)c, \ |e_1| \leq c\rho_1, \ V_0(t,z,d) \leq \alpha_4(c\rho_2+r_3)\}$$

where the positive constants λ , c, ρ_1 , ρ_2 and the class $\mathcal K$ function α_4 are to be specified. Our assumptions should hold in the set Ω_c , i.e., $||e|| < r_1$ and $||z|| < r_2$ for all $(e,z,\sigma) \in \Omega_c$. From Assumption 4 of Chapter 2, upper bounds on e and z are given by

$$||e|| \le |e_1| + |e_2| = |e_1| + |-\sigma - k_1(e_1)e_1 + s|$$

$$\le |\sigma| + (1 + \bar{k}_1)|e_1| + |s| \le c\rho_2$$
 $||z|| \le \alpha_1^{-1}(\alpha_4(c\rho_2 + r_3))$
 (4.9)

where \bar{k}_1 is the maximum of $k_1(e_1)$ over Ω_c , and

$$ho_2 > (1+ar{k}_1)
ho_1 + (2+\delta)$$
 $lpha_4 \overset{\mathsf{def}}{=} lpha_2^{-1} \circ \gamma$

Thus, c should be chosen to satisfy

$$c\rho_2 \leq \min\{r_1, \alpha_4^{-1}(\alpha_1(r_2)) - r_3\}$$
 (4.10)

where $\alpha_4^{-1}(\alpha_1(r_2)) > r_3$ from (2.9).

For (4.8), we take Ω_c as

$$\Omega_c \stackrel{\mathrm{def}}{=} \{(z,e,\sigma): |s| \leq c, \ V(\zeta) \leq c^2 \rho_1, \ V_0(t,z,d) \leq \alpha_4 (c \rho_2 + r_3) \}$$

where

$$V = rac{1}{2} \zeta^T P \zeta + \lambda \int_0^{e_1} \psi(au) d au, \quad \zeta = egin{bmatrix} \sigma \ e_1 \end{bmatrix}, \quad P = egin{bmatrix} p_{11} & p_{12} \ p_{12} & p_{22} \end{bmatrix}$$

The matrix $P=P^T>0$ and the positive constant λ are to be specified. The inequality $||e||\leq c\rho_2$ holds with

$$ho_2 > (2 + \bar{k}_1) \sqrt{\frac{2\rho_1}{\lambda_{\min}(P)}} + 1$$
 (4.11)

and our assumptions are valid in Ω_c if c satisfies (4.10) with ρ_2 as in (4.11).

Let $P_f = P_f^T > 0$ be the solution of the Lyapunov equation

$$P_f A_f + A_f^T P_f = -I$$

and take $V_f(\varphi) = \varphi^T P_f \varphi$. In the first step, we show that φ enters the set

$$\Sigma_{\epsilon} \stackrel{\mathrm{def}}{=} \left\{ arphi \in R^2 : V_f(arphi) \leq \epsilon^2
ho_3
ight\}$$

in a finite time $T_0(\epsilon)$, with $\lim_{\epsilon\to\infty}T_0(\epsilon)=0$, and Σ_ϵ can be made arbitrarily small by choosing ϵ small. The derivative of V_f satisfies

$$|\dot{V}_f \leq -rac{1}{\epsilon}||arphi||^2 + 2||arphi|||P_fB_a||\gamma_1(c)$$

where $\gamma_1(c)=\max\{|b_0(z,e+\nu,d)|+k|a_0(z,e+\nu,d)|\}$ and the maximum is taken over all $(z,e,\sigma)\in\Omega_c,\,d\in D,\,\nu\in\Lambda$ and $\ddot{r}\in\Gamma$. We have

$$|\dot{V}_f < -rac{1}{2\epsilon} ||arphi||^2, \quad ext{for } V_f \geq \epsilon^2
ho_3.$$

where $\rho_3=16||P_fB||^2||P_f||\gamma_1^2(c)$. Thus, $\varphi(t)$ decays to Σ_{ϵ} in a finite time $T_0(\epsilon)$ and stay therein. We choose ϵ small enough that $|N\varphi|<\delta\mu$, where δ is a positive constant to be specified. With $\psi(\cdot)$ satisfying (4.5), the right-side of the slow equation of (4.7) is bounded uniformly in ϵ . Hence, every trajectory in Ω_b , with b< c, is inside Ω_c during $[0,T_1]$, where T_1 is independent of ϵ . We choose ϵ small enough that $T_0(\epsilon)< T_1$. Thus, every trajectory starting at $(e(0),z(0),\sigma(0))\in\Omega_b$ with bounded $\hat{e}(0)$ enters $\Omega_c\times\Sigma_{\epsilon}$ in finite time.

Next, we show that the set $\Omega_c \times \Sigma_\epsilon$ is positively invariant. Choose μ small enough that $\mu(1+\delta) < c$. For $\mu(1+\delta) \le |s| \le c$, we have

$$\operatorname{sgn}\!\left(\phi\!\left(\frac{s-Narphi}{\mu}
ight)
ight)=\operatorname{sgn}\!\left(\frac{s-Narphi}{\mu}
ight)=\operatorname{sgn}(s)$$

and from (2.29), $|\phi(p)| \ge \phi(1) \ge c_3$ for $|p| \ge 1$. Hence

$$s\dot{s} \le |\Delta(\cdot)||s| - c_3 k|a_0||s| \tag{4.12}$$

With the controller gain k taken large enough to satisfy

$$k \ge c_4 + \gamma_2(c) \tag{4.13}$$

where c_4 is a positive constant, $\gamma_2(c) = \max\{|\Delta(z,e,\sigma,\nu,d,\ddot{r})| \ / |c_3a_0(z,e+\nu,d)|\}$, and the maximum is taken over all $(z,e,\sigma) \in \Omega_c$, $d \in D$, $\nu \in \Lambda$ and $\ddot{r} \in \Gamma$, we have

$$s\dot{s} < 0$$
 on $|s| = c$

On $|\sigma| = (1 + \delta)c$, using

$$|s-Narphi(\epsilon)arphi| < c + \delta\mu < |\sigma|$$
 $ext{sign}(\psi(s-Narphi(\epsilon)arphi - \sigma)) = -\operatorname{sign}(\sigma)$

we can show that

$$\sigma\dot{\sigma} = \sigma\psi(s - N\varphi(\epsilon)\varphi - \sigma) < 0$$
, on $|\sigma| = (1 + \delta)c$

From the inequality

$$e_1\dot{e}_1 \leq -k_1(e_1)e_1^2 + |e_1|(|s| + |\sigma|)$$
 (4.14)
 $\leq -\underline{k}_1e_1^2 + e_1(2+\delta)c$

where \underline{k}_1 is the minimum of $k_1(e_1)$ over Ω_c , we have

$$e_1\dot{e}_1 < 0$$
, on $|e_1| = c\rho_1$

if ρ_1 is chosen to satisfy

$$\rho_1 > \frac{2+\delta}{k_1} \tag{4.15}$$

For (4.8), we show that $\dot{V}(\zeta)<0$ on the boundary $V(\zeta)=c^2
ho_1$. The derivative of V is given by

$$egin{aligned} \dot{V} &= -p_{12}\sigma^2 - p_{22}k_1(e_1)e_1^2 - (\lambda k(e_1) - p_{12})\psi(e_1)e_1 + (p_{11} - \lambda)\sigma\psi(e_1) \ &- (p_{22} + p_{12}k_1(e_1))\sigma e_1 + \zeta^T PB_a s + \lambda \psi(e_1)s \end{aligned}$$

By taking $\lambda=p_{11}$ and choosing p_{11} large and $p_{12}>0$, the derivative of V can be arranged in the form

$$\dot{V} \le -\lambda_{\min}(Q)||\zeta||^2 + (||P|| + \lambda c_2)||\zeta|||s| \tag{4.16}$$

where $Q = Q^T > 0$ is given by

$$egin{bmatrix} p_{12} & rac{1}{2}(p_{12}ar{k}_1+p_{22}) \ rac{1}{2}(p_{12}ar{k}_1+p_{22}) & \lambda \underline{\mathbf{k}}_1c_1+p_{22}\underline{\mathbf{k}}_1-p_{12}c_2 \end{bmatrix}$$

and \bar{k}_1 is the maximum of $k_1(e_1)$ over Ω_c . The derivative of V satisfies the inequality

$$\dot{V} < 0$$
, on $V = c^2
ho_1$

when ρ_1 is chosen to satisfy

$$\rho_1 > \frac{(||P|| + \lambda c_2)^3}{2(\lambda_{\min}(Q))^2} \tag{4.17}$$

From (2.7) in Assumption 4, we have $||z|| \ge \gamma(c\rho_2 + r_3)$ on the boundary $V_0 = \alpha_4(c\rho_2 + r_3)$. By (2.8) and the bound of ||e|| in (4.9), we can show that

$$\dot{V}_0 < 0$$
, on $V_0 = \alpha_4(c\rho_2 + r_3)$

Therefore, the set $\Omega_c \times \Sigma_\epsilon$ is positively invariant.

In the third step, we show that every trajectory in $\Omega_c \times \Sigma_{\epsilon}$ enters the set $\Psi_{\mu} \times \Sigma_{\epsilon}$ in finite time and stays therein, where Ψ_{μ} is defined for (4.7) as

$$\Psi_{\mu} \stackrel{\mathrm{def}}{=} \{(z,e,\sigma): |s| \leq \mu_1, \ |\sigma| \leq (1+\delta)\mu, \ |e_1| \leq \mu \rho_1, V_0(t,z,d) \leq \alpha_4(\mu \rho_2 + \mu)\}$$

and for (4.8) as

$$\Psi_{\mu}\stackrel{\mathrm{def}}{=} \{(z,e,\sigma): |s| \leq \mu_1, \ V(\zeta) \leq \mu^2 \rho_1, V_0(t,z,d) \leq \alpha_4 (\mu \rho_2 + \mu)\}$$

Consider s in $\{\mu_1 \leq |s| \leq c\}$. With δ chosen to satisfy

$$\delta<\frac{c_4}{4k}<\frac{1}{4}$$

we have $sgn(\phi(\hat{s}/\mu)) = sgn(\hat{s}/\mu) = sgn(s)$, since $|N\varphi| < \delta\mu < |s|$. If $|\hat{s}| \ge \mu$, inequality (4.12) holds. Using (4.13),

$$s\dot{s} < -c_0c_3c_4|s|$$

where c_0 is defined in (2.2) of Assumption 1. If $|\hat{s}| < \mu$, we have $|\hat{s}| > \mu/2$ and

$$egin{aligned} s\dot{s} & \leq |\Delta(\cdot)||s| - k|a_0(\cdot)|\left|\phi\left(rac{\hat{s}}{\mu}
ight)
ight| ext{sign}\left(\phi\left(rac{\hat{s}}{\mu}
ight)
ight) s \ & \leq |\Delta(\cdot)||s| - rac{c_3k}{2}|a_0(\cdot)||s| \leq -rac{c_0c_3c_4}{2}|s| \end{aligned}$$

Thus, s(t) reaches $\{|s| \leq \mu_1\}$ in finite time and stays therein. Consider σ in $\{(1+\delta)\mu \leq |\sigma| \leq (1+\delta)c\}$. Since $|\hat{s}| < \mu < |\sigma|$, we have $\mathrm{sign}(\psi(\hat{s}-\sigma)) = \mathrm{sign}(\hat{s}-\sigma) = -\mathrm{sign}(\sigma)$ and $|\hat{s}-\sigma| > \delta\mu$. Moreover, $|\hat{s}-\sigma| \leq \mu + (1+\delta)c$ and

$$|\psi(p)| \geq \bar{c}_1|p|$$
, for $|p| \leq \mu + (1+\delta)c$

with $\bar{c}_1 = \min\{c_1, c_1L/(\mu + (1+\delta)c)\}$. Using these facts, we can show that

$$\sigma\dot{\sigma} = \sigma \operatorname{sign}(\hat{s} - \sigma))|\psi(\hat{s} - \sigma)| < -\bar{c}_1\delta\mu|\sigma|$$

Thus, $\sigma(t)$ reaches the set $\{|\sigma| \leq (1+\delta)\mu\}$ in finite time and stays therein. From inequality (4.14), we have

$$e_1\dot{e}_1\leq -rac{k_1}{2}e_1^2,\quad ext{for } |e_1|\geq \mu
ho_1$$

by choosing ρ_1 to satisfy

$$\rho_1 > \frac{4}{k_1} \tag{4.18}$$

Inequality (4.18) implies (4.15). With ρ_1 chosen as above, $e_1(t)$ reaches the set $\{|e_1| \leq \mu \rho_1\}$ in finite time and stays therein.

For (4.8), we consider that $\zeta = [\sigma, e_1]^T$ in $\{V(\zeta) \geq \mu^2 \rho_1\}$. From inequality

(4.16), we show that

$$\dot{V} \leq -rac{\lambda_{\min}(Q)}{2}||\zeta||^2, \quad ext{for } V(\zeta) \geq \mu^2
ho_1$$

by choosing ρ_1 to satisfy

$$\rho_1 > \frac{2(||P|| + \lambda c_2)^3}{(\lambda_{\min}(Q))^2} \tag{4.19}$$

Inequality (4.19) implies (4.17) and from now on, we fix ρ_1 as chosen above. Thus $\zeta(t)$ enters the set $\{V(\zeta) \leq \mu^2 \rho_1\}$ in finite time and stays therein.

Consider z(t) in $\{V_0 > \alpha_4(\mu\rho_2 + \mu)\}$. Using the facts that $||z|| \ge \gamma((\mu\rho_2 + \mu))$ from (2.7), the bound $||e|| \le \mu\rho_2$ (derived similar to (4.9)), $\lim_{t\to\infty} \nu(t) = 0$, and (2.8), we can show that

$$\dot{V}_0 < -\alpha_3(||z||)$$

Therefore, every trajectory in $\Omega_c \times \Sigma_\epsilon$ enters $\Psi_\mu \times \Sigma_\epsilon$ in finite time and stays therein.

Finally, we show that every trajectory in $\Psi_{\mu} \times \Sigma_{\epsilon}$ approaches an equilibrium point

$$ar{\sigma} = -\operatorname{sign}(a_0(\cdot))\mu\phi^{-1}igg(rac{ar{u}(d)}{k}igg)$$

asymptotically. Let $V_1(z, d)$ be a converse Lyapunov function for assumption (2.10) of exponential stability. Consider

$$V_2 = V_1(z,d) + rac{1}{2}\lambda_5 e_1^2 + rac{1}{2}\lambda_6 ilde{\sigma}^2 + rac{1}{2} ilde{s}^2 + arphi^T P_f arphi$$

where $\tilde{\sigma}=\sigma-\bar{\sigma}$, $\tilde{s}=s-\bar{s}$, $\bar{s}=\bar{\sigma}$, and λ_5 and λ_6 are positive constants to be

chosen. The derivative of V_2 can be arranged in the form

$$\dot{V}_{2} \leq -\chi^{T} P_{2} \chi + (\lambda_{7} ||\varphi|| + \lambda_{8} |\tilde{s}| + \lambda_{9} ||z||) ||\nu(t)||
+ (\lambda_{10} ||\varphi|| + \lambda_{11} |\tilde{s}|) |\ddot{r}(t)|$$
(4.20)

where $\chi = [||z|| \ |e_1| \ |\sigma| \ |\tilde{s}| \ ||\varphi||]^T$ and λ_7 to λ_{11} are positive constants, and $P_2 = P_2^T$ has a structure similar to P_2 of (2.43). The matrix P_2 can be made positive definite by choosing λ_5 large enough, then λ_6 large enough, then μ small enough then ϵ small enough.

For (4.8), we consider the Lyapunov function

$$V_2 = V_1(z,d) + \lambda_5 ilde{\zeta}^T P ilde{\zeta} + rac{1}{2} ilde{s}^2 + arphi^T P_f arphi$$

where $\tilde{\zeta} = \zeta - \bar{\zeta}$ and $\bar{\zeta} = [\bar{\sigma}, 0]^T$. The derivative of V_2 has the form similar to (4.20) with $\chi = [||z|| \ ||\zeta|| \ |\tilde{s}| \ ||\varphi||]^T$, and P_2 can be made positive definite by choosing λ_5 large enough then μ small enough then ϵ small enough.

Regional and semiglobal results for the controller (4.2) is stated in Theorem 4 and Corollary 4, respectively, while Theorem 5 and Corollary 5 summarize the results for the controller (4.3).

Theorem 4 Suppose that Assumptions 1 to 4 of Chapter 2 are satisfied and consider the closed-loop system formed of the system (2.5) with relative degree two, the observer (4.4), the output feedback controller (4.2) with the nonlinear integral gain $\psi(\cdot)$ satisfying (4.5), and continuous, bounded and piecewise differentiable nonlinear proportional gain $k_1(\cdot)$. Suppose $\hat{e}(0)$ is bounded and $(z(0), e(0), \sigma(0)) \in \Omega_b$, where b < c and c satisfies (4.10) and (4.13). Then, there exists $\mu^* > 0$ and for each $0 < \mu < \mu^*$, there exists $\epsilon^* = \epsilon^*(\mu) > 0$ such

that for each $0 < \mu < \mu^*$ and $0 < \epsilon < \epsilon^*(\mu)$, all the state variables of the closed-loop system are bounded and $\lim_{t\to\infty} e(t) = 0$.

Corollary 4 Suppose that Assumptions 1 to 4 are satisfied globally, i.e., $U_{\theta} = R^n$, α_1 , α_2 , α_3 and γ are class \mathcal{K}_{∞} functions, and k can be chosen arbitrarily large. For any given compact sets $\mathcal{N} \in R^{n+1}$ and $\mathcal{M} \in R^{\rho}$, choose c > b > 0 and $r_3 \geq 0$ such that $\mathcal{N} \in \Omega_b$, and choose k large enough to satisfy (4.13). Then, there exists $\mu^* > 0$ and for each $0 < \mu < \mu^*$, there exists $\epsilon^* = \epsilon^*(\mu) > 0$ such that for each $0 < \mu < \mu^*$ and $0 < \epsilon < \epsilon^*(\mu)$, and for all initial states $(z(0), e(0), \sigma(0)) \in \mathcal{N}$ and $\hat{e}(0) \in \mathcal{M}$, the state variables of the closed-loop system (4.7), with nonlinear integral gain $\psi(\cdot)$ satisfying (4.5), and continuous, bounded and piecewise differentiable nonlinear proportional gain, are bounded and $\lim_{t\to\infty} e(t) = 0$.

Theorem 5 Suppose that Assumptions 1 to 4 of Chapter 2 are satisfied and consider the closed-loop system formed of the system (2.5) with relative degree two, the observer (4.4), the output feedback controller (4.3) with the nonlinear integral gain $\psi(\cdot)$ satisfying (4.6), and continuous, bounded and piecewise differentiable nonlinear proportional gain $k_1(\cdot)$. Suppose $\hat{e}(0)$ is bounded and $(z(0), e(0), \sigma(0)) \in \Omega_b$, where b < c and c satisfies (4.10) with (4.11), and (4.13). Then, there exists $\mu^* > 0$ and for each $0 < \mu < \mu^*$, there exists $\epsilon^* = \epsilon^*(\mu) > 0$ such that for each $0 < \mu < \mu^*$ and $0 < \epsilon < \epsilon^*(\mu)$, all the state variables of the closed-loop system are bounded and $\lim_{t\to\infty} e(t) = 0$.

Corollary 5 Suppose that Assumptions 1 to 4 are satisfied globally, i.e., $U_{\theta} = R^n$, α_1 , α_2 , α_3 and γ are class \mathcal{K}_{∞} functions, and k can be chosen arbitrarily large. For any given compact sets $\mathcal{N} \in R^{n+1}$ and $\mathcal{M} \in R^{\rho}$, choose c > b > 0

and $r_3 \geq 0$ such that $\mathcal{N} \in \Omega_b$, and choose k large enough to satisfy (4.13). Then, there exists $\mu^* > 0$ and for each $0 < \mu < \mu^*$, there exists $\epsilon^* = \epsilon^*(\mu) > 0$ such that for each $0 < \mu < \mu^*$ and $0 < \epsilon < \epsilon^*(\mu)$, and for all initial states $(z(0), e(0), \sigma(0)) \in \mathcal{N}$ and $\hat{e}(0) \in \mathcal{M}$, the state variables of the closed-loop system (4.8) with nonlinear integral gain $\psi(\cdot)$ satisfying (4.6) and continuous, bounded and piecewise differential nonlinear proportional gain $k_1(e_1)$, are bounded and $\lim_{t\to\infty} e(t) = 0$.

4.3 Simulation Results

Example 1: Reconsider Example 1 of Section 2.5. The simulation results of Figure 2.4 demonstrated that the Universal Integral Controller with nonlinear integrator driven by the augmented error improves the transient performance. In Figure 4.2, we compare two cases where the nonlinear integrator is driven by the augmented error or the tracking error. Figure 4.2 shows the angular velocity, the integrator output and control input for three controllers with the following linear or nonlinear integral gains:

$$\dot{\sigma}=e_1,\quad \dot{\sigma}=\psi_1(\hat{e}_a),\quad \dot{\sigma}=\psi_2(e_1)$$

We use the same system parameters and controller gains of Figure 2.1. The nonlinearities $\psi_1(\cdot)$ and $\psi_2(\cdot)$ are shown in Figure 4.3. Both nonlinear integrators achieve better transient performance than the linear integrator, showing no overshoot and improved settling time.

Example 2: Reconsider Example 2 of Section 2.5. We compare the performance of the nonlinear integrators, driven by the augmented error and the tracking error, for the motion on the level surface. We use the same controller gains as in Figure 4.4.

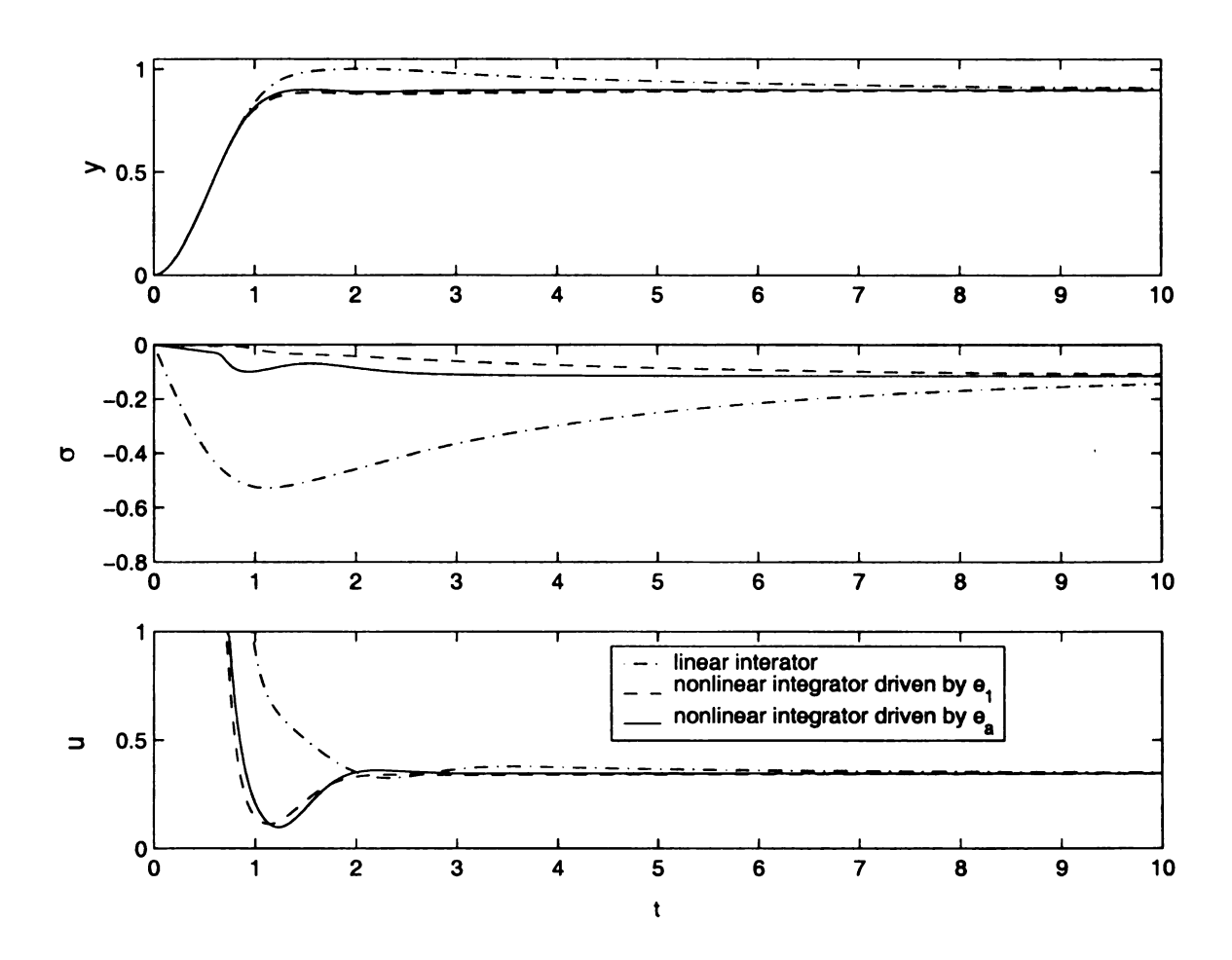


Figure 4.2: Simulation results of the nonlinear PID controllers for the field-controlled DC motor

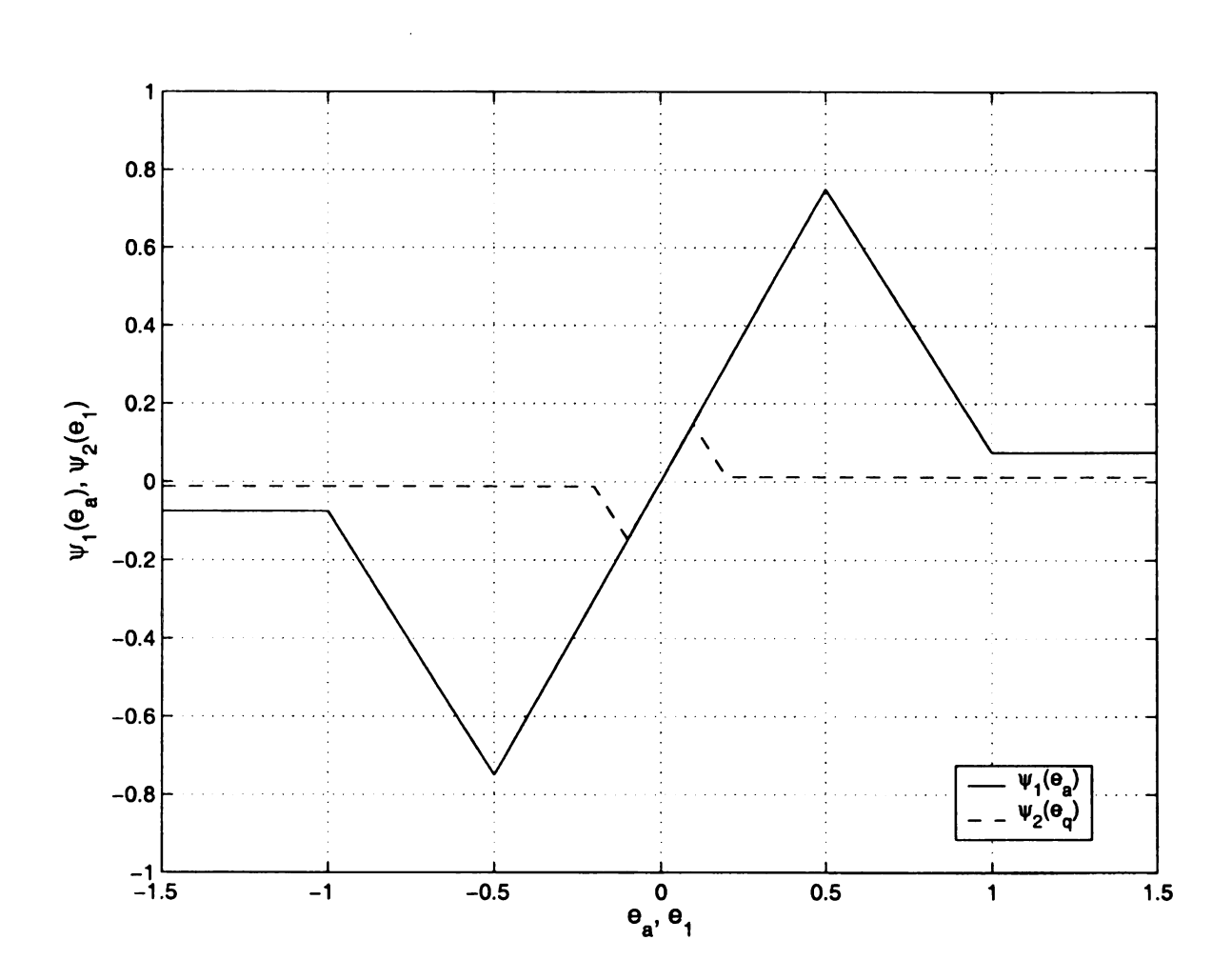


Figure 4.3: Nonlinearities $\psi_1(e_a)$ and $\psi_2(e_1)$ for the simulation of the field-controlled DC motor

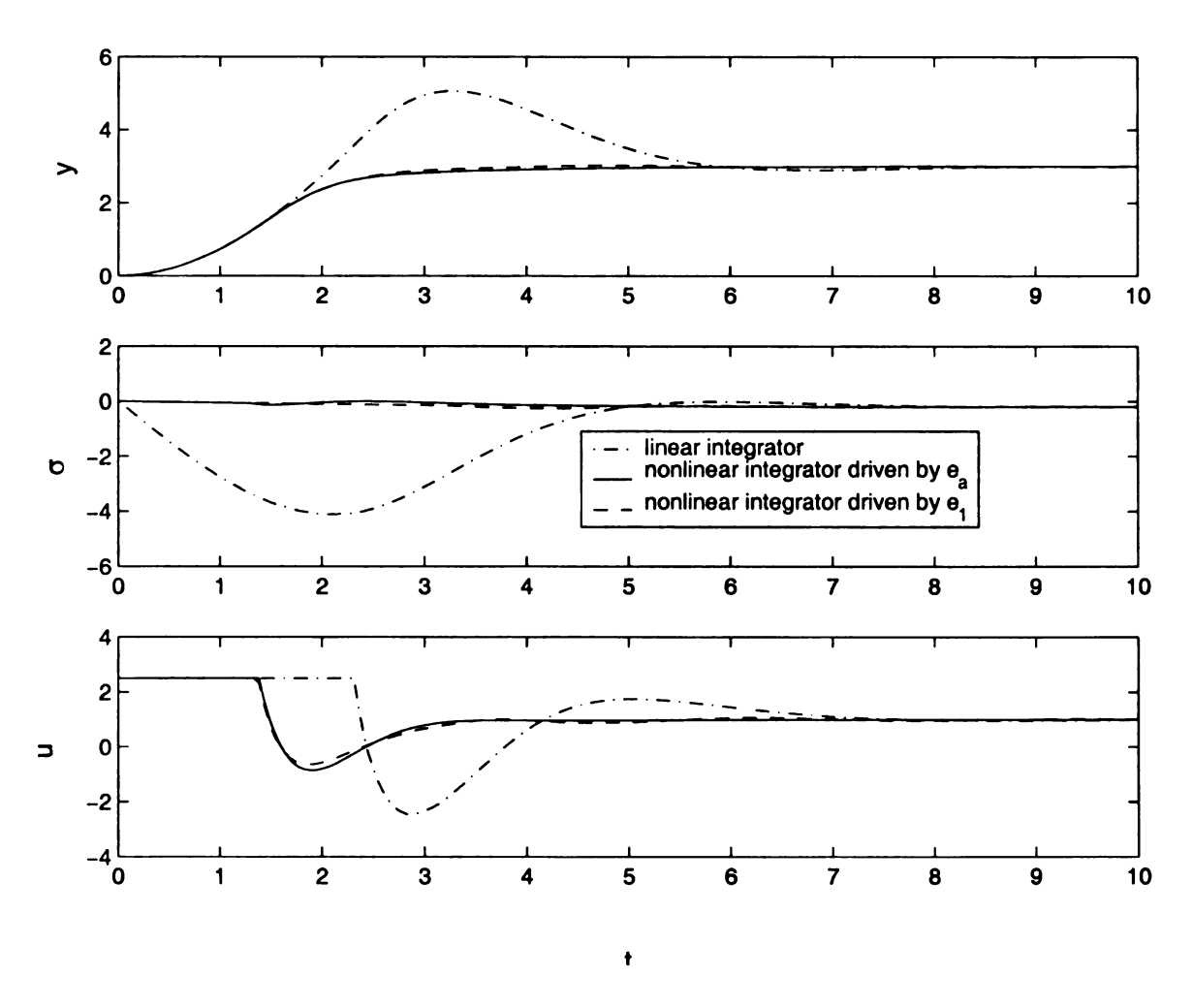


Figure 4.4: Simulation results of the nonlinear PID controllers for motion on a horizontal surface

The nonlinearities $\psi_1(\cdot)$ and $\psi_2(\cdot)$, which are driven by the augmented error and the tracking error respectively, are shown in Figure 4.3. Simulation results are shown in Figure 4.4. Both nonlinear integrators improve the transient performance and show similar performance.

Example 3: An intuitive idea proposed for improving the performance using non-linear gains is to use large proportional gain while the tracking error is large, and decrease the gain as the error becomes small to reduce damping [11] [7]. This idea is not suitable for our case because, inside the boundary layer, the dynamics of the tracking error has the form of a first-order system driven by $(s - \sigma)$:

$$\dot{e}_1 = -k_1e_1 + s - \sigma$$

If the nonlinear integrator keeps σ small, the response of the system will be faster with large k_1 . But k_1 is limited by the control level k, since large k_1 increases the uncertainty $\Delta(\cdot)$, which the controller should overcome (4.13). Nonlinear proportional gain $k_1(e_1)$ can be designed such that the gain is small when the tracking error is large to keep the disturbance $\Delta(\cdot)$ small, and increases as the error becomes small to improve the settling time. For an unstable second-order system with constant disturbance

$$\ddot{y} - \dot{y}^3 - 0.1y^3 = u + 1$$

we designed the nonlinear proportional gain shown in Figure 4.5. A controller with nonlinear integral gain $\dot{\sigma} = \psi_1(\hat{e}_a)$ with $\psi_1(\cdot)$ shown in Figure 4.3, is used with control parameters $\mu = 0.5$ and k = 12 for simulation. The simulation results are shown in Figure 4.6. The controller cannot stabilize the system with linear proportional gain greater than $k_1 = 0.5$, due to the limited control level. The non-

linear proportional gain, shown in Figure 4.5, is designed such that it is small when the tracking error is large and increases as the tracking error becomes small. The nonlinear proportional gain improves the settling time by more than 50%. The simulation results in Figure 4.7 compares the performance of the controllers with the nonlinear integrators $\psi_1(e_a)$, $\psi_2(e_1)$ with the nonlinearities shown in Figure 4.3 and the linear integrator when the nonlinear proportional gain $k_1(e_1)$ is used. The controllers with the nonlinear integrators show similar transient performance improvement. The controller with the linear integrator, driven by the tracking error, cannot stabilize the system with the same control parameters, since the buildup in the integrator increases the uncertainty term.

4.4 Conclusions

In this chapter, we designed a nonlinear PID controller with nonlinear integral and proportional gains for relative-degree-two systems. The nonlinear integrator is driven by the augmented error or the tracking error. We proved regional and semiglobal regulation for both schemes. The simulation results show that nonlinear integrators driven by the tracking error achieve performance improvement similar to integrators driven by the augmented error. The nonlinear proportional gain can be designed to reduce the uncertainty term when the tracking error is large and obtain faster error dynamics inside the boundary layer. Simulation results show that the nonlinear proportional gain can be designed to reduce the settling time.

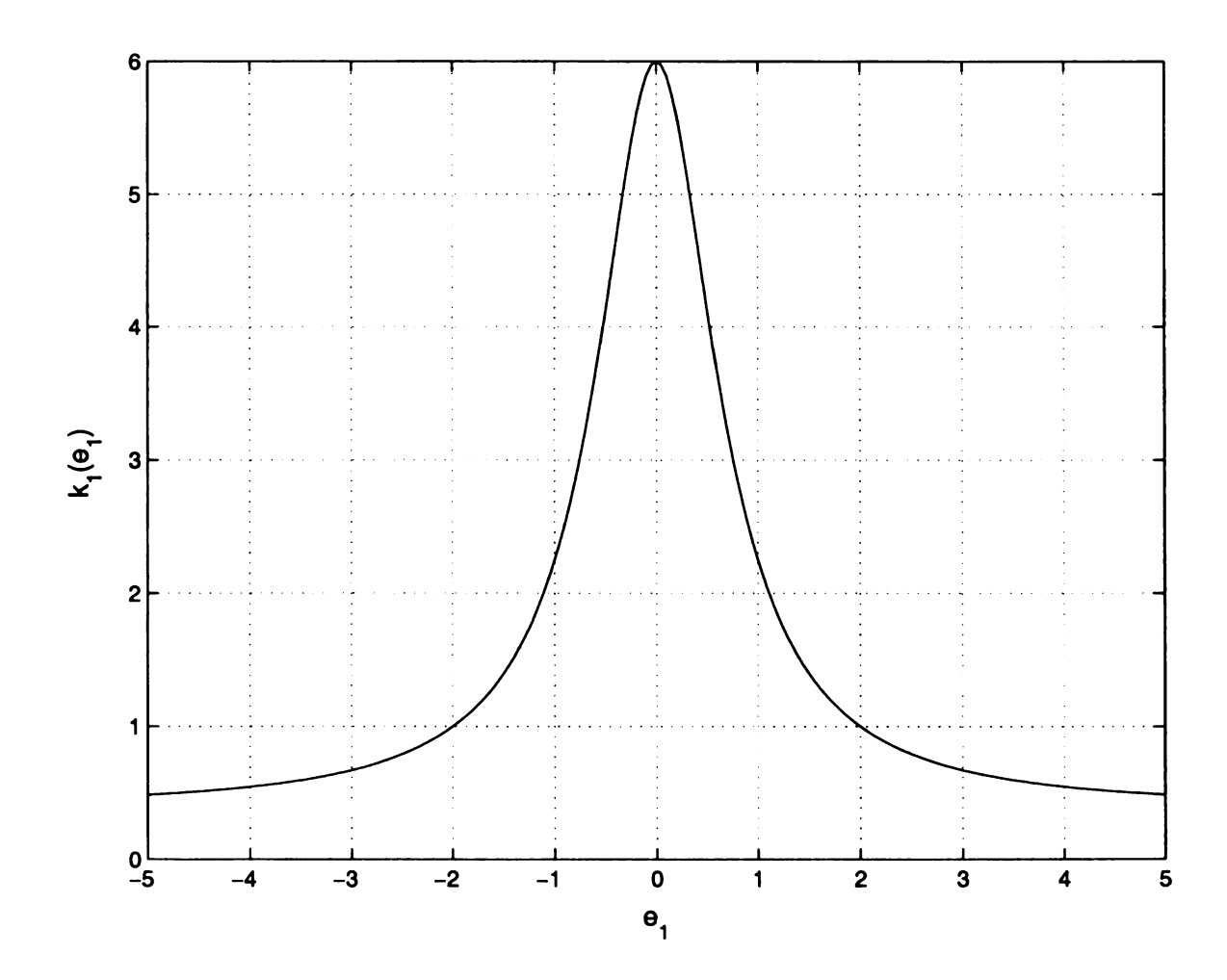


Figure 4.5: Nonlinear proportional gain $k_1(e_1)$ for the simulation of the unstable second-order system

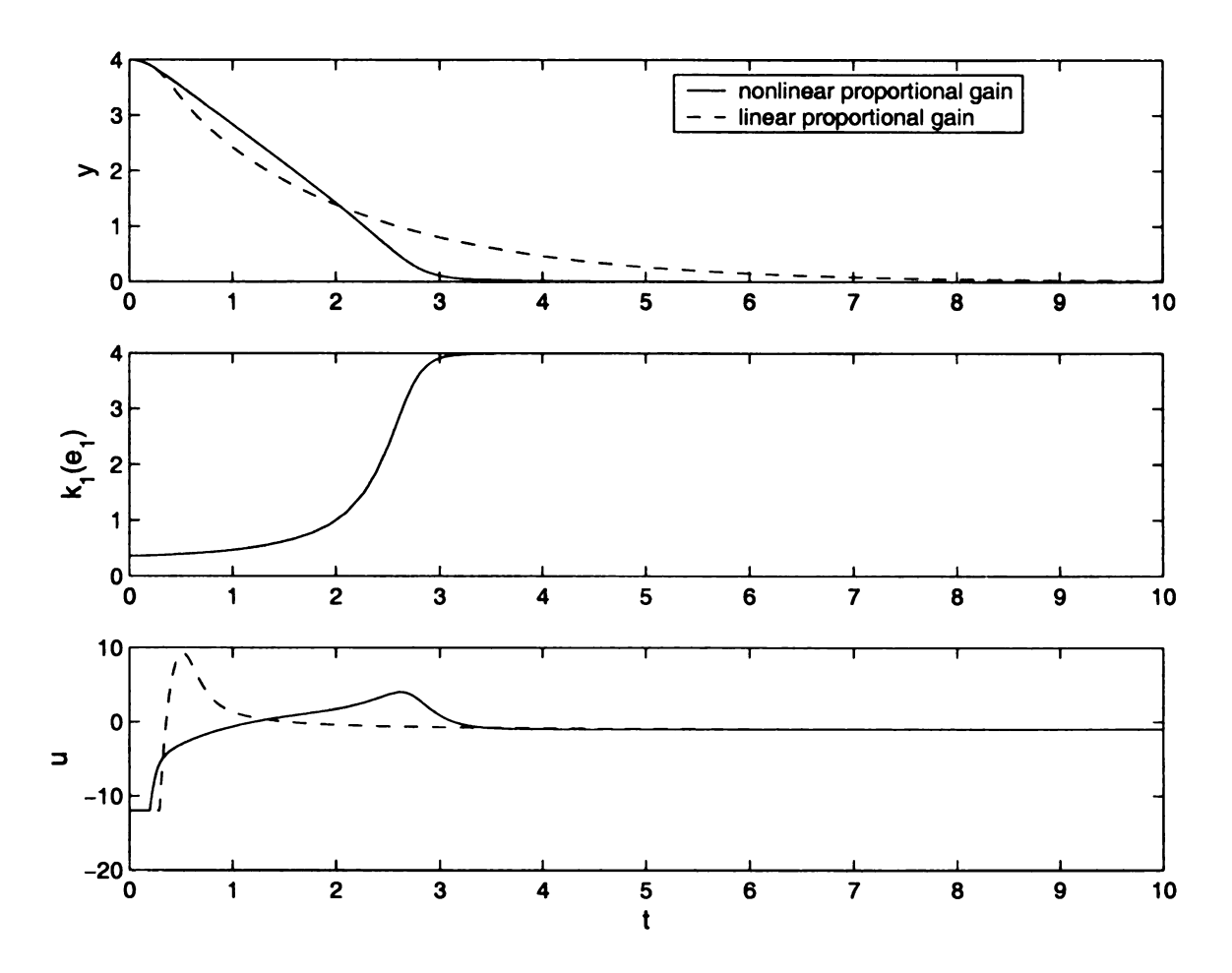


Figure 4.6: Simulation results for the second-order unstable system with nonlinear and linear proportional gains

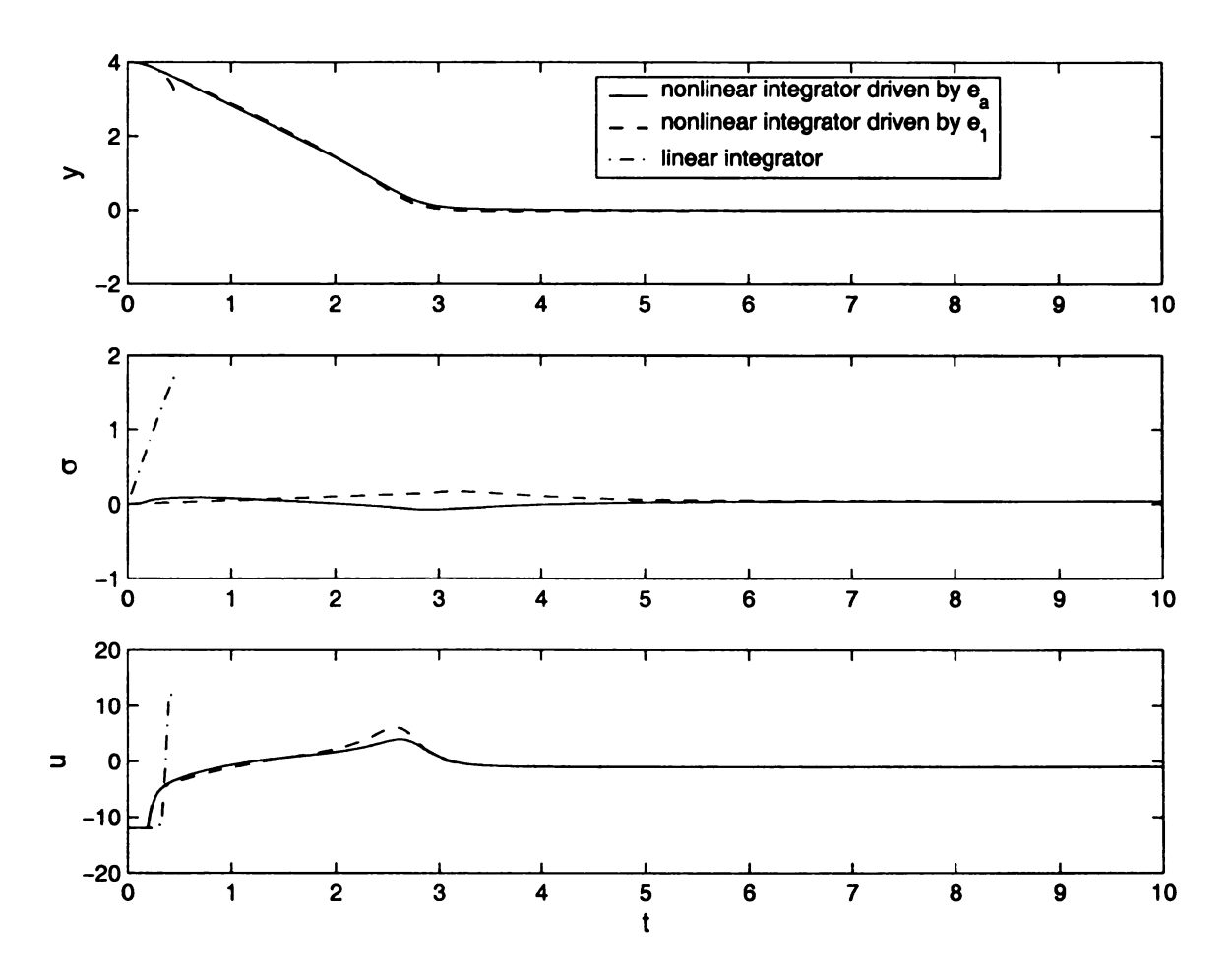


Figure 4.7: Simulation results for the second-order unstable system with linear and nonlinear integrators

Chapter 5

Conclusions

This dissertation provides more freedom in designing controllers which regulate single-input single-output, input-output linearizable, minimum phase nonlinear systems. The structure of the Universal Integral Controller [27] is extended by replacing the controller gains with nonlinear functions of the tracking error and its derivatives, while preserving the regional and semiglobal asymptotic stability. A key idea in our design of the nonlinear gains and analysis of the closed-loop system is that the uncertainty due to nonlinear gains can be overcome by the sliding mode control as long as the system is input-to-state stable inside the boundary layer. The effects of the nonlinear gains on the performance of the controller are investigated by simulation.

In Chapter 2, two possible schemes for nonlinear integration are considered: a nonlinearity placed before or after the integrator. The study of the nonlinear integrator reveals that, when the integrator is driven by the augmented error, the dynamics of the closed-loop system inside the boundary layer are input-to-state stable, which is an essential property for the analysis of asymptotic stability. The closed-loop analysis shows that the Universal Integral Controller with the nonlinear

integrator stabilizes the system regionally and semiglobally. The nonlinear integrator is designed to prevent the buildup during the transient period. In simulations, the Nonlinearity Before Integration scheme achieves superior transient performance over the Nonlinearity After Integration and the linear integrator schemes.

Further extension of the structure of the controller is investigated in Chapter 3. The proportional and derivative gains are replaced by nonlinear functions of the tracking error and its derivatives. By choosing the proportional and derivative gains as nonlinear functions of the form $k_i = k_i(e_i)$, the dynamics inside the boundary layer have the form of a Lure system, and Linear Matrix Inequalities are used to obtain bounds on the nonlinear gains $k_i(e_i)$. Our analysis proves that, if the LMI problem is feasible, the controller with nonlinear proportional, integral and derivative gains achieves regional and semiglobal regulation. Simulation results demonstrate examples where nonlinear gains are utilized to improve the transient performance.

The Universal Integral Controller with nonlinear gains specializes to a non-linear PID controller for relative-degree-two systems. In Chapter 4, more specific results are provided for the nonlinear PID controllers, which are not possible for systems with higher relative degree. We consider the nonlinear integrator driven by the tracking error, which is the classical form of nonlinear integrator found in the literature. The proof of stability is completed analytically, and shows that PID controllers with the nonlinear proportional and integral gains achieves regional and semiglobal regulation for minimum phase nonlinear systems with relative degree two. Simulation results show that the nonlinear integrators, driven by the tracking error or the augmented error, show better transient performance than the linear integrator. The nonlinear proportional gain is designed to improve the settling

time by decreasing the uncertainty that the control input should overcome when the system is far from the equilibrium point.

In this work, we considered the nonlinear proportional and derivative gains of the form $v_i(\cdot) = k_i(e_i)e_i$ among the possible choice of $v_i = v_i(e_1, \dots, e_{\rho-1})$. Finding a more general class of nonlinear functions that preserve the property of input-to-state stability is a challenging but rewarding problem, as it will provide more freedom in the design of the controller.

Application of the Universal Integral Controller with nonlinear gains will be an interesting problem. The structure of the controller could be extended further for a specific problem. For example, the proportional gain of the nonlinear PID controller cannot be taken as $k_1 = k_1(e_1, e_2)$, since it requires that

$$\left[\frac{\partial k_1}{\partial e_2}(e_1,e_2)e_1+1\right]u\neq 0$$

which is not true in general. But the desired proportional gain k_1 and the operating range of a certain application might satisfy the condition.

BIBLIOGRAPHY

- [1] M. Abe. Vibration control of structures with closely spaced frequencies by a single actuator. J. Virbr. Acous. Trans. ASME, 120(1):117-124, Jan. 1998.
- [2] B. Armstrong, D. Neevel, and T. Kusik. New results in npid control: tracking, integral control, friction compensation and experimental results. *IEEE Tran. Contr. Sys. Tech.*, 9(2):399-406, 2001.
- [3] A.N. Atassi and H.K Khalil. A separation principle for the stabilization of a class of nonlinear systems. *IEEE Trans. of Automa. Contr.*, 44:1672-1687, 1999.
- [4] S. Boyd, L.E. Ghaoui, E. Feron, and V. Balakrishnan. Linear Matrix Inequalities in System and Control Theory, volume 15 of SIAM studies in applied mathematics. SIAM, 1994.
- [5] C.I. Byrnes and A. Isidori. Asymptotic stabilization of minimum phase non-linear systems. *IEEE Trans. of Automa. Contr.*, 36(10):1122-1137, 1991.
- [6] H.Y. Chiu, G.B. Stupp, and S.J.Jr. Brown. Vehicle-follower control with variable-gains for short headway automated guideway transit systems. J. Dyn. Syst. Meas. Contr., 99(3):183-189, 1977.
- [7] D.W. Clark. Pid algorithm and their computer implementation. Trans. Inst. Meas. Contr., 6(6):305-316, 1985.
- [8] E.J. Davison. The robust control of a servomechanism problem for linear time-invariant multivariable systems. *IEEE Trans. of Automa. Contr.*, AC-21(1):25-34, 1976.
- [9] C.A Desoer and Y.T. Wang. Linear time-invariant robust servomechanism problems: A self-contained exposition. In C.T. Leondes, editor, *Control and Dynamic Systems*, volume 16, pages 81-129. Academic Press, 1980.
- [10] F. Esfandiari and H.K. Khalil. Output feedback stabilization of fully linearizable systems. *Int. J. Contr.*, 56:1007–1037, 1992.

- [11] H.A. Fertik and R. Sharpe. Optimizing the computer control of breakpoint chlorination. ISA Trans., 19(3):3-17, 1980.
- [12] B.A. Francis. The linear multivariable regulator problem. SIAM J. Contr. Opt., 15(3):486-505, 1977.
- [13] R.A. Freeman and P.V Kokotovic. Optimal nonlinear controllers for feedback linearizable systems. In *Proc. American Control Conference*, pages 2722–2726, Seattle, WA, June 1995.
- [14] T Fukuda, F. Fujiyoshi, F. Arai, and H. Matsuura. Design and dextrous control of micromanipulator with 6 d.o.f. In *Proc. IEEE Int. Conf. Robot. Auto.*, pages 1628–1633, Sacramento, CA, Arp. 1991.
- [15] G.Y. Ghreichi and J.B. Farison. Sampled-data pi controller with nonlinear integrator. In *Proc. IECON*, pages 451-456, Milwaukee, WI, Apr. 1986.
- [16] H. Huang. Error driven controller for electric vehicle propulsion system. In Canadian Conf. Elec. Comp. Eng., volume 2, pages 744-747, St. John, Canada, May 1997.
- [17] J. Huang and W.J. Rugh. On a nonlinear multivariable servomechanism problem. *Automatica*, 26(6):963-972, 1990.
- [18] J. Huang and W.J. Rugh. Stabilization on zero-error manifolds and the nonlinear servomechanism problem. *IEEE Trans. of Automa. Contr.*, 37(7):1009–1013, 1992.
- [19] A. Isidori. A remark on the problem of semiglobal nonlinear output regulation. *IEEE Trans. of Automa. Contr.*, 42:1734-1738, 1997.
- [20] A. Isidori. Nonlinear Control, volume 2. Springer, London, 1999.
- [21] A. Isidori and C.I. Byrnes. Output regulation of nonlinear systems. *IEEE Trans. of Automa. Contr.*, 35(2):131-140, 1990.
- [22] Y Izuno. Speed tracking servocontrol system with speed ripple reduction scheme for traveling-wave-type ultrasonic motor. *Elect. Comm. in Japan*, 81(9):1728-1735, 1998.
- [23] H.S. Kay and H.K. Khalil. Universal integral controllers with nonlinear integrators. In *Proc. ACC*, pages 116-121, Anchorage, AK, May 2002.
- [24] H.S. Kay and H.K. Khalil. Universal integral controllers with nonlinear gains. In *Proc. ACC*, Denver, CO, Jun. 2003. To appear.

- [25] H.K. Khalil. Robust servomechanism output feedback controllers for feedback linearizable systems. *Automatica*, 30(10):1587-1599, 1994.
- [26] H.K. Khalil. High-gain observers in nonlinear feedback control. In H. Nijmeijer and T.I. Fossen, editors, New Directions in Nonlinear Observer Design, volume 244 of Lecture Notes in Control and Information Sciences, pages 249-268. Springer, London, 1999.
- [27] H.K. Khalil. Universal integral controller for minimum-phase nonlinear systems. *IEEE Trans. of Automa. Contr.*, 45(3):490-494, 2000.
- [28] H.K. Khalil. *Nonlinear Systems*. Prentice Hall, Upper Saddle River, NJ, 3rd edition, 2002.
- [29] N.J. Krikelis. State feedback integral control with 'intelligent' integrators. *Int. J. Contr.*, 32(3):465-473, 1980.
- [30] F.J. Luo, R.D. Jackson, and R.J. Hill. Digital controller for thyristor current source. *IEE Proc. B Elect. Pow. App.*, 132(1):46-52, 1985.
- [31] N.A. Mahmoud and H.K. Khalil. Asymptotic regulation of minimum phase nonlinear systems using output feedback. *IEEE Trans. of Automa. Contr.*, 41(10):1402-1412, 1996.
- [32] Y. Ni. Application of a nonlinear pid controller on starcom with a differential tracker. In *Proc. 2nd Int. Conf. Ener. Pow. Deliv.*, volume 1, pages 29-34, Singapore, Mar. 1998.
- [33] Z. Qu. Robust Control of Nonlinear Uncertain Systems. Wiley series in nonlinear science. Wiley, New York, 1998.
- [34] I.W. Sandberg. Global inverse function theorems. *IEEE Tran. Circ. Sys.*, CAS-27(11):998-1004, 1980.
- [35] H. Seraj. A new class of nonlinear pid controllers with robotic applications. J. Robot. Sys., 15(3):161-181, Mar. 1998.
- [36] H. Seraji. Nonlinear and adaptive control of force and compliance in manipulators. *Int. J.Robot. Res.*, 17(5):467-484, May 1998.
- [37] H. Seraji. Nonlinear contact control for space station dextrous arms. In *Proc. IEEE Int. Conf. Robot. Auto.*, pages 899–906, Leuven, Belgium, May 1998.
- [38] S Shahruz and A.L. Schwartz. Nonlinear pi compensators that achieve high performance. J. Dyn. Syst. Meas. Contr., 119:105-110, 1997.

- [39] S.A. Snell and P.W. Stout. Quantitative feedback theory with a scheduled gain for full envelope. J. Guid. Contr. Dyn., 19(5):1095-1101, 1996.
- [40] E.D. Sontag and Y Wang. On characterizations of the input-to-state stability property. Sys. Contr. Lett., 24(5):351-359, 1995.
- [41] A. Teel and L Pray. Global stabilizability and observability imply semi-global stabilizability by output feedback. Sys. Contr. Lett., 22(5):313-325, May 1994.
- [42] H.F. Wang, F.J. Swift, B.W. Hogg, H. Chen, and G. Tang. Rule-based variable-gain power system stabiliser. *IEE Proc. Gen. Trans. Distr*, 142(1):29–32, Jan. 1995.
- [43] Y. Xu, D. Ma, and J.M. Hollerbach. Nonlinear proportional and derivative control for high disturbance rejection and high gain force control. In *Proc. IEEE Int. Conf. Robot. Auto.*, volume 1, pages 752-759, 1993.

